EXPERIMENTAL AND THEORETICAL INVESTIGATIONS ON ALUMINA–WATER NANOFLUID VISCOSITY WITH STATISTICAL ANALYSIS

A THESIS SUBMITTED TO
THE GRADUATE SCHOOL OF NATURAL AND APPLIED SCIENCES
OF
MIDDLE EAST TECHNICAL UNIVERSITY

BY

ELİF BEGÜM ELÇİOĞLU

IN PARTIAL FULFILLMENT OF THE REQUIREMENTS
FOR
THE DEGREE OF MASTER OF SCIENCE
IN
MECHANICAL ENGINEERING

JUNE 2013

Approval of the thesis:

EXPERIMENTAL AND THEORETICAL INVESTIGATIONS ON ALUMINA–WATER NANOFLUID VISCOSITY WITH STATISTICAL ANALYSIS

submitted by **ELİF BEGÜM ELÇİOĞLU** in partial fulfillment of the requirements for the degree of **Master of Science in Mechanical Engineering Department, Middle East Technical University** by,

Prof. Dr. Canan Özgen
Dean, Graduate School of **Natural and Applied Sciences** _____

Prof. Dr. Suha Oral
Head of Department, **Mechanical Engineering** _____

Assoc. Prof. Dr. Almıla Güvenç Yazıcıoğlu
Supervisor, **Mechanical Engineering Dept., METU** _____

Examining Committee Members:

Asst. Prof. Dr. Ahmet Yozgatlıgil
Mechanical Engineering Dept., METU _____

Assoc. Prof. Dr. Almıla Güvenç Yazıcıoğlu
Mechanical Engineering Dept., METU _____

Asosc. Prof. Dr. Derek Baker
Mechanical Engineering Dept., METU NC _____

Asst. Prof. Dr. Mehmet Metin Yavuz
Mechanical Engineering Dept., METU _____

Asst. Prof. Dr. Nilay Sezer Uzol
Mechanical Engineering Dept, TOBB ETÜ _____

Date : **June 24, 2013**

I hereby declare that all information in this document has been obtained and presented in accordance with academic rules and ethical conduct. I also declare that, as required by these rules and conduct, I have fully cited and referenced all material and results that are not original to this work.

Name, Last name : Elif Begüm Elçioğlu

Signature :

ABSTRACT

EXPERIMENTAL AND THEORETICAL INVESTIGATIONS ON ALUMINA–WATER NANOFLUID VISCOSITY WITH STATISTICAL ANALYSIS

Elçioğlu, Elif Begüm
M.S., Department of Mechanical Engineering
Supervisor: Assoc. Prof. Dr. Almıla Güvenç Yazıcıoğlu

June 2013, 119 pages

Nanofluids are nanoparticles' colloidal suspensions. Due to their enhanced thermal conductivity, nanofluids are regarded as advantageous for high efficiency requiring heat transfer applications. On the other hand, the viscosity of nanofluids is greater than those of base fluids. Since the pumping power requirement, which is related to operation cost, is higher for high viscosity fluids, the viscosity of nanofluids should be carefully investigated.

Enhancements in nanofluid thermophysical properties are related to the nanoparticle fraction within the base fluid. Therefore, concentrated nanofluids are more advantageous in terms of their high thermal conductivity. However, viscosity is also high for concentrated nanofluids. Therefore, balancing the advantages of the thermal conductivity enhancement and drawbacks of the viscosity enhancement of nanofluids is important.

The aim of this thesis is to experimentally and theoretically investigate the nanofluid viscosity with detailed statistical analysis. Toward this aim, first a detailed benchmarking of the subject is performed. The unique parts of this thesis are: experimental investigation on Al_2O_3–H_2O nanofluid viscosity for varying nanoparticle volumetric fractions (φ), nanoparticle diameters (d_p), and temperatures (T); and statistical analysis on the experimental data. The experiments showed that, the viscosity of Al_2O_3–H_2O nanofluids increased with φ and d_p, and decreased exponentially with T. The statistical analysis showed that, the main effects of φ, d_p and T, and the interaction effect of T and φ on nanofluid viscosity; and the main effects of φ and d_p on relative viscosity are found to be significant. In addition, new nanofluid viscosity and relative viscosity correlations are presented.

Keywords: Al_2O_3-H_2O nanofluids, nanofluid viscosity, design of experiments, Taguchi Method

ÖZ

ALÜMİNA-SU NANOAKIŞKANININ VİSKOZİTESİNİN TEORİK VE DENEYSEL İNCELEMESİ VE İSTATİSTİKSEL ANALİZİ

Elçioğlu, Elif Begüm
Yüksek Lisans, Makina Mühendisliği Bölümü
Tez Yöneticisi: Doç. Dr. Almıla Güvenç Yazıcıoğlu

Haziran 2013, 119 sayfa

Nanoakışkanlar, nanoparçacıkların kolloidal süspansiyonlarıdır. Nanoakışkanların, yüksek ısıl iletkenliklerinden dolayı, yüksek verim gerektiren ısı transferi uygulamalarında kullanımı avantajlı olarak kabul edilmektedir. Diğer yandan, nanoakışkanların viskozitesi de, baz akışkanlardan daha yüksektir. İşlem maliyeti ile doğrudan ilişkili olan, akışkanı sistem içerisinde sirküle etmek için gerekli pompa gücü, viskozitesi yüksek akışkanlar için daha yüksek olduğundan, nanoakışkanların viskozitesi dikkatle incelenmelidir.

Nanoakışkanların termofiziksel özelliklerinde elde edilen artışlar, baz akışkan içerisindeki nanoparçacık oranına bağlıdır. Bu nedenle, derişik nanoakışkanlar, yüksek ısıl iletkenlikleri ile avantajlıdırlar. Ancak, aynı zamanda, derişik nanoakışkanların viskoziteleri de oldukça yüksektir. Dolayısıyla, nanoakışkanların yüksek ısıl iletkenliklerinin avantajları ile yüksek viskozitelerinin dezavantajlarının dengelenmesi önem taşımaktadır.

Bu tezin amacı, nanoakışkan viskozitesinin teorik, deneysel ve detaylı istatistiksel analiz ile incelenmesidir. Bu amaçla, öncelikle nanoakışkan viskozitesinin karşılaştırmalı değerlendirmesi (benchmark çalışma) yapılmıştır. Bu tezin özgün kısımları: Al_2O_3–H_2O nanoakışkan viskozitesinin değişen sıcaklıklar (T), nanoparçacık hacimsel oranları (φ) ve nanoparçacık çapları (d_p) için deneysel incelemesi ve deneysel verilerin istatistiksel analizidir. Deneyler, Al_2O_3–H_2O nanoakışkanının viskozitesinin φ ve d_p ile arttığını, T ile üstel azaldığını göstermiştir. İstatistiksel analiz, φ, d_p ve T'nin ana etkilerinin ve T ve φ'nin etkileşim etkilerinin nanoakışkan viskozitesi; ve φ ve d_p'nin ana etkilerinin bağıl viskozite üzerine etkilerinin anlamlı olduğunu göstermiştir. Ayrıca, nanoakışkan viskozitesi ve bağıl viskozite için birer korelasyon sunulmuştur.

Anahtar kelimeler: Al_2O_3–H_2O nanoakışkanları, nanoakışkan viskozitesi, deney tasarımı, Taguchi Yöntemi

To my beautiful mother, Prof. Dr. Ömür Şaylıgil Elçioğlu, whom I learnt everything from,

my grandmother Fahriye Şaylıgil, whom I look like and behave as the same,

and my grandfather Remzi Şaylıgil, who had a great wisdom of life.

ACKNOWLEDGEMENTS

First of all, I would like to express my special thanks to my supervisor, Assoc. Prof. Dr. Almıla Güvenç Yazıcıoğlu for her kindness, broadmindedness and everlasting support throughout my graduate education. Studying with her was a privilege and helped me to decide to pursue an academic career. I truly appreciate her encouragement and belief in me. I would like to express my very great appreciation to Prof. Dr. Sadık Kakaç for enlightening me with his academic light throughout the period that I had the chance to work with him. I appreciate his approval on me as a part of his research group for the TÜBİTAK Project. His never ending energy made me rethink on life, studying and success. I would like to thank to Asst. Prof. Dr. Nilay Sezer Uzol for her valuable comments on my studies during our TÜBİTAK Project.

I would like to express my sincere gratitude to Asst. Prof. Dr. Alpaslan Turgut for helping me at every stage of my experiments, and letting me use the facilities of the Energy Laboratory of the Mechanical Engineering Department in Dokuz Eylül University (DEU). I am grateful to him for answering all my questions before, after and during my experiments. I appreciate his kind and perfectionist attitude, as well as his attention on my experiments.

I would like to express my sincere appreciation to Prof. Dr. Ahmet Sermet Anagün at the Industrial Engineering Department of Eskisehir Osmangazi University, for his guidance and help on constructing the statistical methodology of my thesis. I appreciate all the brainstorming we did. He helped me to develop an understanding on the logic of the design of experiments, which I want to use in further studies; and made me understand the value of the multi-disciplinary research.

I would like to thank to my teammates in our TÜBİTAK Project: Büryan Apaçoğlu, Oğuz Kirez and İsmail Ozan Sert for their contributions on my studies, as well as their friendship. I would like to thank to Res. Asst. Tuba Evgin at the DEU Mechanical Engineering for helping me during my experiments and being with me during the lovely times that I spent in İzmir. Her brilliant laboratory skills certainly made things easier for me. I wish to thank Tuğrul Maral for his continuous help, kindness and everlasting positive attitude. My special thanks go to Asst. Prof. Dr. Nurdan Kırımlıoğlu, Res. Asst. Nilüfer Demirsoy and Res. Asst. Hülya Öztürk at the Department of History of Medicine and Ethics, Faculty of Medicine in Eskisehir Osmangazi University for always being with me, their support is very precious.

I thank TÜBİTAK for its financial support during the Project period.

Last but not the least; I want to express my gratefulness to my mother, Prof. Dr. Ömür Şaylıgil Elçioğlu. Being her daughter has been the biggest chance of my life and made me start one move ahead. Her brilliant mind, strong character and big heart have inspired me all my life. Her support, help and love always helped me to go on with life and made me who I am. I also wish to thank to my grandmother Fahriye Şaylıgil and my grandfather Remzi Şaylıgil for loving me so much. I feel very lucky for the lovely times that we spent together.

TABLE OF CONTENTS

LIST OF TABLES

TABLES

LIST OF FIGURES

FIGURES

LIST OF SYMBOLS

A	Heat transfer area (m^2)
A, B, C, D	Factors
AB, AC, BC	Two factor interactions of A, B and C
ABC	Three factor interaction of A, B and C
C	Correction factor in Masoumi et al. correlation [79]
D	Diameter of the circular duct (m)
CF	Critical factor
c_p	Specific heat at constant pressure (J/kgK)
d	Diameter (nm)
D_h	Hydraulic diameter of the duct (m)
d_f	Degree of freedom
d_p	(Nano) particle diameter (nm)
f	Fanning friction factor
F	F value (calculated or table value)
h	Heat transfer coefficient, (W/m^2K)
h	Inter-particle spacing
H_a	Alternative hypothesis
H_0	Null hypothesis
k	Thermal conductivity, (W/mK)
k_H	Huggin's coefficient
L	Duct length, (m)
l	Length of nanotube (nm or μm)
$\dot{m}$	Mass flow rate, (kg/s)
MS	Mean square
N	Total number of observations
N	*N*umber of observations for i^{th} level of a factor
O	Order of terms
P	Power, (W)
r	Particle radius (nm)
Re	Reynolds number, ($\rho u_m D/\mu$)
S	Sum of squares of the cells in the subtotal tables
SS	Sum of squares
SS^l	Pure sum of squares (purified from error)
S_w	Specific surface area (cm^2/g)
T	Temperature (^oC, ^oK)
T	Sum of all observations
u_m	Mean velocity, (m/s)
V	Velocity
Y	All of the observations taken

Greek letters

$[\eta]$	Intrinsic viscosity
η_p	Pump efficiency
λ_0	Wavelength of the 22 mW He-Ne laser of the PSD equipment
Δp	Pressure drop (Pa)
$\dot{\gamma}$	Shear rate
δ	Distance between the nanoparticles
ε	Experimental error
μ	Viscosity
μ	Mean (in Design of Experiments)
ρ	Density (kg/m^3)
φ	(Nano) particle volumetric fraction

Subscripts

a	Aggregate
bf	Base fluid
E	Experimental error
l	Liquid
nf	Nanofluid
p	Particle
r	Relative *(r= nf / bf)*
T	Total
w	Weight (or mass) for particle fraction

CHAPTER 1

INTRODUCTION

In this Chapter, introductory information on nanofluids is given by explaining the components of nanofluids, i.e. nanoparticles and base fluids. The reasons for the outstanding properties of nanoparticles compared to micro- and larger particles are discussed in order to give an opinion on the unforeseen behaviors on nanofluids. After that, nanofluid production and stabilization methods are handled and the importance of the nanofluids' thermophysical properties is emphasized. Finally, the thesis organization is given.

1.1. Need for Efficient Energy Transport

Heat transfer and fluid mechanics practices are very important for industrial applications, especially from the research and development point of view. One of the most important aims of researchers and engineers is to enhance the efficiency of the processes, and this can be done by designing processes in which the energy can be transported in an efficient way.

There are ways to increase the energy transport between the media. One of the most commonly used ways is increasing the heat transfer surface area [1], which can result in an increase in the size of the system, and eventually an increase in the operation cost. Artificial roughness elements [2] may be implemented on the heat transfer surfaces in order to enhance the heat transfer between the media, but this kind of a specific application may not be the solution most of the time.

Relatively poor thermophysical properties of commercial working fluids (e.g, water, ethylene glycol, engine oil, etc.) are regarded as a limitation of the heat transfer performances of the systems. Therefore, improving thermophysical properties of commercial fluids seems to be the best way to achieve high efficiency in heat transfer applications. Suspending small sized particles with enhanced thermophysical properties into the commercial fluids (called "base fluids" from here on) in order to form suspensions that have improved thermophysical properties, thus show improved heat transfer performance mostly, has been considered as a solution for many years.

From this point of view, "nanofluids", which can simply be defined as colloidal dispersions of nanometer sized particles (nanoparticles) in base fluids, are considered as advantageous compared to base fluids, mainly due to their improved thermal conductivity. In addition to the thermal conductivity; thermal diffusivity, thermal absorbtivity, density, and viscosity of nanofluids are higher than those of base fluids, as well. The aforementioned enhancements in thermophysical properties of nanofluids are mainly caused by the high thermophysical properties of dispersed nanoparticles within the base fluids. Detailed information on nanofluids and its components are given in the following sections.

1.2. Nanofluids

Nanofluids are a new class of fluids engineered by dispersing (suspending) nanometer sized materials (nanoparticles, nanofibers, nanotubes, nanowires, nanorods, nanosheets or droplets) within the base fluids. In other words, nanofluids are nanoscale colloidal suspensions containing condensed nanomaterials. They are two-phase systems with one phase (solid phase) in another (liquid phase) [3]. However, nanofluids cannot be considered as totally similar to the commonly used classical suspensions, due to the unforeseen phenomena occurring at the nanometer scale.

The concept nanofluid was introduced by S.U.S. Choi and his co-workers at the Argonne National Laboratory (ANL) in USA. In Choi and Eastman's study [4], nanofluids are defined as: "*innovative new class of heat transfer fluids can be engineered by suspending metallic nanoparticles in conventional heat transfer fluids*" and it is stated that: "*the resulting nanofluids are expected to exhibit high thermal conductivities compared to those of currently used heat transfer fluids, and represent the best hope for enhancement of heat transfer*".

As it is clear from this definition, nanofluids can be simply defined as the combination of nanoparticles and base fluids, as it is illustrated in Figure 1. Information about the components of a nanofluid, i.e. nanoparticles and base fluid as shown in Figure 1, are given in following sub-sections in detail.

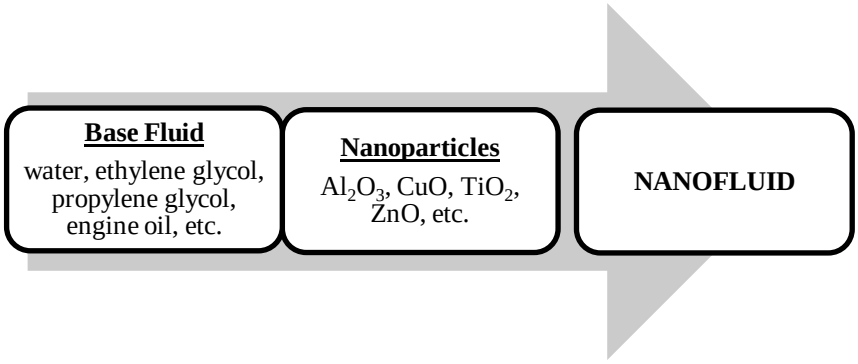

Figure 1. Schematic description of a nanofluid: base fluid in combination with nanoparticles.

1.2.1. Nanoparticles

Nanoparticles are engineered materials, with at least one dimension in the 1-100 nm range. In this definition, size represents an important point. The definition of nanoparticles differs depending upon the materials, fields, and applications concerned. In the narrower sense, they are regarded as the particles smaller than 10 – 20 nm, where the physical properties of solid materials themselves would drastically change [5].

Nanoparticles that are used to improve the thermal conductivity of base fluids can be metals and/or non-metals, since their thermal conductivities are more than one or more order(s) of magnitude(s) higher than those of base fluids. Thermal conductivities of some relevant solids and liquids are provided [6] in Table 1.

Table 1. Thermal conductivities of various solids and liquids

Solids/liquids	Material	Thermal conductivity (W/mK)
Metallic solids	Silver	429
	Copper	401
	Aluminum	237
Nonmetallic solids	Diamond	3300
	Carbon nanotubes (CNTs)	3000
	Silicon	148
	Alumina (Al_2O_3)	40
Metallic liquids	Sodium (at 644 K)	72.3
Nonmetallic liquids	Water (H_2O)	0.613
	Ethylene glycol (EG)	0.253
	Engine oil (EO)	0.145

As is seen in Table 1, thermal conductivities of metallic and non-metallic solids are significantly higher than those of nonmetallic liquids. This is the main idea behind the suspension of particles with enhanced properties into commercial base fluids (which are nonmetallic liquids, mostly).

Some of the commonly used nanoparticles for nanofluid production are: Al, Al_2O_3, Cu, CuO, TiO_2, ZnO, carbon nanotubes (CNTs) (e.g. single walled carbon nanotubes (SWCNTs) and multi walled carbon nanotubes (MWCNTs)), and titanate nanotubes (TNT). In addition to the aforementioned; SiC, SiO_2, Fe_2O_3, Fe_3O_4, Ag, Au, diamond, and $BaZrO_3$ nanoparticles are used, as well.

1.2.1.1. Nanoparticles vs. Microparticles: Which is Advantageous?

With the upsurge in the miniaturization trend, especially towards enhancing the heat transfer performance of the base fluids, mainly by improving their thermal conductivity; suspending small sized particles into the base fluids came to the fore, due to their enhanced thermal conductivity. During the earlier times, micro- ($1\mu m = 10^{-6}$ m) and larger particles were used for this purpose. While some enhancement in heat transfer was obtained this way, some major disadvantages (quick settlement and aggregation of particles, channel clogging, erosion in flow channels, pump damage, etc.) could not be overcome. Later on, suspension of nanoparticles into the commercial base fluids was attempted, in order to enhance the heat transfer performance of the base fluids.

It appeared that, suspending nanoparticles worked better than micro- and larger particles, and developed a new research field. In Figure 2, a general comparison between heat transfer fluids containing microparticles and nanoparticles is illustrated.

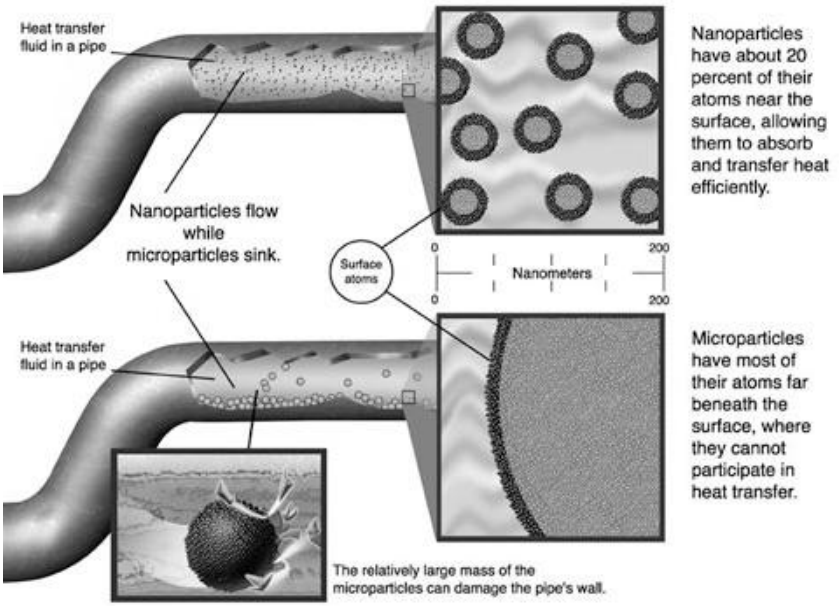

Figure 2. Comparison between heat transfer fluids containing microparticles and nanoparticles. Adapted from [7].

When it comes to fluidic applications, stability is an important concern. While microparticles can easily settle, nanoparticles are mostly stable (remain in suspension almost indefinitely) [8]. This is mostly because of the high surface/volume ratio of the nanoparticles (1000 times higher than that of microparticles), which leads them to be better integrated within the base fluid. As a result, suspending nanoparticles rather than micro- or larger particles into the base fluids is more advantageous due to improved stability and less number of limitations.

1.2.1.2. Why Do Nanoparticles Behave Different?

There are a lot of studies available in literature aimed to explain the possible mechanisms responsible for the unforeseen behaviors of nanoparticles. Behaviors of nanofluids are not similar to those of base fluids, however the base fluid is the biggest component of the nanofluid (considering the volumetric concentrations of nanoparticles (~ 8-10% at most, 1-2% typical), surfactant (little amounts, if used), and base fluid (~ 90-95% at least)). Dispersion of nanoparticles into the base fluids in even very little concentrations can drastically alter the properties of the base fluids, thus leads to the enhanced thermophysical properties of nanofluids. Therefore, it is important to have a fundamental understanding of the possible mechanisms responsible for the unforeseen behaviors of nanoparticles, in order to understand the properties of nanofluids.

The responsible mechanisms are mostly regarded as the size effect and increased surface area of nanoparticles. As the particle size approaches the micrometer range, it tends to be affected by the behavior of atoms or the molecules, and show different properties from those of the bulk [5]. Atoms in a material can be classified as surface atoms and bulk atoms. Surface atoms, which have a high concentration of unsaturated bonds, are different from the bulk atoms, since the termination of the bulk crystalline structure (repeating pattern) occurs at the surface. As the material size decreases, the ratio of atoms lying on the surface, i.e. surface atoms, to the total increases.

The relationship between the particle size and the number ratio of surface atoms to the total (%), with an assumption of atomic distance of 0.2 nm, is provided in Table 2 (adapted from [5]).

Table 2. Solid particle size and the fraction of atoms located at the particle surface.

Number of atoms at the surface	Total number of atoms	Number ratio of surface atoms to the total (%)	Examples of particle size and powder
8	8	100	
56	64	87.5	
488	1.000	48.8	2 nm
58.800	1×10^6	5.9	20 nm (colloidal silica)
6×10^6	1×10^9	0.6	200 nm (titanium dioxide)
6×10^8	1×10^{12}	0.06	2 μm (light calcium carbonate)
6×10^{10}	1×10^{15}	0.006	20 μm (green tea powder, chalk)

Another possible mechanism is the increased surface area of nanoparticles compared to micro- and larger particles. A simple illustration showing the surface areas of cubes (the whole of a cube (left hand side) and a cube divided into smaller cubes on the order of nanometers (right hand side)) is given in Figure 3.

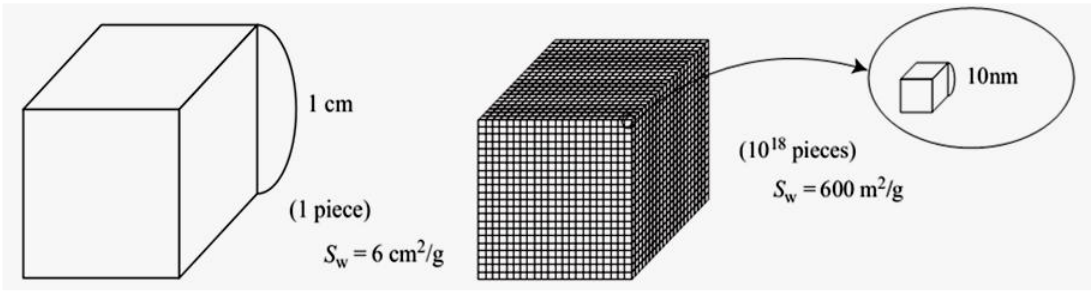

Figure 3. Change of the surface area of a cube. From left to right: the whole of a cube, a cube divided into smaller cubes on the order of nanometers. S_w is the specific surface area. Solid density is assumed to be $1 g/cm^3$. Adapted from [5].

As mentioned, thermophysical properties of nanofluids are different from those of base fluids, and this causes the correlations between the thermophysical properties and ambient parameters for nanofluids to be different than those of base fluids. Therefore, for the measurement and analysis of the thermophysical properties of nanofluids, the aforementioned phenomena are important and should be taken into consideration.

Above, some of the commonly accepted mechanisms responsible for the unforeseen behaviors of nanoparticles were summarized, but there may be other mechanisms that need to be considered, as well. Therefore, observation of the differences between the properties of nanofluids and base fluids is important.

1.2.2. Base Fluids

Some of the commonly used base fluids for nanofluid production are: water (H_2O), ethylene glycol (EG), propylene glycol (PG), and their mixtures (H_2O&EG, H_2O&EG, EG&PG), and engine oil (EO). In addition, decane ($C_{10}H_{22}$), polyalphaolefin (PAO), and gear oil have also been used as base fluids. At this point, it is important to note that, EG and PG are commonly used to lower the freezing point of H_2O, which makes EG and PG mixed H_2O based nanofluids suitable for low temperature applications [9].

1.3. Synthesis of Nanofluids

Nanofluids are synthesized by dispersing (suspending) nanoparticles into the base fluids. The methods used for nanofluid production are "one-step method" and "two-step method (Kool-Aid Method)" [10]. In addition, stability of nanoparticles in the base fluid is a critical concern at all times, including the production step of nanofluids. Nanofluid production and stabilization methods are presented in detail, next.

1.3.1. Nanofluid Production Methods

Methods used for nanofluid production are "one-step method" and "two-step method", which can be classified under top-down approach (producing nanomaterials from bigger materials using micromachining techniques) and bottom-up approach (producing nanomaterials by bringing atoms and molecules together), respectively [11].

In the one-step method, production of nanofluids, i.e. production of nanoparticles and their dispersion into the base fluid, is performed during the same step. This method is usually used for metallic-nanoparticle nanofluid production [12]. In Eastman et al.'s study [13] the authors performed the one-step method for nanofluid production by utilizing direct evaporation technique, in which nanoparticles are solidified into the base fluid from their gas phase. The one-step method can be regarded as advantageous, since the drying, storage, transportation, and dispersion of nanoparticles processes are avoided, the agglomeration of nanoparticles is minimized, and the stability of nanofluids is increased [14].

In the two-step method, the nanofluid production process is performed in two separate steps. In the first step, nanoparticles are produced or purchased from a commercial source. In the second step, their dispersion into the base fluid is performed by some techniques, e.g. high shear and ultrasound [15]. In addition, this method is more suitable for producing oxide nanoparticles [15]. This method can be considered as advantageous for some cases, when laboratory facilities may not be sufficient to produce nanofluids in one step. As mentioned, this method isolates the preparation of the nanofluids from the preparation of nanoparticles. Therefore, agglomeration of nanoparticles may take place in both steps, especially during drying, storage, and transportation stages of nanoparticles [14]. As a result, the possibility of aggregate formation is high in the two-step method.

1.3.2. Nanofluid Stabilization Methods

During (or after) the dispersion of nanoparticles into the base fluid, stabilization methods should be used, in order to obtain a suspension with high stability, i.e. minimum aggregation and settlement of nanoparticles. Nanoparticles can quickly agglomerate before the dispersion and sometimes nanoparticles disperse partially into the base fluids [15]. So as to prevent these unwanted results, stabilization methods are used. The most effective method of breaking and evenly dispersing the nanoparticles in a base fluid is through application of ultrasonic vibration and high speed stirring [16]. Addition of an appropriate stabilizing agent (surfactant) and/or pH adjusting agents into the nanofluids are also used to prevent the agglomeration of the nanoparticles. Nanoparticle aggregation can cause settlement of nanoparticles, due to the increased weight of the nanoparticle aggregates and may result in poor performance. Zeta potential, which is a measure of the potential difference between the dispersion medium (base fluid) and the stationary layer of fluid attached to the particle [3], is a commonly used characterization technique for the determination of the stability of nanofluids. Nevertheless, it is important to note that, the aggregation and settlement of nanoparticles are inevitable in the long term. Therefore, reliable and effective stabilizing methods are required for long-term applications of nanofluids.

1.4. Importance of the Thermophysical Properties of Nanofluids

Due to their improved thermal conductivity and improved heat transfer performance, nanofluids are now regarded as a solution for high efficiency requiring heat transfer applications. However, before the utilization of nanofluids, correct prediction of the thermophysical properties (thermal conductivity, density, viscosity, thermal diffusivity, thermal absorbtivity, etc.) is essential.

For high efficiency requiring heat transfer applications, improved thermal conductivity of nanofluids is a key advantage. As the amount of nanoparticles dispersed within the base fluid increases, the thermal conductivity enhancement obtained with nanofluids always increases [17]. However, the viscosity of nanofluids increases with increasing the amount of dispersed nanoparticles within the base fluid, as well. Enhanced viscosity of nanofluids is a serious limitation, since it results in an increased pressure drop and increased pumping power requirement [18] in the flow channel, and eventually in increased operation cost. Therefore, enhanced viscosity is an unwanted result and should be taken under control. At this point, it is important to define "relative viscosity (μ_r)", which is used to define the viscosity enhancement obtained with nanofluids. Relative viscosity can thus be defined as the ratio of nanofluid viscosity (μ_{nf}) to base fluid viscosity (μ_{bf}), i.e. $\mu_r = \mu_{nf}/\mu_{bf}$.

When the literature is surveyed, it is seen that, the studies interested in particularly with nanofluid viscosity are limited in number, compared to the nanofluid thermal conductivity and heat transfer enhancement studies. However, nanofluid viscosity deserves attention and should be studied comprehensively, as well.

From this point, it is decided to perform a systematic study involving theoretical and experimental investigations along with statistical analysis on Al_2O_3–H_2O nanofluid viscosity. There is a certain need for systematic efforts on the measurement and analysis of nanofluid viscosity.

1.5. Scope and Objectives of the Thesis

In this thesis, nanoparticle volumetric fraction (φ), nanoparticle size (d_p) and temperature (T) dependent viscosity of Al_2O_3–H_2O nanofluids was investigated experimentally. The nanofluid samples used are γ (gamma phase) Al_2O_3–H_2O nanofluids with nanoparticle volume fractions of 1, 2 and 3%, and particle sizes of 10±5 nm and 30±10 nm, which were purchased from Nanostructured & Amorphous Materials, Inc. (NanoAmor), USA. Experiments were carefully designed with Taguchi Method (a Design of Experiments (DOE) approach) before they were performed. Experimental data

were then analyzed with Analysis of Variance (ANOVA), in order to statistically determine the effects of nanoparticle volume fraction, nanoparticle size, and temperature on nanofluid viscosity. It is important to emphasize that, although the trend of viscosity with φ, d_p, and T may be observed through standard experiments, ANOVA helps at the determination of the real magnitudes of the factors, and the factor interactions on the examined parameter. In addition, ANOVA tells whether an effect is due to the experimental error, or it is an actual effect of a factor. The main objectives of this thesis are to provide a reliable nanofluid viscosity database for Al_2O_3–H_2O nanofluids, and have an epistemic understanding on nanofluid viscosity and related concepts by the critical evaluation of the theoretical background. To the knowledge of the author, this will be the first study that is concerned with the statistical determination of the effects of the nanoparticle volumetric fraction, nanoparticle size and temperature with the Taguchi Method.

1.6. Thesis Organization

The thesis is concerned with the evaluation of Al_2O_3–H_2O nanofluid viscosity both theoretically and experimentally, with statistical analysis. Chapter 1 provides introductory conceptual information on nanofluids, its components (nanoparticles and base fluids), why nanofluids have different properties than the commercial working fluids, and the methods and approaches used to produce the nanofluids. After this introduction, a literature survey on nanofluid viscosity is presented in Chapter 2. A benchmark study on nanofluid viscosity and relative viscosity is also presented in the Chapter. After touching on the theoretical background by summarizing the literature and benchmark study, detailed information on the material and method of the present investigation are provided in Chapter 3. After giving the essential points in Chapter 3, the experimental investigation and the statistical evaluation on the Al_2O_3–H_2O nanofluid viscosity and relative viscosity are presented in Chapter 4. The discussion of the results is presented in Chapter 5, and after this Chapter, the summary and conclusions of the present investigation are presented in Chapter 6.

In addition, some materials are provided in the Appendices. In Appendix A, the coefficients of the correlations presented in Chapter 2 are provided. In Appendix B, the MATLAB code that is employed for the calculations required for diluted sample preparation is presented with the program outputs. In Appendix C and Appendix D, the zeta potential and dynamic light scattering results (related to the stability and the particle size distribution) are provided. The data entering for performing ANOVA in order to investigate the effects of the factors on the nanofluid viscosity and relative viscosity is provided in Appendix E. Finally, the entire experimental data are presented in Appendix F.

CHAPTER 2

NANOFLUID VISCOSITY: LITERATURE SURVEY AND BENCHMARK STUDY

In this Chapter, nanofluid viscosity is handled by surveying the related studies in literature, first. Critical evaluation of the previous work is considered to be important, since there have been a lot of inconsistencies in literature. The literature survey consists of the summaries of the manually selected studies from scientific databases. After the literature survey, a benchmark study is performed on the nanofluid viscosity (μ_{nf}) and relative viscosity $\left(\mu_r = \mu_{nf}/\mu_{bf}\right)$ models[1] and correlations[2] via a parametric analysis, in order to summarize the literature objectively. Finally, some conclusions are drawn.

2.1. Introduction

Research on the subject "nanofluids" has been widely conducted all over the world, since Choi and his co-workers introduced "nanofluids" in 1995 [4]. Heat transfer enhancement obtained with nanofluids is one of the most important advantages of nanofluids, and as expected, most of the studies in literature aimed to investigate the superior thermal conductivity of nanofluids, and explain the heat transfer enhancement obtained with nanofluids. The literature survey showed that, the subject "nanofluid viscosity" has not been investigated as comprehensively as the "nanofluid thermal conductivity" and "heat transfer enhancement with nanofluids". However, viscosity and other flow characteristics should gain attention, since they have considerable effect on the flow, just as the thermal conductivity. Figure 4 shows the multi-variability of nanofluid systems and the properties of nanofluids that affect the heat transfer performance.

[1] In this context, the word "model" is used to refer to the widely used and accepted equations developed for conventional mixtures, namely the "Classical Models.

[2] In this context, the word "correlation" is used to refer to the other theoretical and empirical equations.

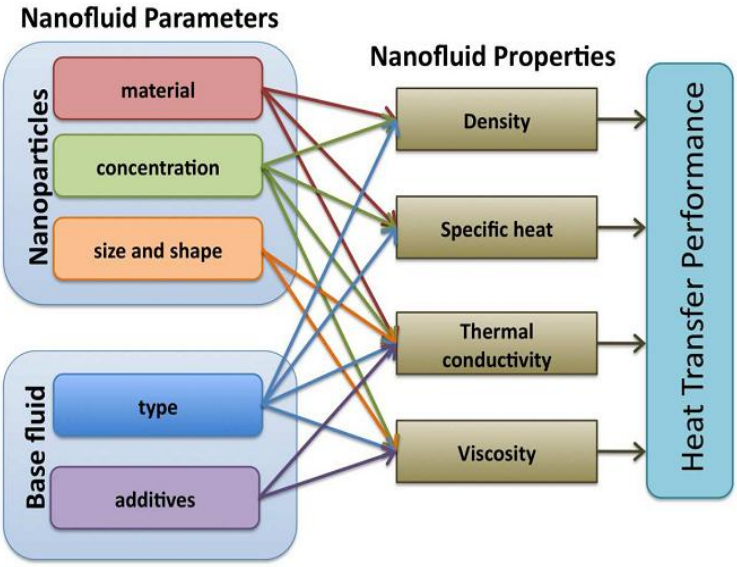

Figure 4. Complexity and multi-variability of nanofluids [19]

As it is seen in Figure 4, viscosity is one of the key properties of nanofluids. Therefore, it should be carefully investigated.

From the heat transfer performance point of view, viscosity is regarded as an important parameter. Heat transfer enhancement between the media is very important, but viscosity enhancement can lead to unwanted results. For turbulent flow, the Fanning friction factor (*f*) is defined with many correlations (for details, see [1] and [20]), but it can be generally defined as: $f = A\,Re^{-n}$. In this definition, *A* and *n* are constants, and *Re* is Reynolds number, $Re = \rho u_m D/\mu$. Using the information given, it can be concluded that, the Reynolds number is lower, thus the friction factor is higher for the high viscosity fluids. The general expression for the frictional pressure drop for flow through a duct of length *L* and the power required by an adiabatic pump for an incompressible stream with a mass flow rate $\dot{m}$ were provided by Kakaç and Liu [20] as in Equation (1) and Equation (2), respectively.

$$\Delta p = 4f\frac{L}{D_h}\frac{\rho u^2{}_m}{2} \tag{1}$$

$$P = \frac{1}{\eta_p}\frac{\dot{m}}{\rho}\Delta p \tag{2}$$

Kakaç and Liu [20] also provided the pumping power per unit heat transfer area (W/m^2) for fully developed turbulent flow in smooth tubes.

$$\frac{P}{A} = \frac{Ch^{3.5}\mu^{1.83}(D_h)^{0.5}}{k^{2.33}c_p{}^{1.17}\rho^2\eta_p} \tag{3}$$

As it is seen in Equation (3), the pumping power per unit area depends strongly on the thermophysical properties of fluids [20], and it is proportional to approximately the square of the working fluid viscosity. Therefore, the fluid viscosity is of great significance in terms of heat transfer performance. In order to have an application with high efficiency, the pumping power should be reduced as much as possible, in order to reduce the operation costs. This is the main reason behind why viscosity is a key property in applications, and why it should be carefully investigated.

The complexity of the nanofluid applications is pretty clear. The reason for the need of nanofluid utilization is the need for high efficiency, and any drawbacks and losses that may be faced during the

applications should be eliminated. Therefore, viscosity of nanofluids should be kept under control, in order to control the pumping power requirement and operation costs of the systems.

2.2. Nanofluid Viscosity: Estimation and Literature Survey

Nanofluids are essentially two-phase mixtures, but this fact does not mean they are totally similar to the conventional suspensions. The reasons for this difference were handled under Section 1.2.1.2.

Equations used to calculate the nanofluid viscosity can initially be classified according to the fluid type that the equations were particularly developed for. Namely, they can be classified as: models proposed for conventional mixtures, and correlations proposed particularly for nanofluids. Models proposed for conventional mixtures, i.e. "Classical Models" can be used to calculate the nanofluid viscosity, but while they are used, their applicability limits should be recalled. The secondary classification can be done according to the methodology used to develop the equations as: theoretical and empirical correlations [21]. Under Section 2.2.1 and 2.2.3, the Classical Models, and the theoretical and empirical correlations are handled in detail.

As aforementioned, the term "relative viscosity" is used to define the viscosity enhancement obtained with nanofluid compared to the viscosity of base fluid. The relative viscosity is defined as the ratio of the viscosity of nanofluid (μ_{nf}) to the viscosity of the base fluid (μ_{bf}), i.e. $\mu_r = \mu_{nf} / \mu_{bf}$.

2.2.1. Viscosity Estimation with Classical Models: The Conventional Approach

The relative viscosity equations proposed for conventional mixtures are called Classical Models. They are widely accepted and used equations in literature for a certain time. A comprehensive review of nanofluid viscosity estimation with the Classical Models, and theoretical and empirical correlations belongs to Kumar et al. [22]. Mahbubul et al. [15] presented the latest developments on the nanofluid viscosity in their review paper. Hosseini et al. [23] reviewed the relations for the physical properties (including viscosity) of nanofluids. In addition, Elçioğlu et al. [21] reviewed the recent literature, in addition to a comparative evaluation on the Classical Models, and theoretical and empirical correlations.

The Classical Models that are used to calculate the viscosity of the conventional suspensions as well as nanofluids are given in Table 3 in their chronological order. To mention briefly, Einstein's work in 1906 [24] can be regarded as the pioneer effort in suspension rheology field and after that, many models and correlations have been proposed, mostly with the aim of extending the Einstein Model [24] to different conditions.
The general expression for the relative viscosity of suspensions is given in Equation (4) [25, 26].

$$\mu_r = \frac{\mu(0)}{\mu_{bf}} = 1 + [\eta]\varphi + k_H([\eta]\varphi)^2 + O(\varphi^3) \quad (4)$$

In Equation 4, $[\eta]$, k_H and $\mu(0)$ denote the intrinsic viscosity, Huggin's coefficient (the interaction parameter characterizing the colloidal interactions between particles as opposed to the purely hydrodynamic effect [26]) and dispersion viscosity at the low shear limiting behavior [25], respectively. As it is seen in Table 3, Einstein [24] and Batchelor [27] predicted the coefficients of φ (which is $[\eta]$) as 2.5 for dilute suspensions and φ^2 (which is $k_H[\eta]^2$) as 6.2, respectively in Equation (4) for suspensions of hard spheres. Batchelor also predicted the coefficient of φ^2 (which is $k_H[\eta]^2$) as 7.6 for extensional flows [25]. Deviations from the particles being hard spheres results in a change of the coefficients of Einstein Model [24] and Batchelor Model [27]. Hence, the dispersion viscosity can be regarded as an indication that may be used to have information on adsorbed layers, particle charge, particle shape, and the fluid nature of the particles [25].

Table 3. Classical Viscosity Models

Reference	Equation	Notes
Einstein, 1906 [24]	$\mu_r = 1 + 2.5\varphi$ (5)	The pioneer model among most of the other viscosity models and correlations, which asumes the particles are non-interacting hard spheres. The model is valid for low particle volumetric fractions ($0< \varphi \lesssim 0.001$) [26].
Andrade, 1934 [28]	$\mu = Dexp(B/T)$ (6)	The model is an empirical model and it defines the viscosity as a function of temperature (D and B are constants).
Brinkman, 1952 [29]	$\mu_r = (1-\varphi)^{-2.5}$ (7)	The model is a modified version of Einstein Model [24] to moderate particle volumetric fractions [33].
Krieger and Dougherty, 1959 [30]	$\mu_r = \left[1 - \frac{\varphi}{\varphi_m}\right]^{-[\eta]\,\varphi_m}$ (8)	$[\eta]$ and φ_m are intrinsic viscosity and maximum particle packing fraction, respectively. $[\eta]$ has a typical value of 2.5 for the mono disperse suspensions of hard spheres. φ_m is 0.495 to 0.54 under quiescent conditions, and 0.605 at high shear rates [26].
Frankel and Acrivos, 1967 [31]	$\mu_r = \frac{9}{8}\left[\frac{(\varphi/\varphi_m)^{1/3}}{1-(\varphi/\varphi_m)^{1/3}}\right]$ (9)	The model is valid for spherical particles in the range of $0.5236 \leq \varphi_m \leq 0.7405$ [22]. φ_m is the maximum particle volumetric fraction, and determined experimentally [46].
Nielsen, 1970 [32]	$\mu_r = (1+1.5\varphi)\exp\left(\frac{\varphi}{1-\varphi_m}\right)$ (10)	The model was proposed to take the particle-particle interactions and aimed to extend the Einstein Model [24] to about $\varphi = 0.04$ [33].
Lundgren, 1972 [34]	$\mu_r = 1 + 2.5\varphi + \frac{25}{4}\varphi^2 + O(\varphi^3)$ (11)	The model is the Taylor Series expansion of Einstein Model [24] with respect to φ. O denotes the order of terms, which is of 3.
Batchelor, 1977 [27]	$\mu_r = 1 + 2.5\varphi + 6.2\varphi^2$ (12)	The model takes the particle-particle interactions into account.
Graham, 1981 [35]	$\mu_r = 1 + 2.5\varphi + 4.5\left[\frac{4}{\frac{h}{d_p}\left(2+\frac{h}{d_p}\right)\left(1+\frac{h}{d_p}\right)^2}\right]$ (13)	The model defines the relative viscosity depending on the particle size (d_p) and inter-particle spacing (h).

For concentrated suspensions, in which the particles interact with each other [25], the rheological behavior cannot be defined with Equation (4). For those cases, Krieger-Dougherty Model [30] (Equation (8) in Table 3) is used. The Model [30] defines the viscosity of suspensions for low and high shear conditions. Substituting the values of $[\eta] = 2.5$ and $\varphi_m = 0.5$ and 0.605 into the Krieger-Dougherty Model, Equation (14) and Equation (15) are obtained for low and high shear conditions. In Equation (14) and Equation (15), $\mu(0)$ and $\mu(\infty)$ denote the viscosity at low and high shear conditions, respectively.

$$\mu_r = \frac{\mu(0)}{\mu_{bf}} = \left[1 - \frac{\varphi}{0.5}\right]^{-[2.5]\,0.5} = \left[1 - \frac{\varphi}{0.5}\right]^{-1.25} \tag{14}$$

$$\mu_r = \frac{\mu(\infty)}{\mu_{bf}} = \left[1 - \frac{\varphi}{0.605}\right]^{-[2.5]\,0.605} = \left[1 - \frac{\varphi}{0.605}\right]^{-1.5125} \tag{15}$$

As it is seen in Table 3, most of the Classical Models (other than Andrade Model [28]) have a lot in common, as can be observed from their polynomial form. This is mostly because of their origin, which is regarded as Einstein Model [24]. Therefore, it may not be wrong to expect them to give similar results. In Table 4, the relative viscosity predictions of Einstein Model [24], Brinkman Model [29], Krieger-Dougherty Model [30] for low and high shear conditions, and Batchelor Model [27] are provided for varying particle volumetric fraction.

Table 4. Relative viscosity predictions of some commonly used Classical Models for varying particle volumetric fraction

φ	Einstein Model (Equation (5))	Brinkman Model (Equation (7))	Krieger-Dougherty Model (Equation (8))		Batchelor Model (Equation (12))
			Low shear condition (Equation (14))	High shear condition (Equation (15))	
0.000	1.000	1.000	1.000	1.000	1.000
0.010	1.025	1.025	1.026	1.030	1.026
0.020	1.050	1.052	1.052	1.052	1.052
0.030	1.075	1.079	1.080	1.080	1.081
0.040	1.100	1.107	1.110	1.109	1.110
0.050	1.125	1.137	1.141	1.139	1.141
0.060	1.150	1.167	1.173	1.171	1.172
0.070	1.175	1.199	1.207	1.204	1.205
0.080	1.200	1.232	1.244	1.239	1.240
0.090	1.225	1.266	1.282	1.276	1.275
0.100	1.250	1.301	1.322	1.314	1.312

As it is seen in Table 4, the predictions of the Classical Models are quite close to each other. Because, as aforementioned, they have similar equation forms, as most of the models or correlations proposed after Einstein Model [24] have the aim to extend it to different conditions. The modifications are classified in Wang and Mujumdar's review paper [36] as follows.

1. Extension of the Einstein Model to higher particle volume concentrations by including particle-particle interactions as: $\mu_r = (1 + c_1\varphi + c_2\varphi^2 + c_3\varphi^3 + \cdots)$.

2. Taking into account the fact that the effective viscosity of a mixture becomes infinite at the maximum particle volume concentration φ_{max} and including the effect of non-spherical particle concentrations.

3. The equation obtained through item 2 usually has the term $[1-(\varphi/\varphi_{max})]^{\alpha}$ in the denominator, which can be expressed in a form similar to the Einstein Model [36].

In literature, the validity of some of the Classical Models was evaluated by comparing the estimations of Classical Models and the experimental data. In addition, some theoretical and empirical correlations were proposed, and they were also compared with the Classical Models. Conclusions of literature about the validity of the Classical Models are given in literature survey presented in the next Section.

2.2.2. Survey on the Experimental Nanofluid Viscosity Literature

This Section provides a literature survey on the experimental nanofluid viscosity field. Critical evaluation of the previous work is considered to be important, since there have been a lot of inconsistencies in literature. In order to address this issue, the studies that were selected manually from the scientific databases were outlined in detail.

In Table 5, the experimental parameters of the studies outlined in the literature survey are summarized. The summary based on the experimental parameters is essential, since differences in experiment parameters may lead to significantly different experiment results.

After the parameter based summary of literature given in Table 5, a review of the literature including the conclusions of the outlined studies is provided in this Section. In the review; the shear rate, nanoparticle volumetric fraction, temperature and nanoparticle diameter are denoted as γ, φ, T, and d_p, respectively. In the review of the literature provided in this Section, the correlations (see Table 6 in Section 2.2.3) proposed in the studies are referred with their equation numbers.

Table 5. Parameter based summary of literature

Reference	Nanofluid Type		T (^{o}C)	Particle Size **	φ ***
	Nanoparticle	Base Fluid*			
Pak and Cho, 1998 [37]	Al_2O_3; TiO_2	(Distilled H_2O) + pH adjuster (HCl or NaOH)	~15–75 (Al_2O_3); ~20–65 (TiO_2)	d_p=13 nm (Al_2O_3); d_p= 27 nm (TiO_2)	0.01–0.10
Wang et al., 1999 [38]	Al_2O_3	Distilled H_2O; EG	–	d_p=28 nm	0.01–0.0625 (Al_2O_3–H_2O); 0.00125–0.0035(Al_2O_3–EG)
Tseng and Lin, 2003 [39]	TiO_2	DDW	25	d_p=7–20 nm	0.05–0.12
Prasher et al., 2006 [40]	Al_2O_3	PG	30, 40, 50, 60	d_p=27, 40, and 50 nm	0.005, 0.02, 0.03
Namburu et al., 2007-a [41]	CuO	EG&H_2O (60:40)	-35–50	d_p=29 nm	0.01–0.0612
Namburu et al., 2007-b [42]	SiO_2	EG&H_2O (60:40)	-35–50	d_p=20, 50, 100 nm	0.02–0.10
Chen et al., 2007 [43]	TiO_2	Pure EG	20–60	d_p=25 nm, d_a=120–150 nm	0.01–0.018
He et al., 2007 [44]	TiO_2	(Distilled H_2O) + pH adjuster	22	d_p=20 nm; d_a =95, 145, 210 nm	0.0024, 0.006, 0.0118
Chevalier et al., 2007 [45]	SiO_2	EtOH	Ambient temperature	d_p=35±3, d_a=97nm; d_p=94±5, d_a=195 nm; d_p=190±8 nm, d_a=352 nm	0.011–0.07
Nguyen et al., 2007 [46]	Al_2O_3; CuO	(H_2O) + chemical dispersants (not specified)	22–75	d_p=36, 47 nm (Al_2O_3), d_p=29 nm (CuO)	0.01–0.12
Murshed et al., 2008 [47]	Al_2O_3; TiO_2	(DIW; EG; EO) + surfactant (CTAB)	–	d_p=80nm (Al), d_p=80 nm (Al_2O_3), d_p=15 nm (TiO_2)	0.01–0.05

Table 5 (cont'd)

Reference	Nanofluid Type		T (^{o}C)	Particle Size **	φ ***
	Nanoparticle	**Base Fluid***			
Chen et al., 2008 [48]	TNT	(Distilled H_2O) + pH adjuster (NaOH)	25 (φ= 0.0012, 0.0024); 25-50 (φ= 0.006)	d_p=10nm, l =100nm, d_a =260 nm	0.0012, 0.0024, 0.006
Tavman et al., 2008 [49]	SiO_2; Al_2O_3	DIW	20–50	d_p=12nm (SiO_2); d_p=30nm (Al_2O_3);	0.0045, 0.0185, and 0.04 (SiO_2); 0.005 and 0.015 (Al_2O_3)
Garg et al., 2008 [50]	Cu	EG	25	d_p=200 nm	0.004–0.02
Lee et al., 2008 [51]	Al_2O_3	DIW	21–39	d_p=30±5 nm	0.0001–0.003
Xie et al., 2008 [52]	Al_2O_3	EG; Distilled H_2O	–	–	0.01–0.05
Anoop et al., 2009 [53]	Al_2O_3; CuO	(H_2O; EG) + pH adjuster	20–50	d_p<50 nm, d_a=100 nm; d_a =95 nm; d_a =152 nm	0.005–0.06
Chen et al., 2009 [54]	TNT	EG	20–60	d_p=10 nm, l =100 nm, d_a =260 nm	0.01–0.018
Turgut et al., 2009 [55]	TiO_2	DIW	13–55	d_p=21 nm	0.002–0.03
Duangthongsuk and Wongwises, 2009 [56]	TiO_2	H_2O	15–35	d_p=21 nm	0.002–0.02
Phuoc and Massoudi, 2009 [33]	Fe_2O_3	(DIW)+ dispersant (PVP or (PEO))	25	d_p=20–40 nm	0.01–0.04
Garg et al., 2009 [57]	MWCNT	(DIW) + GA	15–30	d_p=10–20 nm , l =0.5–40 μm	0.01 ***

Table 5 (cont'd)

Reference	Nanofluid Type		T (^oC)	Particle Size **	φ ***
	Nanoparticle	**Base Fluid***			
Timofeeva et al., 2009 [58]	Al_2O_3	(Laboratory grade EG& DIW (50:50)) + dispersant (monovalent acids: nitric, acetic or formic)	15–85	9 nm (platelet); 60x10 nm (blade); 80x10 nm (cylinder); 40 nm (brick)	0.01–0.084
Zhao et al., 2009 [59]	SiO_2	DIW	25	d_p=7, 12, 16, 20, 40 nm	0.0001–0.02
Pastoriza-Gallego et al., 2009 [60]	Al_2O_3	Milli-Q-Grade H_2O	15–60	d_p=40–50 nm, d_a=43±23 nm (S1); d_p<50 nm, d_a=32±23 nm (S2); d_p<20 nm, d_a=8±3 nm (S3)	0.0013–0.029
Naik et al., 2010 [61]	CuO	PG&H_2O (60:40)	-15–60	d_p< 50 nm	0.00025–0.012
Godson et al., 2010 [62]	Ag	DIW	50–90	d_p=60 nm	0.003–0.009
Tavman and Turgut, 2010 [63]	SiO_2, TiO_2, Al_2O_3	DIW		d_p=12 nm (SiO_2); d_p=21 nm (TiO_2); d_p=30 nm (Al_2O_3)	0.0045, 0.0185 (SiO_2); 0.002, 0.01, 0.02 (TiO_2); 0.005, 0.015 (Al_2O_3)
Kole and Dey, 2010 [64]	Al_2O_3	PG&H_2O (50:50))	10–50	d_p< 50 nm	0.001–0.015
Chandrasekar et al., 2010 [65]	Al_2O_3	Distilled H_2O	Room temperature	d_p= 43 nm	0.01–0.05
Xie et al., 2010 [66]	MgO	EG	10–60	–	0.005–0.05
Lee et al., 2011 [67]	SiC	DIW	~ 28– ~ 72	d_p< 100 nm	0.00001–0.03
Suresh et al., 2011 [68]	Al_2O_3–Cu (hybrid)	(DIW) + dispersant (SLS)	32	d_p= 17 nm	0.001–0.02
Kole and Dey, 2011 [69]	CuO (spherical)	(Gear oil) + surfactant ($C_{18}H_{34}O_2$)	10–80	d_p= 40 nm; d_a~ 7d_p	0.005–0.025

Table 5 (cont'd)

Reference	Nanofluid Type		T (^{o}C)	Particle Size **	φ ***
	Nanoparticle	Base Fluid*			
Pastoriza-Gallego et al., 2011 [70]	CuO	Mili-Q-Grade H_2O	10–50	d_p= 33±13 nm (S1); d_p= 11±3 nm (S2)	0.0016–0.017
Kim et al., 2012 [71]	Al_2O_3 (spherical and fibrous)	EG	25–80	d_p= 80 nm (spherical)	0.055
Aladağ et al., 2012 [72]	Al_2O_3; MWCNT	(H_2O) + surfactant (not specified)	2–10	d_p= 30 nm (Al_2O_3); d_p= 9 μm (MWCNT), l= 200 μm	0.01 ***
Utomo et al., 2012 [73]	Al_2O_3; TiO_2	H_2O	20±0.1	d_p= 50–60 nm (Al_2O_3), d_a=200 nm; d_p= 20–30 nm (TiO_2), d_a= 140 nm	~0.005–0.06 (TiO_2); ~0.005–0.10 (Al_2O_3)
Suganthi and Rajan, 2012 [74]	ZnO	(H_2O) + stabilizer (SHMP)	10–55	d_p= 35–40 nm,	0.0025–0.015
Nabeel Rashin and Hemalatha, 2013 [75]	CuO	Coconut oil	35–55	d_p= 20 nm	0.005–0.025***
Syam Sundar et al., 2013 [76]	Fe_3O_4	Distilled H_2O	20–60	d_p= 13 nm	0.002–0.02

* **Abbreviations and Chemical formulae.** HCl: hydrochloric acid, EtOH: Ethanol; DDW: Double distilled H_2O; CTAB: cetyl trimethyl ammonium bromide; TNT: Titanate nanotubes; NaOH: sodium hydroxide; DIW: Deionized H_2O; PVP: polyvinylpyrrolidone; PEO: poly (ethylene oxide); MWCNT: multi wall carbon nanotube; GA: Gum Arabic; SLS: sodium lauryl sulphate; $C_{18}H_{34}O_2$: oleic acid; SHMP: sodium hexa-metaphosphate.

** The symbols d_p, d_a and l denote the nanoparticle diameter, aggregate diameter (the diameter of the nanoparticle cluster) and nanotube length.

*** The sign indicates that the nanoparticle fraction is given by weight. For all the other cases, the nanoparticle fraction is given by volume.

Pak and Cho [37] investigated the viscosities of Al_2O_3–H_2O and TiO_2–H_2O nanofluids for varying $\dot{\gamma}$, φ, and T. The Al_2O_3–H_2O nanofluids at φ= 0.03, and TiO_2–H_2O nanofluids at φ= 0.10 started to behave as shear-thinning fluids. The viscosities of Al_2O_3–H_2O and TiO_2–H_2O nanofluids increased with increasing φ (the increase for Al_2O_3–H_2O nanofluids were higher than that of TiO_2–H_2O nanofluids) and decreased asymptotically with increasing T. The experimental results were significantly higher than the predictions of Batchelor Model [27].

Wang et al. [38] investigated the viscosity of Al_2O_3–H_2O nanofluids produced by mechanical blending (method 1), coating particles with polymers (method 2), and filtration (method 3), and Al_2O_3–EG nanofluids for varying φ. The nanofluids produced by methods 2 and 3 had lower viscosity, indicating that the particles were better dispersed. The H_2O and EG based nanofluids had a similar viscosity increase with increasing φ.

Tseng and Lin [39] investigated the viscosity of TiO_2–H_2O nanofluids for varying $\dot{\gamma}$ and φ. The relative viscosity increased exponentially with φ (see Equation (16)), and the increase became more pronouncedly as $\varphi > \sim 0.1$. This exponential relationship was attributed to the particle interactions (more specifically, the attractive interparticle potential), which became more pronounced as φ was increased. The nanofluids generally exhibited pseudoplastic flow behavior (indicating an existence of particle aggregations), and they became apparently thixotropic as $\varphi > 0.1$.

Prasher et al. [40] investigated the viscosity of Al_2O_3–EG nanofluids for varying $\dot{\gamma}$, φ, d_p, and T. The nanofluids exhibited Newtonian behavior. The relative viscosity was largely independent of d_p, which was regarded as a sign of Newtonian behavior. The nanofluid viscosity increased with increasing φ (see Equation (19)) and the relative viscosity did not varied significantly with T. In the study, the applicability of nanofluids for laminar and turbulent flow was discussed.

Namburu et al. investigated the viscosity of CuO–EG&H_2O (60:40) nanofluids for varying $\dot{\gamma}$, T, and φ [41] and the viscosity of SiO_2–EG&H_2O (60:40) nanofluids for varying $\dot{\gamma}$, φ, d_p, and T [42]. The most concentrated CuO–EG&H_2O nanofluids exhibited Newtonian behavior, which was attributed to the Newtonian nature of the base fluid EG&H_2O, such that it dominated the rheological property of the nanofluid. The d_p= 50 nm SiO_2–EG&H_2O nanofluid exhibited Newtonian behavior for $T > -10^oC$, whereas it exhibited non-Newtonian behavior for $T < -10^oC$. The viscosity of both CuO–EG&H_2O and SiO_2–EG&H_2O nanofluids decreased exponentially with increasing T (see Equation (20)) and increased with increasing φ. The authors provided the correlations of the coefficients A and B dependent on nanoparticle weight fraction for CuO–EG&H_2O and SiO_2–EG&H_2O nanofluids, which are given in Table 6. The relative viscosity of CuO–EG&H_2O decreased with increasing T and the rate of this decrement was higher for higher φ; whereas for lower φ, the change in relative viscosity over T was found to be minimal. For φ= 0.08, the SiO_2–EG&H_2O nanofluids with the highest d_p showed the lowest viscosity. The relative viscosity of SiO_2–EG&H_2O nanofluids modestly decreased with increasing T.

Chen et al. [43] investigated the viscosity of TiO_2–EG nanofluids for varying $\dot{\gamma}$, φ, and T. The nanofluids exhibited Newtonian behavior. The viscosity of nanofluids increased with increasing φ in a nonlinear manner, and the experimental results were significantly higher than the predictions of Einstein Model [24]. The nanofluid viscosity decreased exponentially with increasing T (see Equation (21)). The authors provided the values of the coefficients A, B, and C dependent on nanoparticle weight fraction, which are provided in Appendix A, Table 30. The relative viscosity increased with increasing φ (see Equation (22)) but it was independent of T.

He et al. [44] investigated the viscosity of TiO_2–H_2O nanofluids for varying $\dot{\gamma}$, φ, and d_p. The TiO_2–H_2O nanofluids exhibited shear-thinning behavior. The viscosity of nanofluids increased with φ in a nonlinear manner, and increased with d_p. The non-linearity of the viscosity dependence on φ was more considerable than that on d_p. The experimental results were much higher than the predictions of Einstein Model [24], which was considered as an indication of nanoparticle interactions.

Chevalier et al. [45] investigated the viscosity of SiO_2–EtOH nanofluids for varying $\dot{\gamma}$, φ, and d_p. The nanofluids exhibited Newtonian behavior. The viscosity of nanofluids increased with increasing φ and decreased with increasing d_p. The experimental results were significantly higher than the predictions of Einstein Model [24] and consistent with Krieger-Dougherty Model [30]. The linear regression only holds for d_p= 190 nm diameter nanofluids (see Equation (25)). The strong enhancement of the relative

viscosity with increasing φ was attributed to nanoparticle aggregation. In addition, the causes of nanoparticle aggregation were evaluated in terms of the Peclet number.

Nguyen et al. [46] investigated the viscosity of Al_2O_3–H_2O and CuO–H_2O nanofluids for varying φ, d_p, and T. The viscosity of nanofluids increased significantly with increasing φ (see Equation (26), Equation (27) and Equation (28)), decreased with increasing T (see Equation (29) and Equation (30)) and decreased with increasing d_p. The viscosity of CuO–H_2O nanofluids was found to be similar to Al_2O_3–H_2O nanofluids for $\varphi< 0.04$; whereas for higher φ, the viscosity increase was greater than that for Al_2O_3–H_2O nanofluids. The experimental results were significantly higher than the predictions of Einstein [24], Brinkman [29], Lundgren [34], Batchelor [27] and Graham [35] Models, except at very low φ. In addition, a critical T was observed beyond which irreversible damage seemed to happen to the nanofluid properties, and hysteresis behavior was observed. The authors attributed the differences between their study and the literature to various factors, such as nanofluid production methods.

Murshed et al. [47] investigated the viscosity of Al_2O_3–H_2O and TiO_2–H_2O nanofluids for varying φ. The viscosity of nanofluids increased with increasing φ. The authors attributed the differences of the findings of this study and literature to the differences in the size of the particle clusters, the dispersion techniques and the use of surfactant in this study. In addition, the predictions of Krieger-Dougherty Model [30] and Nielsen Model [32] were found to be lower than the experimental results.

Chen et al. [48] investigated the viscosity of TNT–EG nanofluids for varying $\dot{\gamma}$, φ, and T. The nanofluids exhibited shear-thinning behavior. The viscosity of nanofluids decreased with increasing T. The experimental results for $\varphi< 0.0012$ were in an agreement with the Einstein Model [24] and Branner and Condiff Equation (which was given as $\mu_r/\mu_l = 1 + [\mu]\varphi + O(\varphi^2)$ in the article), whereas for $\varphi= 0.0024$ and $\varphi= 0.0060$, the predictions of the aforementioned models were lower than the experimental results. In addition, high shear viscosity of TNT nanoparticle nanofluids was considerably higher than that of spherical TiO_2 nanoparticle nanofluids, indicating the effect of nanoparticle shape on the rheological behavior.

Tavman et al. [49] investigated the viscosity of SiO_2–H_2O and Al_2O_3–H_2O nanofluids for varying φ and T. The decrease in viscosities of the SiO_2–H_2O and Al_2O_3–H_2O nanofluids with increasing T was exponential (similar to that of water [77]) for low φ. Viscosity of nanofluids increased dramatically with increasing φ, which was attributed to not using any surfactant or chemical additives. In addition, the experimental results were much higher than the predictions of Einstein Model [24].

Garg et al. [50] investigated the viscosity of CuO–EG nanofluids for varying $\dot{\gamma}$ and φ. The nanofluids exhibited Newtonian behavior. The viscosity of nanofluids increased with increasing φ in a linear manner (see Equation (31)), but were higher than the predictions of Einstein Model [24].

Lee et al. [51] investigated the viscosity of Al_2O_3–H_2O nanofluids for varying φ and T. The viscosity of nanofluids decreased significantly with increasing T, and increased slightly with increasing φ. The experimental results were higher than the predictions of Einstein Model [24] even for very low φ (which was considered as an indication of particle-particle interactions) and the relation between the relative viscosity and φ was nonlinear (while the Einstein Model [24] predicts a linear relationship).

Xie et al. [52] investigated the viscosity of Al_2O_3–H_2O and Al_2O_3–EG nanofluids for varying $\dot{\gamma}$, φ, nanoparticle morphologies (different specific surface areas, i.e. 122 m^2g^{-1}, and 124 m^2g^{-1}), nanoparticle agglomeration and pH values. The nanofluids exhibited Newtonian behavior for $\varphi< 0.03$, whereas they exhibited shear-thinning behavior for $\varphi> 0.05$. The viscosities of Al_2O_3–H_2O nanofluids were higher than Al_2O_3–EG nanofluids. Viscosities of Al_2O_3 (124 m^2g^{-1})–EG nanofluids were found to be smaller than the viscosities of Al_2O_3 (122 m^2g^{-1})–EG nanofluids, indicating the effect of nanoparticle status on the rheological behavior of nanofluids. The effect of pH on the viscosity of nanofluids was investigated in terms of the isoelectric point and dispersion characteristics. The viscosities of Al_2O_3 (122 m^2g^{-1})–EG, Al_2O_3 (124 m^2g^{-1})–EG and Al_2O_3 (122 m^2g^{-1})–H_2O nanofluids were found to be much higher than the predictions of Batchelor Model [27], which was attributed to the electrical viscosity effect.

Anoop et al. [53] investigated the viscosities of Al_2O_3–H_2O, Al_2O_3–EG and CuO–EG nanofluids for varying $\dot{\gamma}$, φ, and T. The H_2O based and EG based nanofluids exhibited Newtonian behavior. The relative viscosity increased with increasing φ, and decreased with increasing T. The effect of T on viscosity was more severe for EG-based nanofluids than for H_2O based nanofluids. The viscosities of

nanofluids were found to be higher than the theoretical predictions. The differences between H_2O and EG based nanofluids were attributed to the fact that, the H_2O based nanofluid was electrostatically stabilized (which forms an electrical double layer that introduces additional increase in viscosity, see Equation (32)) whereas the EG based nanofluids (see Equation (33)) were not. It was also noted that the viscosity might be higher for suspensions containing smaller particles than for suspensions with larger particles. The authors stated that, since pH values, particle sizes and methods of nanofluid preparation vary in literature and some are not reported precisely, exact predictions were not possible. The equal importance of the electroviscous effects as the particle agglomeration on the viscosity of nanofluids was emphasized.

Chen et al. [54] investigated the viscosity of TNT–EG nanofluids for varying $\dot{\gamma}$, φ, nanoparticle shape, and T. The nanofluids exhibited strong shear thinning behavior especially at $\varphi > 0.02$ (by weight), which was different than the rheological behavior of spherical TiO_2–EG nanofluids [26]. The viscosity of TNT–EG nanofluids exponentially decreased with increasing T (see Equation (21)), and increased with increasing φ. The Einstein Model [24] and the Brenner and Condiff Equation (which was given as $\mu_r/\mu_l = 1 + [\mu]\varphi + O(\varphi^2)$ in the article) greatly under predicted the experimental results. The high-shear viscosity of TNT–EG nanofluids was found to be much higher than that of the spherical TiO_2–EG nanofluids, which indicated a strong particle shape effect on the viscosity of nanofluids. In addition, based on the modified Krieger-Dougherty Model [30], it was stated that the effective volume fraction of aggregates (φ_a) are much higher than the φ, and this fact was considered as the reason for the experimentally observed high-shear viscosity even for very dilute nanofluids. Therefore, the authors suggested that, the demarcations defining the dilute and semi-concentrated dispersions should be changed by using the effective volume fraction.

Turgut et al. [55] investigated the viscosity of TiO_2–H_2O nanofluids for varying φ and T. The decrease in the viscosities of the TiO_2–H_2O nanofluids with increasing T was found to be similar to that of water, which can be considered as exponential [77] for low φ. The viscosity of nanofluids increased dramatically with increasing φ, and this was considered as a result of not using any surfactant or chemical additives. The experimental results were much higher than the predictions of Classical Models, which were considered as an indication of nanoparticle interactions.

Duangthongsuk and Wongwises [56] investigated the viscosity of TiO_2–H_2O nanofluids for varying φ and T. The viscosity of nanofluids increased significantly with decreasing T, and increased with increasing φ (see Equation (34)). The authors provided the values of the coefficients a, b and c dependent on temperature, which are provided in Appendix A, Table 31. In addition, the experimental results were much higher than the predictions of Einstein Model [24], Brinkman Model [29] and Batchelor Model [27], whereas they were closer to the predictions of the correlation proposed by Wang et al.

Phuoc and Masoudi [33] investigated the viscosity of Fe_2O_3–H_2O nanofluids for varying $\dot{\gamma}$ and φ. The nanofluids exhibited Newtonian behavior when $\varphi < 0.02$ whereas they transformed to non-Newtonian and shear-thinning behavior when $\varphi > 0.02$. The viscosity of nanofluids increased exponentially with increasing φ.

Garg et al. [57] investigated the viscosity of MWCNT–H_2O nanofluids for varying $\dot{\gamma}$, ultrasonication times, and T. MWCNT–H_2O nanofluids exhibited shear-thinning behavior. The viscosity of the nanofluids increased with sonication time until a maximum value was reached and decreased thereafter, and decreased with increasing T. The initial increase was associated with declustering of CNT bundles, which resulted in a better dispersion. The latter decrease in viscosity was explained by the increased breakage rate of CNTs, resulting in shorter nanotubes, and hence, inferior networking of CNTs in dispersion.

Timofeeva et al. [58] investigated the viscosity of Al_2O_3–EG&H_2O (50:50) nanofluids for varying φ, nanoparticle shapes, and T. The viscosity of nanofluids decreased with increasing T, and increased with increasing φ (see Equation (35)). The experimental results were higher than the predictions of the Einstein-Batchelor Equation (which is same as the Batchelor Model [27] in this text), which was considered as an indication of strong particle-particle interactions. Regarding nanoparticle shapes, the viscosity increase with increasing φ in Al_2O_3–EG&H_2O nanofluids at T= 25°C was described low to high sequence as: blades< bricks<< cylinders< platelets. The values of the coefficients A_1 and A_2 in Equation (35) at 25°C for different nanoparticle shapes are provided in Appendix A, Table 32. Platelet and blade shaped nanoparticle nanofluids exhibited Newtonian behavior, whereas the brick and

cylinder shaped nanoparticle nanofluids exhibited shear-thinning behavior. In addition, the relationship between the pH and the nanofluid viscosity was examined and as a result, it was stated that nanofluid viscosity can be modified with almost no effect on nanofluid thermal conductivity.

Zhao et al. [59] investigated the viscosity of SiO_2–H_2O nanofluids for varying φ, d_p, and pH values. The viscosity of nanofluids increased with increasing φ, and the relative viscosity increased rapidly as d_p was decreased. The viscosity of nanofluids was strongly dependent on d_p, especially for d_p< 20nm. For smaller d_p, larger nanofluid viscosity values were obtained. For small d_p, the relative viscosity was a strong function of φ (the relative viscosity increased with increasing φ), whereas with an increase of d_p, the relative viscosity was inversely correlated with φ. The viscosity of nanofluids fluctuated with pH value. The fluctuation was more pronounced for d_p= 7 nm than d_p= 12 and d_p= 16 nm, whereas for d_p> 20 nm, viscosities remained unchanged with varying pH. In addition, the aggregate diameter to nanoparticle diameter ratios (d_a/d_p) varied slightly with the pH, which was an indication of the effects of the fractal dimension change of aggregates and the electrical double layer of particles on the viscosity fluctuation with pH.

Pastoriza-Gallego et al. [60] investigated the viscosity of Al_2O_3–H_2O nanofluids for varying φ, T, and dispersion techniques. The viscosity of nanofluids increased with increasing φ, and decreased with increasing T. The viscosity of the sample with smaller d_p was larger than that of the sample with larger d_p. The experimental results were higher than the predictions of Einstein Model [24] whereas they were closer to the predictions of Krieger-Dougherty Model [30] with variable and constant d_a/d_p values.

Naik et al. [61] investigated the viscosity of CuO–PG&H_2O nanofluids for varying $\dot{\gamma}$, φ, and T. The nanofluids exhibited Newtonian behavior. The viscosity of nanofluids decreased exponentially with increasing T and increased with increasing φ. The Einstein Model [24], Brinkman Model [29] and Batchelor Model [27] were found to be suitable to predict the viscosity of examined nanofluids.

Godson et al. [62] investigated the viscosity of Ag–H_2O nanofluids for varying φ and T. The viscosity of the nanofluid increased with increasing φ (see Equation (36)), and decreased with increasing T. The experimental results were much higher than the predictions of Einstein Model [24], Brinkman Model [29], and the correlation proposed by Wang et al. The results showed that the viscosity depends on nanoparticle material, size, and shape, φ, random motion of the nanoparticles, and the operating T.

Tavman and Turgut [63] investigated the viscosity of SiO_2–H_2O, TiO_2–H_2O and Al_3O_3–H_2O nanofluids for varying φ and T. The viscosity of nanofluids increased with increasing φ. The decrease in the viscosities of the TiO_2–H_2O nanofluids with increasing T was found to be similar to that of water, which can be considered as exponential [77] for low φ. The experimental results of SiO_2–H_2O nanofluids were significantly higher than the predictions of Einstein Model [24], Krieger-Dougherty Model [30] and Nielsen Model [32], whereas the experimental results of TiO_2–H_2O nanofluids were also higher than the predictions of Einstein Model [24].

Kole and Dey [64] investigated the viscosity of Al_2O_3–PG&H_2O (50:50) nanofluids for varying $\dot{\gamma}$, φ, and T. The base fluid, engine coolant (PG&H_2O (50:50)) exhibited Newtonian behavior, and with the addition of φ= 0.001 Al_2O_3 nanoparticles, the behavior of the nanofluid transformed to non-Newtonian. The viscosity of nanofluids increased with increasing φ, and decreased exponentially with increasing T. The predictions of Einstein Model [24], Brinkman Model [29], Batchelor Model [27], Krieger-Dougherty Model [30], Kitano Model [78] and the modified version Krieger-Dougherty Model proposed by Chen et al. [26] were lower than the experimental results. The failure of Krieger–Dougherty Model [30], and its modified version proposed by Chen et al. [26] were considered as an indication of the absence of the aggregation of Al_2O_3 nanoparticles in the engine coolant based nanofluid. The T dependent viscosity of nanofluids were in a strong agreement with the predictions of the correlation proposed by Namburu et al. [41], and the authors provided the values of the coefficients A and B dependent on nanoparticle volumetric fraction, which are provided in Appendix A, Table 33. The correlation proposed by Masoumi et al. [79], which fairly explained the nanoparticle volumetric fraction and viscosity relationship, did not give acceptable agreement to the T dependence.

Chandrasekar et al. [65] investigated the viscosity of Al_2O_3–H_2O nanofluids for varying $\dot{\gamma}$ and φ. The nanofluids exhibited Newtonian behavior. The viscosity of nanofluids increased with increasing φ (see Equation (37)). The relative viscosity increase was almost linear up to φ= 0.02 and agreed well with the Einstein Model [24], whereas for φ> 0.02, the increase in relative viscosity showed a nonlinear

relationship with φ. This behavior was attributed to the hydrodynamic interactions between particles at higher φ.

Xie et al. [66] investigated the viscosity of MgO–EG nanofluids for varying $\dot{\gamma}$, φ, and T. The MgO–EG nanofluids exhibited Newtonian behavior. The viscosity of nanofluids increased with increasing φ in a non-linear manner, and decreased rapidly with increasing T. The non-linear relationship between the relative viscosity and φ was attributed to nanoparticle aggregation. The experimental results were higher than the predictions of Einstein Model [24], Brinkman Model [29] and Batchelor Model [27].

Lee et al. [67] investigated the viscosity of SiC–H_2O nanofluids for varying φ and T. The viscosity of nanofluids increased with increasing φ (see Equation (38)), and decreased with increasing T. The experimental results were higher than the predictions of Brinkman Model [29] and Batchelor Model [27] even at very low φ. The overall effectiveness of nanofluids as heat transfer fluids were evaluated in terms of the equations suggested by Prasher et al. [40]. The nanofluids investigated in this study were found to be not beneficial to convection heat transfer applications.

Suresh et al. [68] investigated the viscosity of Al_2O_3&Cu (hybrid, 90:10 by weight)–H_2O nanofluids for varying $\dot{\gamma}$ and φ. The nanofluids exhibited Newtonian behavior. The viscosity of nanofluids increased with increasing φ. In addition, the difference between the viscosities of the Al_2O_3&Cu–H_2O hybrid nanofluids and Al_2O_3–H_2O nanofluid at lower nanoparticle volumetric fractions was small, while the viscosity of Al_2O_3&Cu–H_2O hybrid nanofluids was higher than the Al_2O_3–H_2O nanofluid at higher φ. The experimental results were higher than the predictions of Einstein Model [24], Brinkman Model [29] and Batchelor Model [27], and this difference was attributed to the nanoparticle aggregation. The roles of the nature of the nanoparticle surface, ionic strength of the base fluid, surfactants, pH values, inter-particle potentials such as repulsive (electric double layer force) and attractive (van der Waals force) forces were considered as significant on the viscosity of nanofluids, in addition to the φ and nanoparticle diameter. Finally, the viscosity of the hybrid nanofluid with the functionalized Al_2O_3 was higher than that corresponding to the nanofluid made of simple Al_2O_3 or CuO due to the increased effective density of hybrid nanoparticles.

Kole and Dey [69] investigated the viscosity of CuO–Gear oil nanofluids for varying $\dot{\gamma}$, φ, and T. The nanofluids showed non-Newtonian behavior. The viscosity of nanofluids increased with increasing φ, and decreased asymptotically with T (strongly following Equation (21), which belongs to Chen et al. [26, 43]), and the authors provided the values of the coefficients A, B, and C dependent on nanoparticle weight fraction, which are provided in Appendix A, Table 34. The predictions of Einstein Model [24], Brinkman Model [29], Batchelor Model [27], Nielsen Model [32], Frankel and Acrivos Model [31], Kitano Model [78], correlations proposed by Wang et al. and Choi et al. were lower than the experimental results, and this behavior was attributed to nanoparticle aggregation, since the experimental results were in a good agreement with the predictions of Krieger-Dougherty Model [30].

Pastoriza-Gallego et al. [70] investigated the viscosity of CuO–H_2O nanofluids for varying φ and T. It was found that the nanofluids produced by different methods (which also had different d_p) showed different viscosity trends. The viscosity increased with increasing φ, decreased with increasing d_p, and increasing T. The relative viscosity increase with φ did not follow a classical trend. The viscosity increase was examined considering the nanoparticle aggregation and particle size distribution (PSD) analysis. The unforeseen viscosity increase was attributed to the aggregation behavior of nanoparticles (as defined by the Krieger-Dougherty Model [30]), and both approaches (state of nanoparticle aggregation or the PSD alone) provided a qualitative correct description of the nanofluid viscosity in both cases, but as d_p decreased the deviations were larger. The authors stated that, the simplified viscosity theories might be insufficient to describe the complex behavior of these nanofluids, thus other effects (e.g. interparticle interactions, solid–fluid interactions, friction, particle anisotropy, etc.) should be introduced in the existing viscosity theories.

Kim et al. [71] investigated the viscosity of Al_2O_3–EG nanofluids for varying φ, nanoparticle shapes (fibrous and spherical), and T. The viscosity of nanofluids increased with increasing φ and decreased with increasing T. At T= 25°C, the relative viscosity of fibrous Al_2O_3–EG nanofluids was higher than that of spherical Al_2O_3–EG nanofluids. As T increased, the decrease in the relative viscosity was higher for fibrous Al_2O_3–EG nanofluids than that of spherical Al_2O_3–EG nanofluids, which was considered as an indication of severe aggregation occurred in fibrous Al_2O_3–EG nanofluids.

Aladag et al. [72] investigated the viscosity of Al_2O_3–H_2O and MWCNT–H_2O nanofluids for varying $\dot{\gamma}$ and T. The viscosity of nanofluids decreased with increasing T. The MWCNT–H_2O nanofluids exhibited shear-thinning behavior, whereas the Al_2O_3–H_2O nanofluids exhibited shear-thickening behavior. The difference in non-Newtonian behavior of Al_2O_3–H_2O and MWCNT–H_2O nanofluids was attributed, at least partially, to different particle shape and aspect ratio, agglomeration and disagglomeration kinetics due to the interaction between the surfactant and the nanoparticles. The predictions of Brinkman Model [29] were lower than the experimental MWCNT–H_2O results, and this finding was attributed to nanoparticle aggregation.

Utomo et al. [73] investigated the viscosity of Al_2O_3–H_2O and TiO_2–H_2O nanofluids for varying $\dot{\gamma}$ and φ. The viscosity of nanofluids increased with increasing φ, and at the same φ, the relative viscosity of TiO_2-H_2O nanofluid was higher than that of Al_2O_3–H_2O nanofluid. The viscosity of the nanofluids was considered to be dependent on many factors, (e.g. surface chemistry and size of the particle, shape of the primary particle, base fluid, pH, T and dispersion method), which in turn influence the morphology of suspension of nanoparticles/nanofluids by electro-viscous effect and the interaction between particles/aggregates due to attractive van der Waals force and repulsive electrostatic force. In addition, the experimental results were higher than the predictions of the Einstein–Batchelor Model (which is same as the Batchelor Model [27] in this text), whereas they were in a better agreement with the predictions of Krieger–Dougherty Model [30]. This was considered as a confirming fact that, the aggregation can increase the viscosity of nanofluids by increasing the effective volume fraction of nanoparticles.

Suganthi and Rajan [74] investigated the viscosity of ZnO–H_2O nanofluids for varying φ, T, and ultrasonication times. The viscosity of nanofluids increased with increasing φ (see Equation (39)), and decreased with increasing T in a similar manner to that of water, which can be considered as exponential (see Equation (40)). The zeta potential and hence the magnitude of inter-particle forces in a stable dispersion was considered as not effective on the trend of viscosity and T relationship. The predictions of Einstein Model [24] were found to be lower than the experimental results.

Nabeel Rashin and Hemalatha [75] investigated the viscosity of CuO–Coconut oil nanofluids for varying $\dot{\gamma}$, φ, and T. The CuO–Coconut oil nanofluids exhibited shear-thinning behavior. The viscosity of nanofluids increased with increasing φ (see Equation (41)) and decreased exponentially with increasing T (see Equation (42)). The authors provided the values of the coefficients a and b in Equation (41) dependent on T in Appendix A, Table 35, and c in Equation (42) dependent on nanoparticle weight fraction in Appendix A, Table 36. The experimental results were not in exact agreement with the predictions of Einstein Model [24], Batchelor Model [27] and the correlation proposed by Wang et al., but they were either closer, or slightly higher.

Syam Sundar et al. [76] investigated the viscosity of Fe_3O_4–H_2O nanofluids for varying $\dot{\gamma}$, φ, and T. The Fe_3O_4-H_2O nanofluids exhibited Newtonian behavior. The viscosity of nanofluids increased with increasing φ (see Equation (43)), and decreased with increasing T. The experimental results were in an agreement with predictions of Einstein Model [24], Brinkman Model [29] and Batchelor Model [27] for low φ, whereas they failed to predict the values with the effect of T.

With the light of this literature survey, one can conclude that the inconsistencies in literature are abundant. The inconsistencies are mainly on the rheological properties of nanofluids (whether the nanofluid exhibit Newtonian or non-Newtonian behavior), the effect of the properties of nanofluids (φ, d_p, nanoparticle type and morphology, base fluid type, etc) and ambient parameters (temperature, pressure, etc.) on nanofluid viscosity, and the type of the correlations proposed (linear, exponential, and other types of non-linear relations).

2.2.3. Viscosity Estimation with Theoretical and Empirical Correlations: The New Approach

Considering the fact that the concept nanofluid was introduced by Choi and his co-workers in 1995, the equations proposed before 1995 were presented for conventional suspensions. Correlations for the thermophysical properties of nanofluids have been shared in literature after 1995. Classical Models proposed for conventional suspensions can be used to calculate the viscosity of nanofluids. From this point forth, Classical Models were employed to calculate the nanofluid viscosity, but in general, most of the Classical Models turned out to give rough results compared to the experimental results [27, 33, 39, 40, 43-56, 58, 60, 62-69, 72-74]. A few studies [61, 75, 76] claimed that the Classical Models were suitable in estimating the nanofluid viscosity dependent on nanoparticle volumetric fraction. Therefore, the need for more accurate results leads researchers to propose empirical correlations. The empirical correlations in the studies summarized in Table 5 are given in Table 6 below in their chronological order.

Table 6. Theoretical and Empirical Correlations of Studies Outlined in Table 5

Reference	Correlation		Notes
Tseng and Lin, 2003 [39]	$\mu_r = 13.47\, e^{35.98\varphi}$	(16)	The exponential relationship of μ_r with φ was observed. Thus, the correlation gives considerably high relative viscosity values for high φ (provided in Table 7) compared to common literature.
Maïga et al., 2004 [80]	$\mu_r = \frac{\mu_{nf}}{\mu_{bf}} = 123\varphi^2 + 7.3\varphi + 1$	(17)	Equation (17) and Equation (18) were proposed for Al_2O_3–H_2O and Al_2O_3–EG nanofluids, respectively.
	$\mu_r = \frac{\mu_{nf}}{\mu_{bf}} = 306\varphi^2 - 0.19\varphi + 1$	(18)	
Prasher et al., 2006 [40]	$\mu_r = 1 + 10\varphi$	(19)	
Namburu et al., 2007-a [41], Namburu et al., 2007-b [42]	$\log(\mu_{nf}) = Ae^{-BT}$	(20)	The curve-fit values A and B in Equation (20) are provided in the Equations (20.1.a), (20.1.b) for CuO–EG&H_2O nanofluids [41], and the Equations (20.2.a) and (20.2.b) for SiO_2–EG&H_2O nanofluids [42].
	$A = 1.8375(\varphi)^2 - 29.643(\varphi) + 165.56$	(20.1.a)	
	$B = 4 \times 10^{-6}(\varphi)^2 - 0.001(\varphi) + 0.0186$	(20.1.b)	
	$A = 0.1193(\varphi)^3 - 1.9289(\varphi)^2 - 2.245(\varphi) + 167.17$	(20.2.a)	
	$B = -7 \times 10^{-6}(\varphi)^2 - 0.0004(\varphi) + 0.0198$	(20.2.b)	
Chen et al., 2007 [26, 43], Chen et al., 2008 [48], Chen et al., 2009 [54]	$\ln(\mu_{nf}) = A + B \times 1000/(T + C)$	(21)	In Equation (21), the empirical constants A, B and C were given for different φ (by weight) in Appendix A, Table 30. In Equation (23), D is the fractal index, $[\eta]$ is the intrinsic viscosity, φ_a is the effective volume fraction of aggregates, φ_m is the maximum packing fraction of aggregates, a_a is the radius of the aggregate, and a is the radius of the particle. In Equation (24), r is the radius of the particle.
	$\mu_r = 1 + 10.6\varphi + (10.6\varphi)^2$	(22)	
	$\mu_r = \left(1 - \frac{\varphi_a}{\varphi_m}\right)^{-[\eta]\varphi_m}$; $\varphi_a = \varphi\left(\frac{a_a}{a}\right)^{3-D}$	(23)	
	$[\eta] = \frac{0.312r}{(\ln 2r) - 1.5} + 2 - \frac{0.5}{(\ln 2r) - 1.5} - \frac{1.872}{r}$	(24)	

Table 6. Theoretical and Empirical Correlations of Studies Outlined in Table 5

Reference	Correlation	Notes
Chevalier et al., 2007 [45]	$\mu_r = 1 + 8.2\varphi$ (25)	The Equation was derived for d_p= 190 nm nanofluids.
Nguyen et al., 2007 [46]	$\mu_r = \frac{\mu_{nf}}{\mu_{bf}} = 0.904e^{0.148\varphi}$ (26) $\mu_r = 1 + 0.025\varphi + 0.015\varphi^2$ (27) $\mu_r = 1.475 - 0.391\varphi + 0.051\varphi^2 + 0.009\varphi^3$ (28) $\mu_{nf} = \mu_{bf}(1.1520 - 0.0007\,T)$ (29) $\mu_{nf} = \mu_{bf}(2.1275 - 0.0215\,T + 0.0002\,T^2)$ (30)	Equation (26) and Equation (27) were proposed for d_p=47 nm and d_p= 36nm Al_2O_3–H_2O nanofluids, respectively, whereas the Equation (28) was proposed for CuO–H_2O nanofluids. Equation (29) and Equation (30) were proposed for φ= 0.01 and φ= 0.04 Al_2O_3–H_2O, Al_2O_3–EG and CuO–EG nanofluids, respectively. In Equation (29) and Equation (30), the temperature units are ^oC.
Garg et al., 2008 [50]	$\mu_r = \frac{\mu_{nf}}{\mu_{bf}} = 1 + 11\varphi$ (31)	
Anoop et al., 2009 [53]	$\mu_r = 1 + 10\varphi$ (32) $\mu_r = 1 + 5\varphi$ (33)	The Equation (32) was proposed for electrostatically stabilized Al_2O_3–H_2O nanofluids, whereas the Equation (33) was proposed for EG based nanofluids which were not stabilized.
Duangthongsuk and Wongwises, 2009 [56]	$\frac{\mu_{nf}}{\mu_w} = a + b\varphi + c\varphi^2$ (34)	In Equation (34), the values of the empirical constants *a*,*b* and *c* are given in Appendix A, Table 31.
Timofeeva et al., 2009 [58]	$\mu_{nf} = \mu_{bf}(1 + A_1\varphi + A_2\varphi^2)$ (35)	In Equation (35), the values of the empirical constants A_1 and A_2 at 25^{o}C are given in Appendix A, Table 32.
Godson et al., 2010 [62]	$\frac{\mu_{nf}}{\mu_w} = 1.005 + 0.497\varphi - 0.1149\varphi^2$ (36)	

Table 6 (cont'd)

Reference	Correlation	Notes
Kole and Dey, 2010 [64]	The correlation proposed by Namburu et al [41, 42] (Equation (20)) was stated to give the best fit to the experimental data in [64].	The values of the empirical constants *A* and *B* in correlation proposed by Namburu et al. [41, 42] are provided in Appendix A, Table 33.
Chandrasekar et al., 2010 [65]	$\mu_r = 1 + b\left(1 - \frac{\varphi}{1-\varphi}\right)^n$ (37)	In Equation (37), b=5300 and n=2.8.
Lee et al., 2011 [67]	$\mu_r = 1 + 33\varphi$ (38)	
Kole and Dey, 2011 [69]	The correlation proposed by Chen et al. [26, 43, 54] (Equation (21)) was stated to give the best fit to the experimental data in [69].	The values of the empirical constants *A*, *B*, and *C* in correlation proposed by Chen et al. [26, 43] are provided in Appendix A, Table 34.
Suganthi and Rajan, 2013 [74]	$\mu_r = 1 + 11.97\varphi$ (39) $\mu_{nf} = A\, e^{-BT}$ (40)	In Equation (39), the value of *B* has substantially similar range between 0.465 and 0.174. For φ= 1.5% nanofluid, *A*= 5.254 (maximum), while for φ= 2.5% nanofluid, *A*= 4.676. Equation (40) is valid for 10-35°C and φ= 0-15% (R^2= 0.98 and standard deviation= 0.0087).
Nabeel Rashin and Hemalatha, 2013 [75]	$\mu_{nf} = \mu_{bf}(1 + a\varphi + b\varphi^2)$ (41) $\mu_{nf} = ce^{-0.03\,T}$ (42)	The values of the empirical constants *a* and *b* of Equation (41) and the values of the empirical constant *c* of Equation (42) are given in Appendix A, Table 35 and Table 36.
Syam Sundar et al., 2013 [76]	$\mu_{nf} = \mu_{bf}\left(1 + \frac{\varphi}{12.5}\right)^{6.356}$ (43)	Equation (43) is valid for 0< φ< 2% and 20°C< T <60°C.
Masoumi et al., 2009 [79]	$\mu_{nf} = \mu_{bf} + \frac{\rho_p V_B {d_p}^2}{72C\delta}$ (44)	The correction factor *C* in Equation (44) can be calculated by $C = {\mu_{bf}}^{-1}\left[\left(c_1 d_p + c_2\right)\varphi + \left(c_3 d_p + c_4\right)\right]$. The coefficients c_1, c_2, c_3 and c_4 are; -0.000001133, -0.000002771, 0.00000009 and -0.000000393.

As it is seen in Table 6, many correlations were proposed based on the experimental data or theoretical considerations. Since the validity of Classical Models appeared to be questionable for nanofluids, researchers started to propose new correlations, mostly based on the experimental data. Although the validity of the empirical correlations seems to be enhanced since they are based on experimental data, it is important to note that, the empirical correlations were obtained for a particular experimental data set. Therefore, their range of applicability is limited with the experimental conditions, and their extrapolation to the wider intervals of the experiment parameters may lead to erroneous results.

With the light of this theoretical outline, it can be concluded that, the Classical Models may be used to have an opinion and obtain preliminary nanofluid viscosity or relative viscosity values, rather than using them to get the actual values of nanofluid viscosity or relative viscosity for applications.

2.3. Benchmark Study on Nanofluid Viscosity and Relative Viscosity

In this Section, a benchmark study on nanofluid viscosity and relative viscosity is done by a parametric analysis on the relative viscosity and nanofluid viscosity models and correlations with respect to the nanoparticle fraction (mostly given as volumetric fraction, rarely given as weight fraction; information on this issue is provided when required.) and temperature. The parametric analysis involves some of the Classical Models given in Table 3 and some empirical correlations given in Table 6. This kind of a benchmark study is needed in order to point out to the inconsistencies in the nanofluid viscosity literature.

2.3.1. Nanofluid Viscosity Dependent on Nanoparticle Fraction

Viscosity of conventional suspensions depends on the solid content in the mixture. This behavior is consistent with nanofluids, but it does not follow a classical trend, mostly. The predictions of some Classical Models and empirical correlations proposed for different types of nanofluids for a wide interval of (nano) particle volumetric fraction are provided in Table 7.

Table 7. Relative viscosity predictions of some Classical Models (Einstein Model, Batchelor Model, and Krieger-Dougherty Model) and empirical correlations (proposed by Tseng and Lin, Maïga et al., and Suganthi and Rajan)

φ	Einstein Model (Equation (5))	Batchelor Model (Equation (12))	Krieger-Dougherty Model (Equation (14))	Tseng and Lin (Equation (16))	Maïga et al. (Equation (17))	Suganthi and Rajan (Equation (39))
0.000	1.000	1.000	1.000	13.470	1.000	1.000
0.020	1.050	1.053	1.052	27.662	1.195	1.239
0.040	1.100	1.110	1.110	56.807	1.489	1.479
0.060	1.150	1.173	1.173	116.660	1.881	1.718
0.080	1.200	1.242	1.244	239.575	2.371	1.958
0.100	1.250	1.315	1.322	491.993	2.960	2.120

As it is seen in Table 7, the relative viscosity of nanofluids increases with increasing nanoparticle fraction, but the predictions of Classical Models and empirical correlations differ significantly from each other. Especially, the correlation proposed by Tseng and Lin [39] predicts approximately 491 times viscosity increase for a nanoparticle volumetric fraction of φ= 0.10, which is considerably high compared to the common literature. This behavior was also mentioned in review paper of Mahbubul et al. [23] as an unrealistic increment of the viscosity with increasing nanoparticle volumetric fraction.

A closer look at Table 7 leads to further discussion. The empirical correlations, whose results were illustrated in Table 7, were proposed for different types of nanofluids, meaning the nanoparticle and base fluid material, nanoparticle diameter, and experiment conditions are different for these correlations. At this point, it can be concluded that, the effect of nanoparticle fraction is significant on nanofluid viscosity. However, when predicting the viscosity of nanofluids, some other parameters should certainly be taken into account, as well as the nanoparticle volumetric fraction. For this purpose, further comparisons are presented under Sections 2.3.2, 2.3.3, 2.3.4 and 2.3.5, for evaluating the effects of different nanoparticle shapes, nanoparticle materials, temperatures, and nanoparticle aggregation levels on nanofluid viscosity and relative viscosity.

2.3.2. Nanofluid Viscosity Dependent on Nanoparticle Shape

Nanoparticle shape is a very important parameter, and it is usually desired to be under control at the nanoparticle production stage [21]. There are a few studies in literature examining the effects of nanoparticle shape on nanofluid viscosity. Timofeeva et al. [58] and Kim et al. [71] discussed the effect of nanoparticle shape on nanofluid viscosity. Timofeeva et al. [58] proposed correlations for the relative viscosity of nanofluids containing different shaped Al_2O_3 nanoparticles. In Figure 5, the correlations proposed by Timofeeva et al. [58] and some other correlations proposed for Al_2O_3 nanoparticle nanofluids together with Einstein Model [24] are compared within their validity limits.

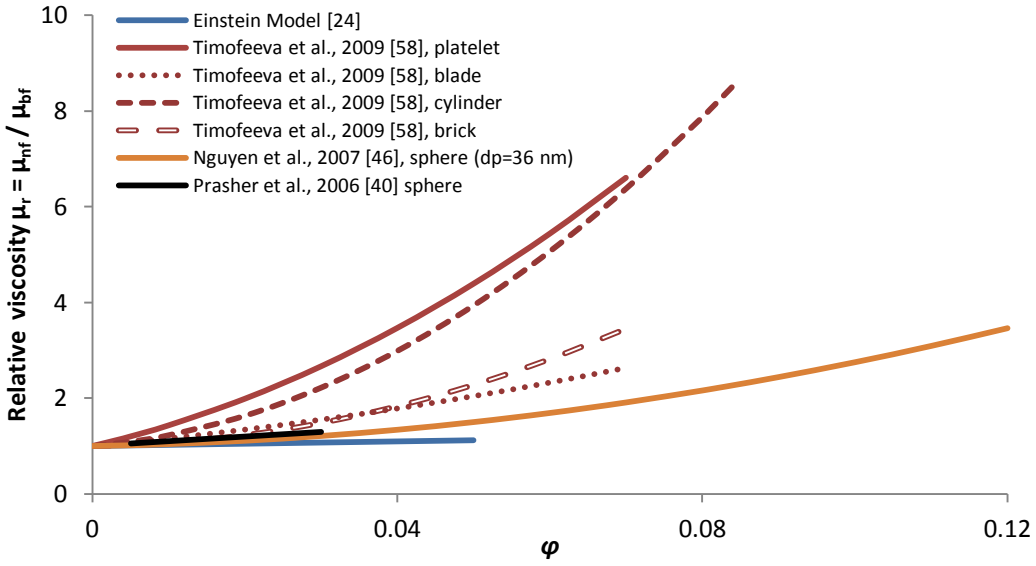

Figure 5. Relative viscosity of nanofluids dependent on φ for different nanoparticle shapes. Behavior of a Classical Model (Einstein Model for non interacting hard spheres) and empirical correlations are presented.

In this comparison, the empirical correlations proposed only for Al_2O_3 nanoparticle nanofluids are used in order to avoid other parameters' (nanoparticle type, etc) effects, and strengthen the sensitivity of the analysis. As it is seen in Figure 5, the relative viscosity of nanofluids increases with increasing nanoparticle volumetric fraction. The relative viscosity is greater than 1, meaning the viscosities of nanofluids are greater than the base fluids studied. In addition, the behaviors of the relative viscosity correlations proposed for nanofluids containing different shaped nanoparticles, are significantly different from each other, and Einstein Model. Therefore, it can be concluded that, the effect of nanoparticle shape is significant on nanofluid viscosity.

2.3.3. Nanofluid Viscosity Dependent on Nanoparticle Material

Although nanoparticles with their enhanced surface to volume ratios constitute a relatively small percentage of nanofluids, they are regarded as one of the responsible factors for the unforeseen behaviors of nanofluids. From this point of view, nanoparticle material is a critical factor. In Figure 6, the frequency values of nanoparticles dispersed within nanofluids evaluated in studies summarized in the literature survey (see Table 5) are provided.

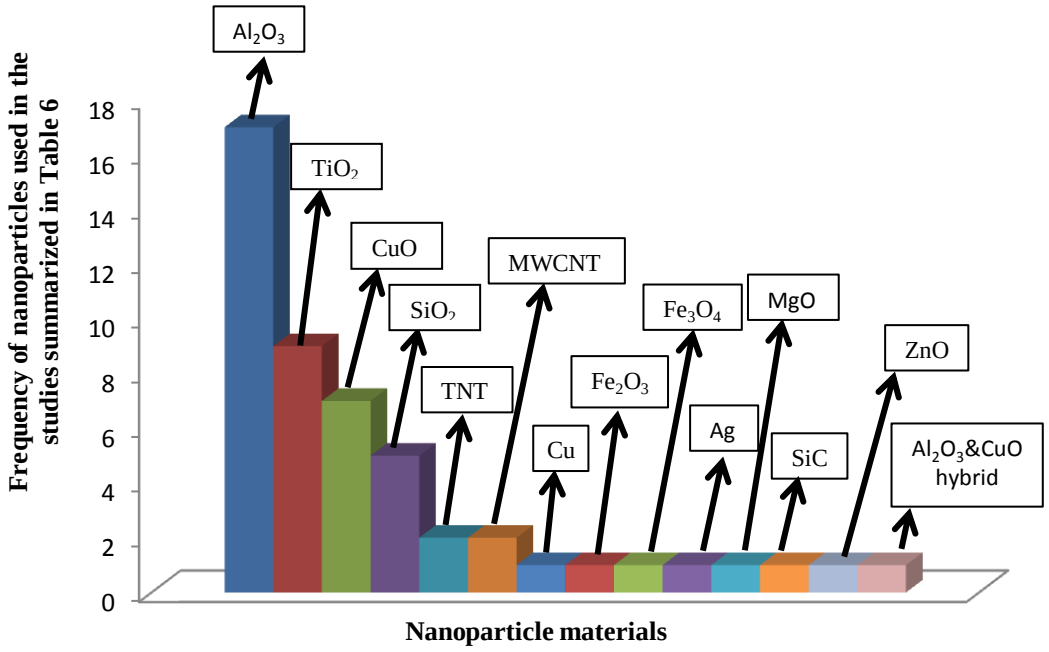

Figure 6. Nanoparticle frequency plot obtained from the literature survey given in Table 5.

As it is seen in Figure 6, a significant amount of research was done on the viscosity of Al_2O_3, TiO_2 and CuO nanoparticle nanofluids, but Al_2O_3 nanoparticle nanofluids come to the fore with 17 studies outlined among 41 studies.

In Figure 7, the relative viscosity correlations proposed for different nanoparticle materials together with Einstein Model [24] are compared within their validity limits.

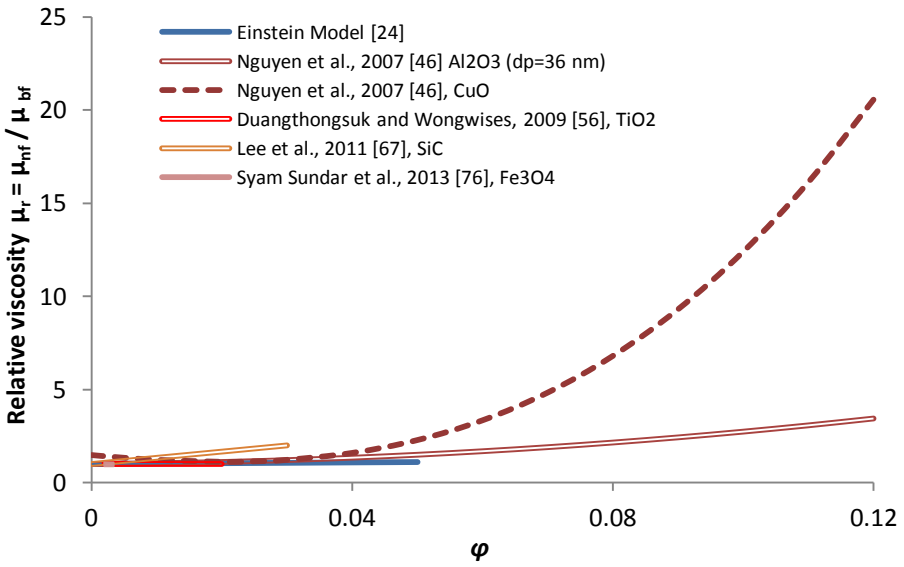

Figure 7. Relative viscosity of nanofluids dependent on φ for different nanoparticle materials. Behavior of a Classical Model (Einstein Model) and empirical correlations are presented.

In this comparison, the empirical correlations proposed for Al_2O_3, CuO, TiO_2 (at 25°C), and SiC nanoparticle nanofluids are used. Empirical correlation proposed for the viscosity of Ag nanoparticle nanofluids by Godson et al. [62] is not included into the Figure, in order to strengthen the sensitivity of the analysis, since the regarding correlation was presented for the viscosity of Ag-H_2O nanofluids, at high temperatures (50-90°C), whereas the others presented in the Figure are approximately at room temperature (20-30°C). Regarding the nanoparticle diameters of the empirical correlations proposed for varying nanofluids, they were selected as close as possible (e.g. for the correlations proposed by Nguyen et al. [46], the correlation proposed for d_p= 36 nm nanofluid is employed rather than the correlation proposed for d_p= 47 nm nanofluid) in order to avoid nanoparticle size effects, and strengthen the sensitivity of analysis.

As it is seen in Figure 7, the relative viscosity of nanofluids increases with increasing nanoparticle volumetric fraction, and is greater than 1, meaning the viscosity of nanofluids are greater than that of the base fluids studied. In addition, the behaviors of the relative viscosity correlations proposed for different nanoparticle materials are significantly different from each other and Einstein Model. Since the parameters other than the nanoparticle shape and nanoparticle volumetric fraction could not be kept constant in this analysis, it is not for certain that the differences in the results presented in Figure 7 are due to the nanoparticle material effect, only. Nevertheless, it still seems to be an important factor, and have significant effect on nanofluid viscosity.

2.3.4. Nanofluid Viscosity Dependent on Temperature

Viscosity is very sensitive to temperature, thus particular attention must be given to temperature when determining viscosity [81]. The exponential variation of the viscosity of pure water with temperature is an explanatory example on the effect of temperature on viscosity [77]. In Figure 8, the relative viscosity and nanofluid viscosity correlations are compared within their validity limits.

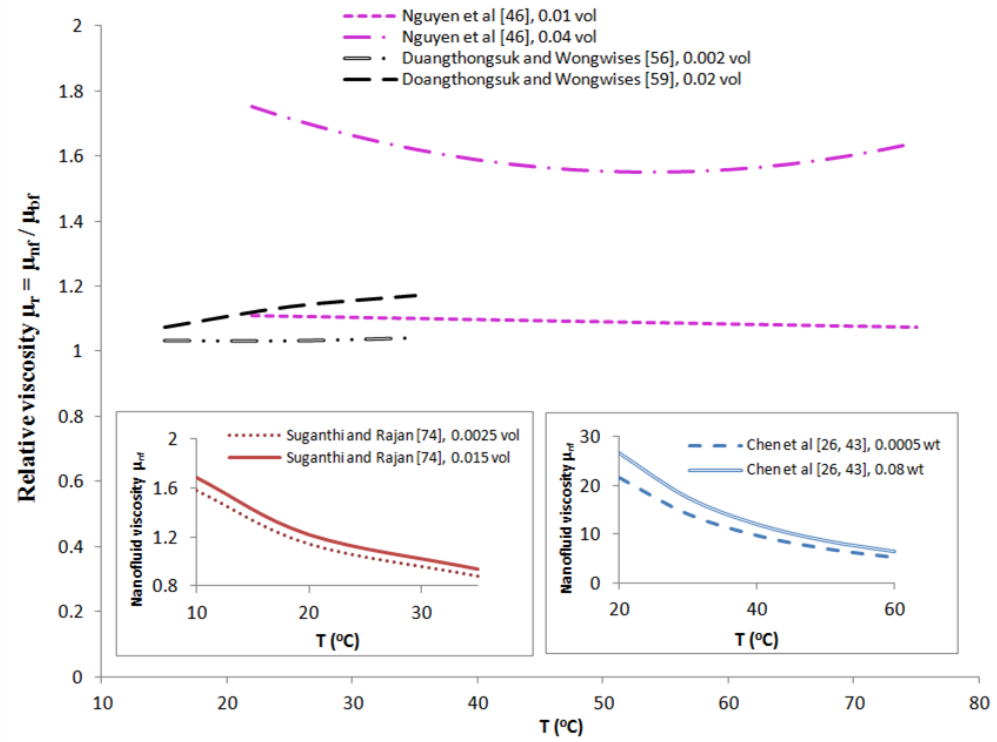

Figure 8. Relative viscosity and nanofluid viscosity dependent on *T*. Behavior of empirical correlations are presented.

As it is seen in Figure 8, the viscosity of nanofluids decreases significantly with increasing temperature. It is important to recall from the literature survey that, the nonlinear decrease in the nanofluid viscosity with increasing temperature is a commonly observed fact. However, explaining the relative viscosity dependence on temperature may not be as simple as the nanofluid viscosity dependence on temperature. As aforementioned, the temperature dependence of the base fluids (e.g. water) is also very dominant. Therefore, when evaluating the relative viscosity and temperature relationship, evaluation of the dependence of the nanofluid viscosity, as well as the base fluid viscosity on temperature is necessary. The behaviors seen in Figure 8 for relative viscosity are good examples in this issue. Nevertheless, the temperature dependence of viscosity is widely known. The viscosities of fluids dependent on temperature should be carefully investigated within the bounds of experimental facilities [21], and it can be concluded that, the effect of temperature is significant on nanofluid viscosity.

2.3.5. Nanofluid Viscosity Dependent on Nanoparticle Aggregation

Aggregation is an inevitable behavior of nanoparticles. As it is seen in Figure 9, nanoparticles tend to come together and form particle pairs, multi particles, and aggregates. Since this behavior is inevitable in the long term, and has strong effect on nanofluid viscosity, developing an understanding of nanofluid viscosity from the nanoparticle aggregation point of view is important.

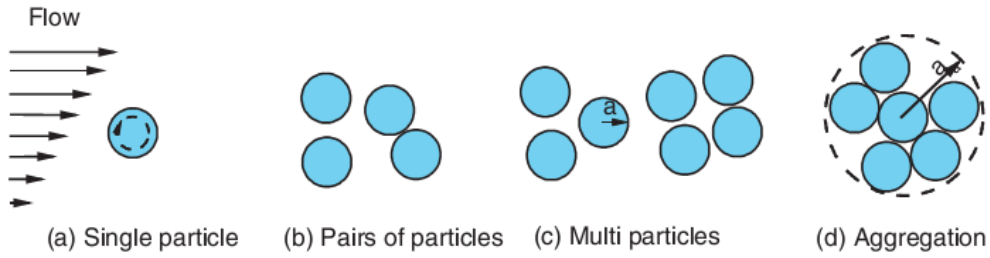

Figure 9. Schematic illustrations of the particle conditions within shear flow (a and a_a refer to particle and aggregate radius, respectively) [26]

The parameters that are used to define the nanoparticle aggregation are correlated with the relative viscosity by Chen et al. [26, 43, 54] as in Equation (23), which are a_a/a, D, φ_m and $[\eta]$. The intrinsic viscosity $[\eta]$ should be calculated using Equation (24) for nanoparticles other than spherical shaped, which is done for TNT (cylindrical) nanoparticle nanofluids, in the present study.

The aggregate size is mostly defined as the aggregate diameter (d_a) or aggregate radius (a_a). These parameters define the size of an aggregate as a mean value, since the aggregates do not have a uniform shape. In literature, some of the studies [40, 43, 54, 59, 60, 69, 70, 73] reported the measured d_a / d_p (or, a_a / a) values. In Table 8, the d_a / d_p (or, a_a / a), D, φ_m and $[\eta]$ values reported in the studies outlined in the literature survey are given.

Table 8. The values of d_a / d_p (or, a_a / a), D, φ_m and $[\eta]$ reported in the experimental studies outlined in Table 5

	d_a / d_p (or, a_a / a)	D	φ_m	$[\eta]$
Prasher et al. [40]	3.17	1.8	0.605	2.5
Chen et al. [43]	3.34	1.8	0.605	2.5
Chen et al. [54] *	9.46	2.1	0.30	Calculated using Equation (24)
Zhao et al. [59]	4.48 (d_p= 40 nm); 16.29 (d_p= 7 nm)	1.9	0.605	2.5 (d_p= 40 nm); 2.8 (d_p= 7 nm)
Pastoriza-Gallego et al. [60]	2.7 (S1**); 5.1 (S3**)	1.8	0.605	2.5
Kole and Dey [69]	7.15	1.7	0.5	2.5
Pastoriza-Gallego et al. [70]	2.5 (S1**); 7.5 (S2**)	1.8	0.605	2.5
Utomo et al. [73]	4 (Al_2O_3); 4.7 (TiO_2)	2.6 (Al_2O_3); 2.0 (TiO_2)	0.62	2.5

* The sign indicates that the nanoparticles were cylindrical. For all the other cases, the nanoparticles were spherical.
** S denotes the "sample" in the studies of Pastoriza-Gallego et al. [60, 70].

In addition to Table 8, Chevalier et al. [45] reported φ_a/φ_m values of 3.4, 2.4 and 2.1 for d_p= 35, 94 and 190 nm nanofluids, respectively. They found a relatively good agreement between Equation (45) (below) and their experimental results.

$$\mu_r = \left(1 - \frac{\varphi_a}{\varphi_m}\right)^{-2} \quad , \quad \varphi_a = \left(\frac{d_a}{d_p}\right)^{1.2} \varphi \tag{45}$$

In Figure 10, the relative viscosity correlations are compared within their validity limits for different nanoparticle aggregation levels.

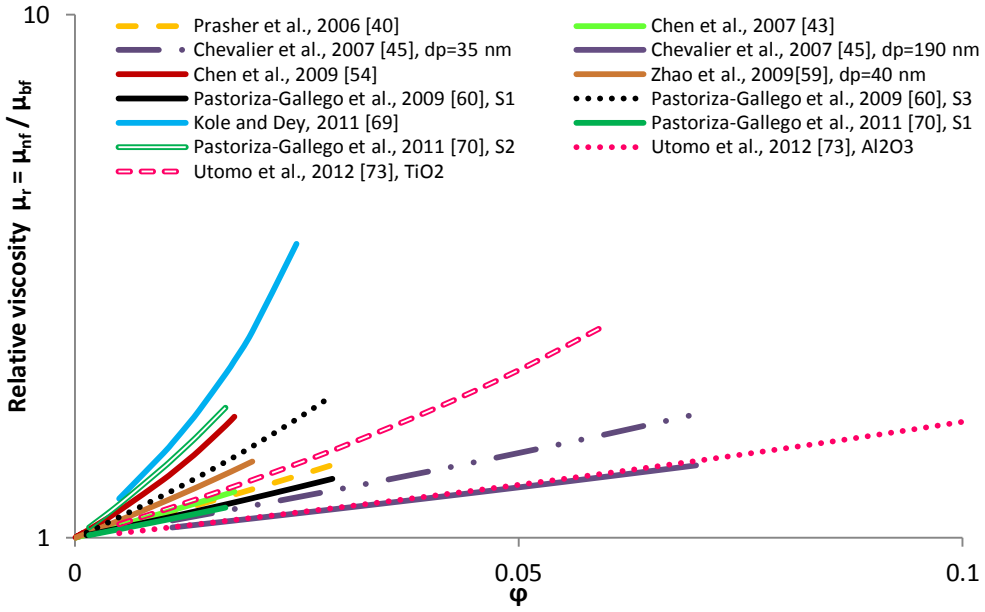

Figure 10. Relative viscosity of nanofluids dependent on φ for different nanoparticle aggregation levels (see Table 8). Behavior of empirical correlations is presented.

In this comparison, the relative viscosity of nanofluids is evaluated in terms of nanoparticle aggregation. Figure 10 shows the behavior of modified Krieger-Dougherty Model proposed by Chen et al. [26, 43, 54] (given as Equation (23)) for different nanoparticle aggregation levels and varying d_a / d_p (or, a_a / a), D, φ_m, and $[\eta]$ values.

As it is seen in Figure 10, the relative viscosity of nanofluids increases with increasing nanoparticle volumetric fraction, which also results in an increase in the effective volumetric fraction of aggregates, thus an increase in nanoparticle aggregation. Therefore, it can be concluded that, the effect of nanoparticle aggregation is significant on nanofluid viscosity.

2.3.6. Concluding Remarks from the Benchmark Study

Nanofluid viscosity can be easily affected by many parameters, and some of them were shown under Section 2.3. The Section provides an objective summary of the literature by comparing the empirical correlations and some Classical Models within their validity limits. It was found from the benchmark study that, the effects of nanoparticle fraction, nanoparticle shape, nanoparticle material, temperature, and nanoparticle aggregation on the nanofluid viscosity are significant, and should certainly be taken into consideration while estimating nanofluid viscosity.

The complexity of the nanofluid systems and the lack of a universally accepted nanofluid viscosity model make this subject even more complicated [21]. Regarding this issue, Godson et al. [62] stated that, *"Since the thermophysical properties of nanofluids depend on various factors, such as particle size, particle shape, nature of material, and pH value, it is hard to develop a universal model"*. On the other hand, nanofluid viscosity as an easily affected property by many parameters should be carefully investigated, in order to have a fundamental understanding on the applications.

2.4. Conclusion

This Chapter provided a literature survey and a benchmark study on the nanofluid viscosity and relative viscosity. The literature survey and the benchmark study lead to develop insights for further experimental studies. The important points that came to the fore are the nanofluid types that can be examined experimentally, and the effects of parameters that can be examined on nanofluid viscosity. As aforementioned, although the nanoparticles constitute a relatively small percentage of nanofluids, they are regarded as one of the responsible parameters from the unforeseen behaviors of nanofluids. From this point of view, selection of the nanoparticle material is of great importance for the applications.

Regarding the nanofluid type, the frequency plot for the nanoparticle materials examined in the literature review was provided in Figure 6. It was seen in the Figure 6 that, a significant amount of research was done for Al_2O_3 nanoparticle nanofluids. In the statistical review paper of Sergis and Hardalupas [82], a similar but a more comprehensive frequency distribution based on the examined nanofluid types was presented. Among the 141 studies, 85 of the studies examined Al_2O_3–H_2O nanofluids, which made the Al_2O_3–H_2O nanofluids the most commonly examined nanofluid [82]. In addition, due to the relatively accessible cost of Al_2O_3 nanoparticles, the industry may be established on Al_2O_3 nanoparticles (nanofluids). This is the main idea on selecting Al_2O_3–H_2O nanofluids for the experimental investigation presented in this thesis.

Regarding the effects of parameters to be examined on nanofluid viscosity in the current work, the literature review was consulted. In the literature survey presented in Section 2.2.2, the examined parameters on nanofluid viscosity were provided. It was seen that, the effects of the nanoparticle fraction and temperature should certainly be examined, since their effects are proven to be significant by many studies. In addition to the nanoparticle fraction and temperature, the effect of nanoparticle diameter was thought to be very important as well; however it was not examined as comprehensively as the nanoparticle fraction and temperature.

Another conclusion that can be drawn based on the literature review is that, the experiments were mostly done on randomly selected parameters. This may be due to the experimental resources in hand, and the sample supplying opportunities; since the nanofluid industry is still emerging. In addition, an actual experimental design based on statistics was not seen to be done before the experiments were performed, which is a very important point.

CHAPTER 3

MATERIAL HANDLING AND METHODOLOGY

In this Chapter, information on the materials used in the experimental study (see Chapter 4) is given, first. The Chapter emphasizes the algorithm of the Taguchi Method, which is used for the experimental design. The algorithm steps are given for the present experimental investigation. The experimental setup and the experimental procedure are also introduced. The statistical methodology employed in this thesis is a novel approach for the field nanofluid viscosity. Finally, some conclusions are drawn.

3.1. Introduction

Nanofluid viscosity is still an emerging research area; therefore systematic investigations are needed in order to develop a fundamental understanding in this field. For this purpose, nanofluid viscosity has been investigated both theoretically and experimentally. Still, inconsistencies in literature are very significant and clear to see. Reasons of the inconsistencies in literature are very difficult to keep under control and nearly impossible to eliminate at this point. However, the aforementioned facts do not make comparing the findings of researches with each other unnecessary, in fact, it strengthens this requirement, but in a more efficient and meaningful way, from which drawing conclusions will be more objective.

From this point of view, systematic investigations combining both the experiments and theoretical background are required. The present experimental study was performed at the Energy Laboratory of the Mechanical Engineering Department in Dokuz Eylül University in İzmir, Turkey.

At this point, it is considered as necessary to provide required information on the properties of the experiment samples. Because if the required information is not present, interpretation of the experimental results on a solid basis is not possible.

The methodology used to construct the experiments is very important, as well. Design of Experiments (more specifically, Taguchi Method) is used to design the experimental study. Utilization of such a statistical methodology is novel for the field "nanofluid viscosity", as far as the author's literature investigation is concerned.

3.2. Material

In the experiments, the viscosity of Al_2O_3–H_2O nanofluids (supplied from NanoAmor (USA)) is comprehensively investigated. The nanofluid samples contained two different sized Al_2O_3 nanoparticles (d_p= 10±5 nm and d_p= 30±10 nm). Initially, the weight fractions of Al_2O_3 nanoparticles were 20% within the nanofluids, as it was provided by the manufacturer. But, they were diluted with medical grade deionized water supplied from the Department of Nephrology in Eskisehir Osmangazi University Hospital, to φ= 1, 2 and 3% (by volume) nanofluids. The nanofluids involve Acetic Acid as a surfactant. The concentration of Acetic Acid is 0.1–0.3% by weight, in all samples. Table 9 summarizes the characteristics of the nanofluids.

Table 9. Characteristics of nanofluids used in the experiments

Material: Al_2O_3–H_2O		
d_p (nm)	10±5 nm	30±10 nm
φ	1, 2, and 3 vol%	1, 2, and 3 vol%

3.2.1. Sample Preparation

The weight fractions of nanoparticles within both nanofluids were provided as 20% by the manufacturer. It is useful to convert the weight fraction of nanoparticles to volumetric fraction, since a significant part of the information provided in the literature is based on volumetric fraction, rather than weight fraction. For this purpose, Equation (46) [83] was used.

$$\varphi = \frac{\varphi_w \rho_l}{\rho_p + \varphi_w \rho_l - \varphi_w \rho_p} \tag{46}$$

In Equation (46), the parameters $\varphi, \varphi_w, \rho_l$ and ρ_p denote the nanoparticle volumetric fraction, nanoparticle weight (mass) fraction, liquid (H_2O) density, and nanoparticle (Al_2O_3) density. The density of the Al_2O_3 nanoparticles was specified as 3700 g/cm^3 by the manufacturer. The density of H_2O was taken as 1000 g/cm^3 [83]. The weight fraction of nanoparticles was 0.20 within the nanofluids. Using Equation (46), the volume fraction of nanoparticles is estimated to be approximately 0.0633. Thus, for the Al_2O_3–H_2O nanofluids considered, φ_w= 20% corresponds to $\varphi \cong$ 6.33 vol%.

In experiments, the φ= 0.01, 0.02 and 0.03 nanofluids (each are 50 ml in volume) are examined. The sample volumes are specified as 50 ml considering the possible material losses, since the volume of approximately 40 ml and 10 ml samples can be used in experiments, depending on the measurement type. Detailed information regarding with this issue is provided in Chapter 4, Section 4.2.1.2.

For the sample preparation, the $\varphi \cong 0.0633$ nanofluids were diluted to φ= 0.01, 0.02, and 0.03 nanofluids. In order to dilute the $\varphi \cong 0.0633$ Al_2O_3–H_2O nanofluids, certain amounts of deionized water were added to $\varphi \cong 0.0633$ samples. The amounts of water to be added to $\varphi \cong 0.0633$ nanofluids for dilution are calculated using MATLAB Program. The Code and detailed program outputs are provided in Appendix B. The program outputs regarding the amounts of deionized water and nanofluid ($\varphi \cong 0.0633$) to be mixed in order to prepare φ =0.01, 0.02 and 0.03 nanofluids (50 ml, each) are given in Table 10.

Table 10. Required volumes of nanofluid and deionized water for diluted sample preparation

φ of diluted samples	Volume of $\varphi \cong 6.33\%$ nanofluid (ml)	Volume of deionized water (ml)	Volume of resulting nanofluid (ml)
0.01	7.9	42.1	50
0.02	15.8	34.2	50
0.03	23.7	26.3	50

The dilution of the nanofluids was done very precisely using AXYGEN Single Channel Micropipette AP–10ML with a measurement range of 1000 µl to 10000 µl (Figure 11a). The diluted samples were ultrasonicated with Misonix Sonicator 3000 (Figure 11b, 11c) in order to ensure the stability of nanofluids after dilution.

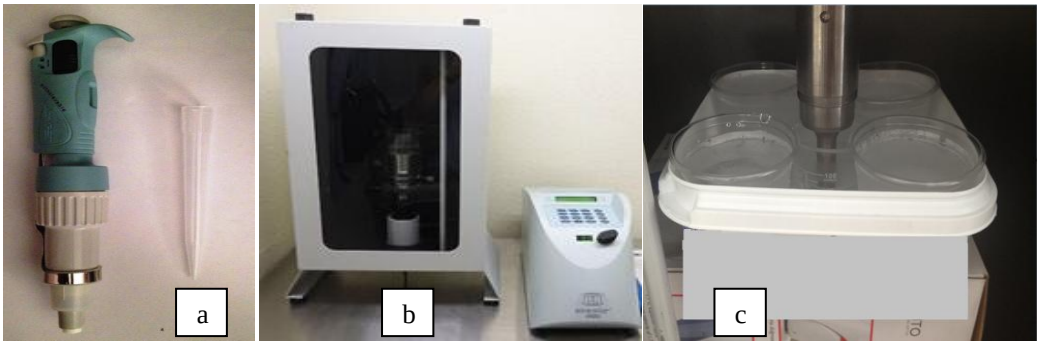

Figure 11. a) AXYGEN Single channel micropipette with its tip. b, c) Misonix Ultrasonicator 3000. Figure 11.b is adapted from [84]

The prepared six Al_2O_3–H_2O nanofluid samples of $\varphi = 0.01$, 0.02, and 0.03; d_p= 10 nm and d_p= 30 nm after ultrasonication are given in Figure 12.

Figure 12. The nanofluids after ultrasonication

In order to prevent sunlight exposure and other unwanted results, the prepared samples were stored in dark colored glass bottles, as it is seen in Figure 12. Foams that were caused by the ultrasonication process can be seen in some of the bottles. However, after the relaxation of the samples for a few hours, the foams disappeared.

3.2.2. Determination of the Colloidal Behavior of Nanofluids by Zeta Potential Measurements

Aggregation and sedimentation of nanoparticles are inevitable in the long term. They are directly related to the stability of nanofluids. Aggregate formation of nanoparticles is guided by the electromagnetic forces (attractive forces: van der Waals force and repulsive forces: electrical double layer force [47]) between the nanoparticles and the fluid medium. If these forces balance each other, the net charge will be zero, and the particles tend to come together and form aggregates (see Figure 9 in Section 2.3.5), which will result in an unstable nanofluid.

The measure of "zeta potential" comes to the fore at this point. Zeta potential is a measure of the stability of colloidal dispersions. Colloids with high zeta potential (negative or positive) are electrically stabilized, while colloids with low zeta potentials tend to coagulate [3]. As a generally accepted rule, colloids with zeta potential higher than 30 mV (negative or positive) are regarded as stable [83], whereas colloids with zeta potential lower than 30 mV (negative or positive) are regarded as unstable, and prone to aggregation and sedimentation. The ranges of zeta potential corresponding to stable and unstable behavior are illustrated in Figure 13.

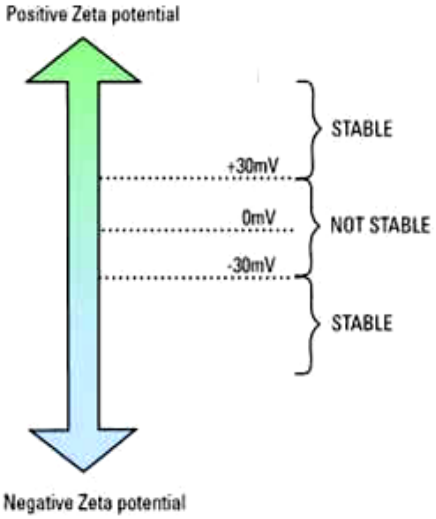

Figure 13. Zeta potential ranges of colloids [85]

The Zeta Potential measurements of nanofluids were done with MALVERN Nano ZS90 at Middle East Technical University, Central Laboratory. The measurements were done on the most diluted nanofluid samples, i.e. φ= 0.01, d_p= 10 and φ= 0.01, d_p= 30 nm. The graphs showing the zeta potential of the φ= 0.01, d_p= 10 and φ= 0.01, d_p= 30 nm Al_2O_3–H_2O nanofluids are given in Figure 14. The detailed results are provided in Appendix C.

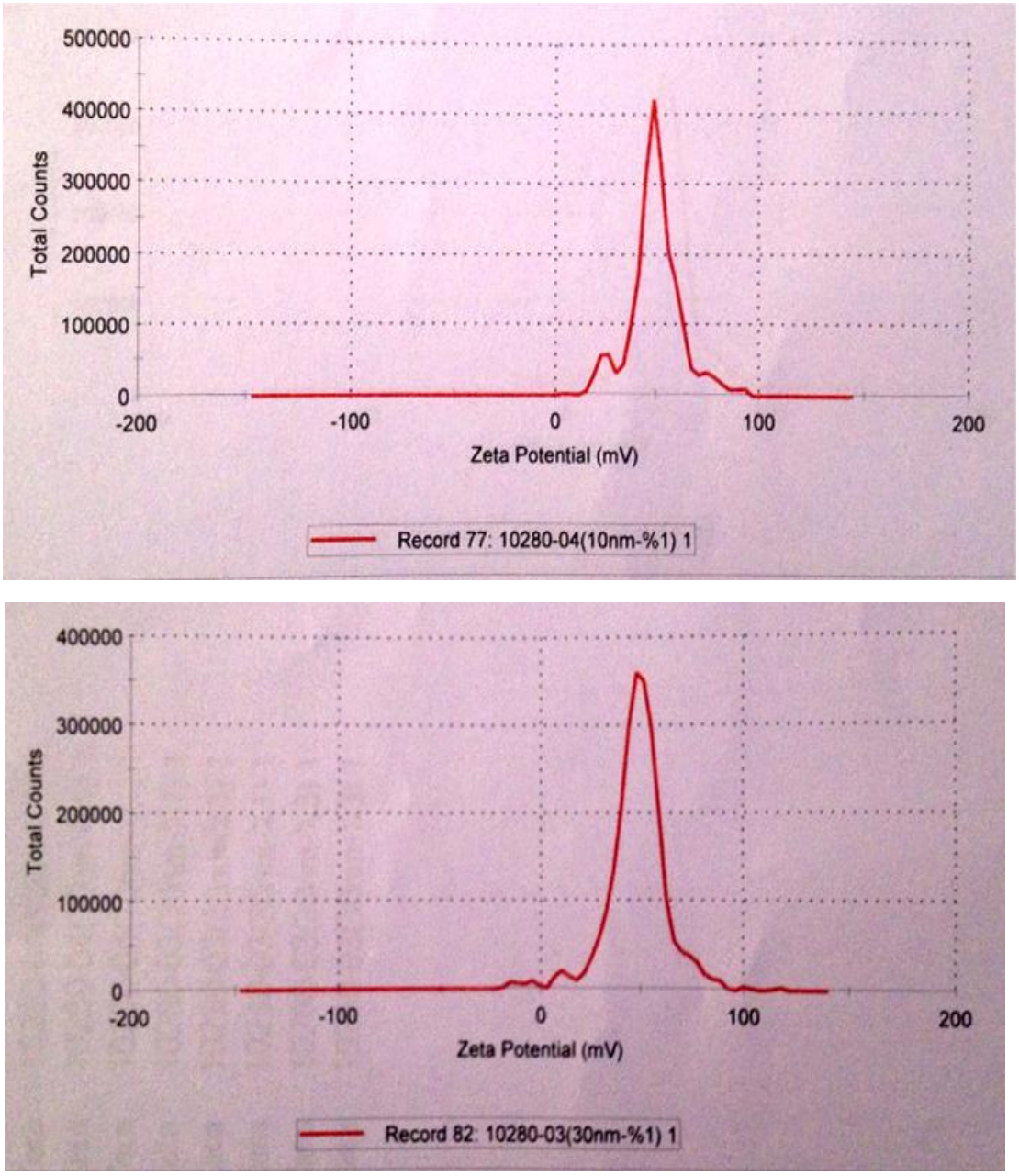

Figure 14. Zeta potentials of φ= 0.01, d_p= 10 nm and φ= 0.01, d_p= 30 nm nanofluids

The mean zeta potential of φ= 0.01, d_p= 10 nm nanofluid is 49.2 mV, whereas the mean zeta potential of φ= 0.01, d_p= 30 nm nanofluid is 48 mV. Both zeta potential values are higher than 30 mV, indicating the nanofluids are highly stable.

3.2.3. Particle Size Distribution of Nanofluids with Dynamic Light Scattering Measurements

The particle size distribution (PSD) analyses on the most diluted nanofluid samples, i.e. φ= 0.01, d_p= 10 nm and φ= 0.01, d_p= 30 nm nanofluids, were done with Dynamic Light Scattering (DLS) measurements, using ALV/CGS-3 compact goniometer system (Malvern Instruments, Inc, UK) in

Eskisehir Osmangazi University, Polymer Laboratory. The system is equipped with He-Ne laser at λ_0= 632.8 nm, 22 mW, photodiode detector with high quantum efficiency and an ALV/LSE–5003 multi tau digital correlator electronic system. The measurements were done with 90^o constant angle scatterings on the suspensions, and the data were processed using secondary cumulant analysis.

Although the nanoparticle sizes were provided by the manufacturer, it is important to confirm these values before/after the experiments, since the particle size is a dynamic parameter. Unfortunately, due to the experimental opportunities, the confirmation experiments on the nanoparticle sizes were done one month after the viscosity experiments.

The unweighted results of the PSD of the φ= 0.01, d_p= 10 nm and φ= 0.01, d_p= 30 nm nanofluids are given in Figure 15. The detailed results are provided in Appendix D.

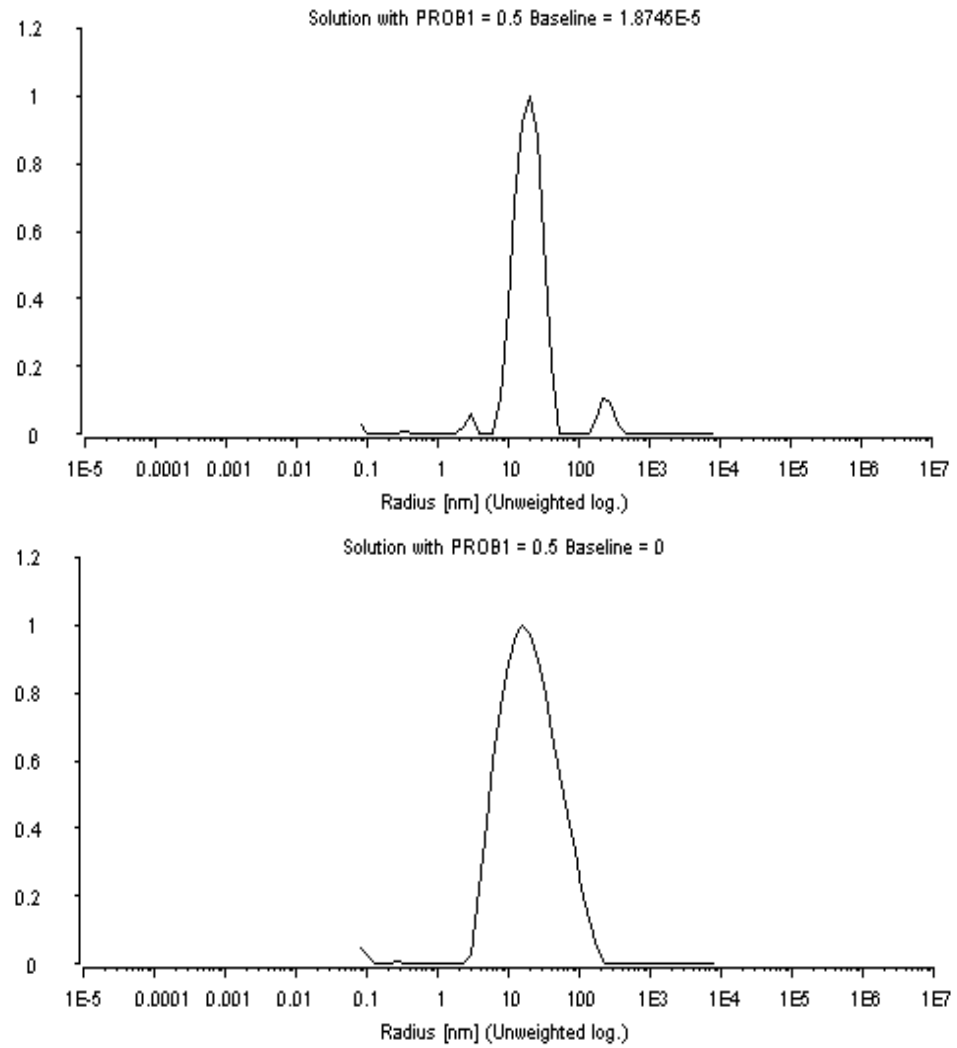

Figure 15. Particle size distribution of φ= 0.01 d_p= 10 nm (top) and φ= 0.01 d_p= 30 nm (bottom) nanofluids.

The average particle sizes of the nanoparticles dispersed in nanofluids are specified as d_p= 10±5 nm (minimum d_p= 5 nm, maximum d_p= 15 nm) and d_p= 30±10 nm (minimum d_p= 20 nm, maximum d_p= 40 nm) by the manufacturer. The results presented in Figure 15 seem to be a bit higher than the

information provided by the manufacturer, but suggesting that the measured and provided (by the manufacturer) particle sizes being totally inconsistent would not be correct, since the PSD results depend on many factors, such as the nanoparticle aggregation (not seem to be happened, though), and the equipment type and resolution. (The effect of the equipment type can be observed through comparing the PSD results in Appendix C and Appendix D.) Nevertheless, in Figure 15, the average particle sizes for φ= 0.01 d_p= 10 nm and φ= 0.01 d_p= 30 nm nanofluids are shown as nearly consistent and within the minimum and maximum values specified by NanoAmor. Therefore, it can be concluded that, the results in Figure 15 (for detailed results, see Appendix D) are acceptable.

3.3. Method

The method employed to construct the experimental study is Taguchi Method, which is classified under the approach "Design of Experiments (DOE)". DOE is a statistical tool and it was founded by Ronald A. Fisher [86, 87, 88]. It gives a clear arrangement of the both experiment plan and experimental results, and it is used to determine the effects of the experimental parameters on the measured parameter.

Scientific investigations are important not only for academic research, but also in industry. Recognition is being given to the necessary link between the scientific study of industrial processes, and the quality of the goods produced [89]. For continuous production and high quality, the processes should be carefully designed, the process inputs and outputs should be thoroughly examined, and optimized process conditions should be sought in order to minimize the losses occurring during the process and to procure the optimized results (or products). Hence, the importance of the careful experimentation and the statistical evaluation is critical for both academic and industrial advance. The DOE can be employed in order to design the processes with minimal expense on both cost and time, since experimentation in a trial-and-error manner and changing one factor at a time is the most expensive approach. A far more effective method is to apply a computer-enhanced and systematic approach to experimentation, one that considers all factors simultaneously [90], all of which are what DOE is capable of.

DOE can be used for process characterization, optimization, and modeling. The method DOE is widely accepted in many fields for improving the product performance and reliability, the process capability and yield. By employing DOE, a lot of information can be obtained with a minimum number of experiments, which is of great importance for today's industry [91].

3.3.1. Conceptual Introduction to Design of Experiments

In this Section, some important concepts of DOE defined below are handled.

- Experiment: An operation under controlled conditions to determine an unknown effect; to illustrate or verify a known law; a test to establish a hypothesis [92].

In experiments, the measurements are done to observe the behavior of a parameter, which is dependent on some experiment parameters. Here, the observed parameters (the outputs) are the dependent variables, whereas the parameters that are controllably varied that affect the dependent variables (the inputs) are the independent variables. From this point of view, the concepts "factor", "quality characteristic" and "level" are defined below.

- Factor: The input parameter. The independent variable considered in experiments, for which the dependent variable is examined. The factors are denoted with capital letters, such as: *A*, *B*, *C*, etc.

- Quality (performance) characteristic: The output parameter. The dependent variable examined in experiments.

- Level: In experiments, effects of a factor on the quality characteristic can be examined for different values of the factor. The different values of the factors are denoted as the levels of a factor. The levels of a factor are denoted with lower case letters, such as: *a, b, c*, etc.

Using DOE, the effects of the factors on the quality characteristic can be evaluated. The effects of the factors can be classified as main effect (which is the summation of the simple effects) and interaction effects.

- Simple effect: The very own effect of a factor on the quality characteristic. When the effect of a factor is kept as constant, the difference between the other factors levels gives the simple effect. Table 11 gives an explanatory example on the simple effects of parameters in a two leveled two factor experiment.

Table 11. The simple effects of factors A and B in a two leveled (1, 2) two factor (*A, B*) experiment

	Factor	*B*		The simple effect of *B*
Factor	Level	*b1*	*b2*	
A	*a1*	*(a1b1)*	*(a1b2)*	*(a1b1)-(a1b2)*
	a2	*(a2b1)*	*(a2b2)*	*(a2b1)-(a2b2)*
	The simple effect of *A*	*(a1b1)-(a2b1)*	*(a1b2)-(a2b2)*	

- Interaction (AB): The synergistic effect of two or more factors [92].

The other concepts that are used when performing DOE are also given below.

- Experimental error: The variation observed when products are tested under "identical" conditions; a portion of which is instrumentation repeatability [92].

- Orthogonal matrix (array): A matrix which assures a balanced, fair comparison of levels of any factor or interaction of factors; all columns can be evaluated independently of one another [92].

- Degrees of freedom (d_f): The number of independent measurements available to estimate pieces of information; the number of independent (fair) comparisons that may be made within a set of data [92].

- F test: The hypothesis test that determines whether the means (μ) of two different populations are different or not (the name of the test is eponym of Ronald A. Fisher). On the evaluation of results, the F table is used, in which reference values are present [93].

- Hypothesis: In statistics, hypotheses are used in order to evaluate whether there is a difference between the two values for a particular case. For this purpose; two different hypotheses, i.e. the null hypothesis (H_0) and the alternative hypothesis (H_a) are employed. As a rule of thumb, the H_0 is tested. The only hypothesis that is accepted or rejected is H_0. If the H_0 is rejected, then the H_a is accepted.

The acceptance of a hypothesis does not mean that the hypothesis is true. The measure of the sensitivity of the decision made on acceptance/rejection of a hypothesis is related to the alpha (α) error, which is defined below.

- Alpha (α) error: The probability of the null hypothesis (H_0) will be rejected, when in fact it is true [92].

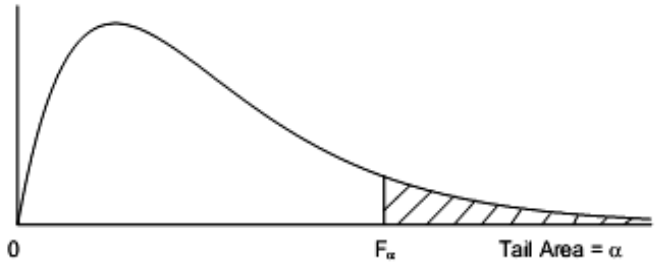

Figure 16. F distribution: The value of the alpha (α) error and its corresponding *F* value [93]

In Figure 16, the *F* distribution is given. The total area under the curve and the tailed area correspond to 1 and α, respectively. According to the definition of the α error, the untailed area, which is 1-α, belongs to the situation that the H_0 is accepted when it is true.

Regarding the experimental data, choosing the appropriate analysis method is of great importance. Usage of statistical methods with experiments works extremely well, since statistics is a very efficient tool on the evaluation and interpretation of the experimental results in an unbiased way. With straightforward algorithms, DOE can be used to draw critical conclusions. For the analysis, the analysis of variance (ANOVA) is used, which is defined below.

- ANOVA: A procedure to isolate one source of variation from another; a method to decompose the total variation present into accountable sources; a method to make a statistically based decision as to the causes of variation in an experiment [92].

Lu et al. [94] published a review paper regarding statistical methods for quality improvement and control in nanotechnology. In the study, the importance of using statistical approaches when studying nanotechnology was emphasized as: *"Because statistical techniques have made sizable impacts in many technology fields in the past, statistics are expected to play an important role in tackling these challenges and boosting the development of nanotechnology."* The difficulties of controlling the effects of ambient parameters on the newly developing and experiment based fields were mentioned, and the requirement of studying the effects of each factor and their interactions using advanced statistical techniques was emphasized. Finally, the important points of the statistical methodology to be used when studying nanotechnology were noted, such as: the choice of experimental design methods, analysis of experimental data, use of computer simulations and interaction between statisticians and experts in material science, physics, and other disciplines.

3.3.2. The Algorithm of Taguchi Method

Taguchi Method is a robust design method with straightforward steps. Since the Taguchi Method is classified under DOE, the algorithm is based on mostly DOE, but it involves Taguchi-specific steps. The DOE algorithm is mainly divided into three phases, which are: the planning phase, the conducting phase, and the analysis phase, respectively. The DOE algorithm involving Taguchi-specific steps is given in Figure 17. The analysis steps are adapted from [92], and after that, they are explained for the present experimental investigation.

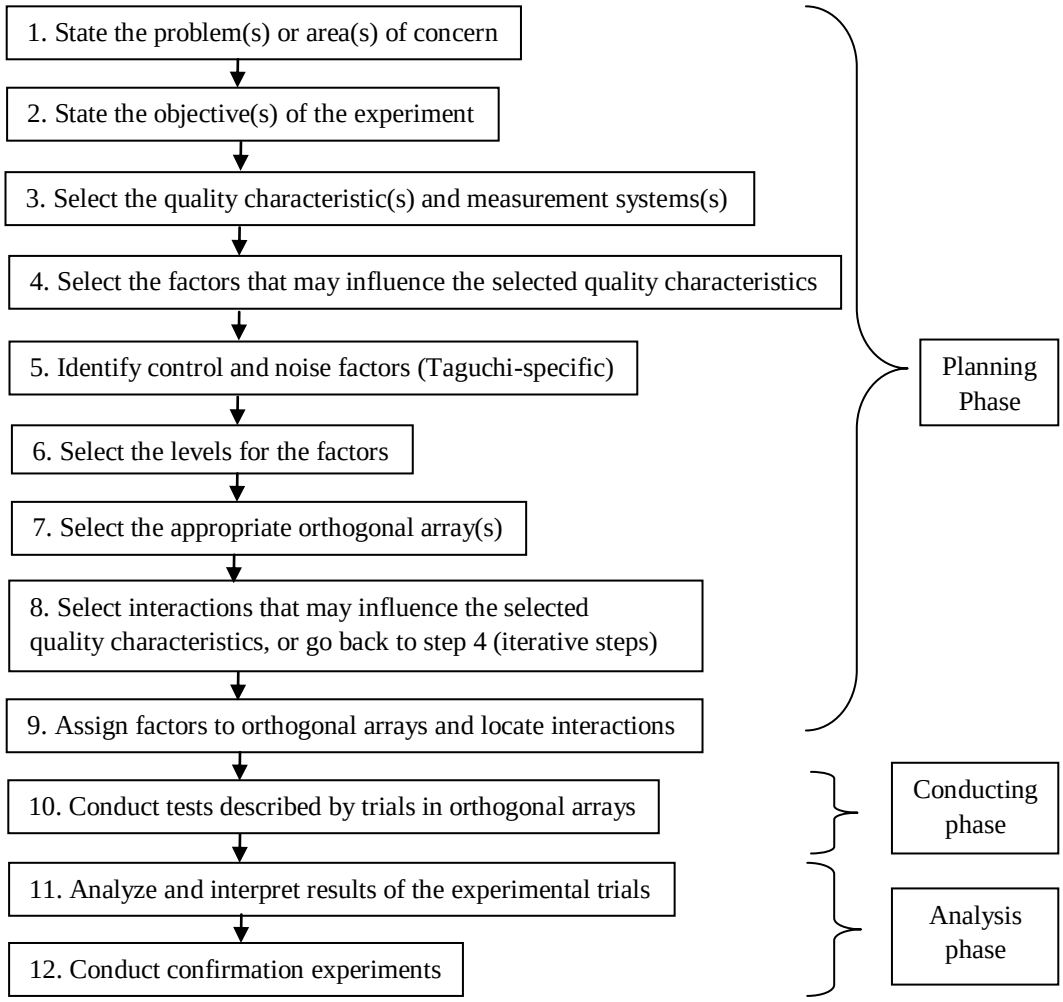

Figure 17. The DOE algorithm involving Taguchi-specific steps. Adapted from [92]

The steps given in Figure 17 are fundamentally the same regardless of whether one is designing a Taguchi-based experiment or a classical design. In addition to the classical experimental design, Taguchi approach relies on the assignment of factors in specific orthogonal arrays to determine these test combinations [92].

Nanofluids is still an emerging research field, and the inconsistencies in literature are abundant. Therefore, systematic studies are needed, in order to obtain objective, unbiased and interpretable results. Investigating the thermophysical properties of nanofluids in a systematic way is a good start and thus, it will strengthen the background in this area.

Regarding the thermophysical properties of nanofluids, it is seen that the viscosity of nanofluids has not been investigated as comprehensively as the thermal conductivity of nanofluids. Since the viscosity is of great importance for applications, systematic investigations are needed in nanofluid viscosity field.

In Sections 3.3.2.1, 3.3.2.2 and 3.3.2.3, the phases of the DOE: the planning phase, the conducting phase, and the analysis phase are described for the present experimental investigation.

3.3.2.1. Planning Phase

Step 1. Problem statement: The viscosity of working fluids is critical for the applications, since it is directly proportional to the pumping power required to circulate the fluid in the system. The viscosity of nanofluids is higher than the conventional working fluids (unless any additive is used to reduce the viscosity). Therefore, it is important to keep the viscosity of nanofluids under control, in order to have an application with high efficiency, and minimum expense.

Step 2. Objective of the experiment: Determining the effects of some observable and controllable parameters that have significant effect on nanofluid viscosity and relative viscosity.

Step 3. Selection of the quality characteristic and measurement systems: The viscosity of Al_2O_3–H_2O nanofluids is measured with a Sine Wave Vibro Viscometer SV-10 located at the Energy Laboratory of the Mechanical Engineering Department in Dokuz Eylül University. The temperature of the nanofluid samples is regulated with a WiseCircu circulating water bath WCR-P8 with 0.1°C stability.

Step 4. Selection of the factors that may influence the quality characteristics: This step requires the critical evaluation of the previous work, in order to have insight on the factors that may have considerable effect on the quality characteristic (nanofluid viscosity, and relative viscosity). In order to clearly illustrate the factors that can affect the quality characteristic, a cause and effect diagram (fishbone diagram) can be used. The cause and effect diagram (fishbone diagram) showing some effective factors on nanofluid viscosity is given in Figure 18.

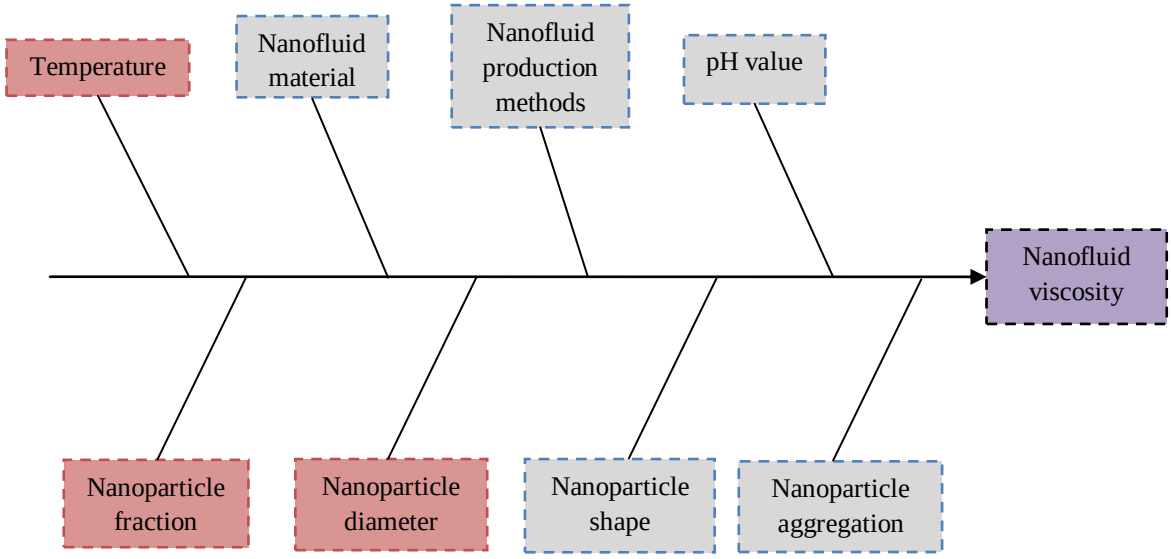

Figure 18. The cause & effect diagram (fishbone diagram) showing some factors that have considerable effect on nanofluid viscosity

As it is seen in Figure 18, the parameters that have considerable effect on the nanofluid viscosity are a lot in number. Although their effects are considered as significant, assigning some of them as factors to the experiment is very hard, since some of them are controlled by the manufacturer, or some of them are hard to controllably change during the experiments. As a consequence, the parameters in the pink blocks (temperature, nanoparticle fraction, and nanoparticle diameter) are controllably varied in experiments, whereas the parameters in the gray blocks are tried to kept as constant.

Step 5. Identification of the control and noise factors: The control factors are selected as the temperature, nanoparticle fraction and nanoparticle diameter, whereas some of the noise factors can be listed as the relaxation time of the nanofluid samples (as the relaxation time increases, the samples are being more prone to aggregation, sedimentation, or evaporation), level of the nanofluid in the sample cup, position of the sensor plates that are submerged within the nanofluid sample, and experiment personnel.

Step 6. Selection of the levels of the factors: The factors and the levels of the factors are provided in Table 12 (adapted from [92]).

As it was stated in Section 3.2.1, the experiments are done for φ= 0.01, 0.02 and 0.03 and d_p= 10 nm and 30 nm nanofluids, for T= 20, 30, 40 and 50^{o}C. The statistical analysis is concerned with the determination of the effects of the factors (φ, d_p and T) on the quality characteristic (nanofluid viscosity and relative viscosity). For the analyses, it is decided to consider the levels of these factors, which corresponds to their minimum and maximum values, in order to see the differences in the nanofluid viscosity and relative viscosity, i.e. for φ=0.01 and 0.03 and d_p= 10 nm and 30 nm and T= 20 and 50^{o}C. The reason for this selection is to see the effects of the factors more clear, whereas the reason for the additional experimentation for T= 30 and 40^{o}C and φ=0.02 is to be able to see the behavior of the nanofluid viscosity and thus relative viscosity for the intermediate values, and to be sure of the behavior for the whole interval of the factors, and to interpret the results with a more solid basis, in addition to the aim to provide a wide database for the Al_2O_3–H_2O nanofluid viscosity. In addition, with this approach, the standard orthogonal array L_8 can be used (see Table 13).

Table 12. The factors and their levels

	Factors		Level 1		Level 2	
Nanofluid viscosity experiment	*A*	Temperature (^{o}C)	a_1	20	a_2	50
	B	Nanoparticle volumetric fraction	b_1	0.01	b_2	0.03
	C	Nanoparticle diameter (nm)	c_1	10	c_2	30

Step 7. Selection of the appropriate orthogonal array (matrix): The selection of the appropriate orthogonal array should be done considering the number of factors and interactions of interest, the number of levels for the factors of interest, and the desired experimental resolution or cost limitations [95]. In the present experimental investigation, three factors with two levels are considered, thus the L_8 orthogonal array is selected. The detailed information on the L_8 standard orthogonal array is provided in Table 13.

Table 13. The L_8 standard orthogonal array

	Column						
Experiment	**1**	**2**	**3**	**4**	**5**	**6**	**7**
1	1	1	1	1	1	1	1
2	1	1	1	2	2	2	2
3	1	2	2	1	1	2	2
4	1	2	2	2	2	1	1
5	2	1	2	1	2	1	2
6	2	1	2	2	1	2	1
7	2	2	1	1	2	2	1
8	2	2	1	2	1	1	2

By employing L_8 design, a maximum of seven different factors' effects on the quality characteristic(s) can be determined. However, for the present experimental investigation, the three factors (*A, B, C*) and their interactions (*AB, AC, BC* and *ABC*) fill the columns of the L_8 matrix (see Table 14). Therefore, for the present experimental investigation, it will be possible to determine the effects of the interactions of the factors on the quality characteristic, as well as the simple effects of the factors.

Step 8. Selection of the interactions that may influence the selected quality characteristic: This step is already handled, since all the interaction effects will be examined for the present experimental investigation.

Step 9. Assigning factors to orthogonal array and locate interactions:

The factors (*A, B* and *C*; and their interactions *AB, AC, BC* and *ABC*) are located into the L_8 orthogonal array. The corresponding array is given in Table 14.

Table 14. The L_8 orthogonal array for the present experimental investigation

	Column						
	A	***B***	***AB***	***C***	***AC***	***BC***	***ABC***
Experiment	**1**	***2***	***3***	***4***	***5***	***6***	***7***
1	1	1	1	1	1	1	1
2	1	1	1	2	2	2	2
3	1	2	2	1	1	2	2
4	1	2	2	2	2	1	1
5	2	1	2	1	2	1	2
6	2	1	2	2	1	2	1
7	2	2	1	1	2	2	1
8	2	2	1	2	1	1	2

At this point, deciding on the interaction(s) to be examined is very important. Using the L_8 orthogonal array, two different cases for the interaction evaluation can be done. The linear graphics for the regarding cases are given in Figure 19.

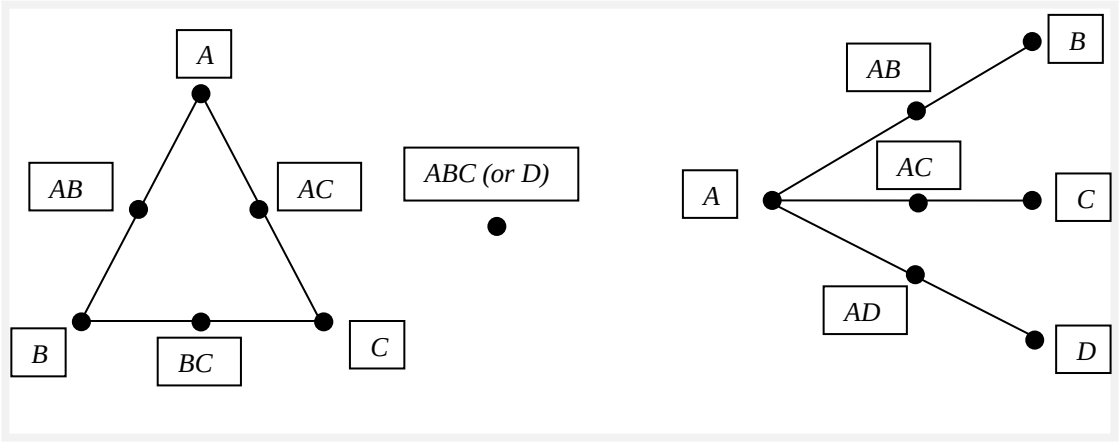

Figure 19. Linear graphics for the L_8 orthogonal array, in which the factors and their interactions of the present experimental investigation are located. Adapted from [96]

Regarding the linear interaction graphics given in Figure 19, the following explanations can be given. The left hand side interaction is appropriate for the following two cases:

Case 1: The simple effects of the three factors (*A, B* and *C*), all the two factor interactions of these factors (*AB, AC* and *BC*), and their three factor interaction (*ABC*) are to be examined.

Case 2: The simple effects of the four factors (*A, B, C* and *D*) and the two factor interactions of the three factors (*AB, AC* and *BC*) are to be investigated.

The right hand side interaction is appropriate for the cases in which the simple effects of the four factors (*A, B, C* and *D*) and two sided interactions of a single factor with other factors (e.g. *AB, AC* and *AD*) are to be investigated. With the light of the above given explanation, it is concluded that, the left hand side interaction with *Case 1* fits the present experimental investigation.

3.3.2.2. Conducting Phase

Step 10. Conducting tests described by trials in orthogonal arrays: The samples examined in experiments were selected as Al_2O_3–H_2O nanofluids. The experiments are done following the L_8 orthogonal array given in Table 14. During the experiments, data are collected via four repetitions. The experiments are done by the same person. In the next two sub-sections, information on the experimental setup and the experimental procedure are given in detail.

3.3.2.2.1. Experimental Setup

In the experiments, the viscosities of φ= 0.01, 0.02 and 0.03; d_p= 10 nm and d_p= 30 nm Al_2O_3–H_2O nanofluids were measured with a Sine Wave Vibro Viscometer SV-10, for the temperatures of 20, 30, 40 and 50^{o}C. The temperatures of the samples were regulated with WiseCircu circulating water bath WCR-P8 with 0.1^{o}C stability. Pictures of the experimental setup are provided in Figure 20.

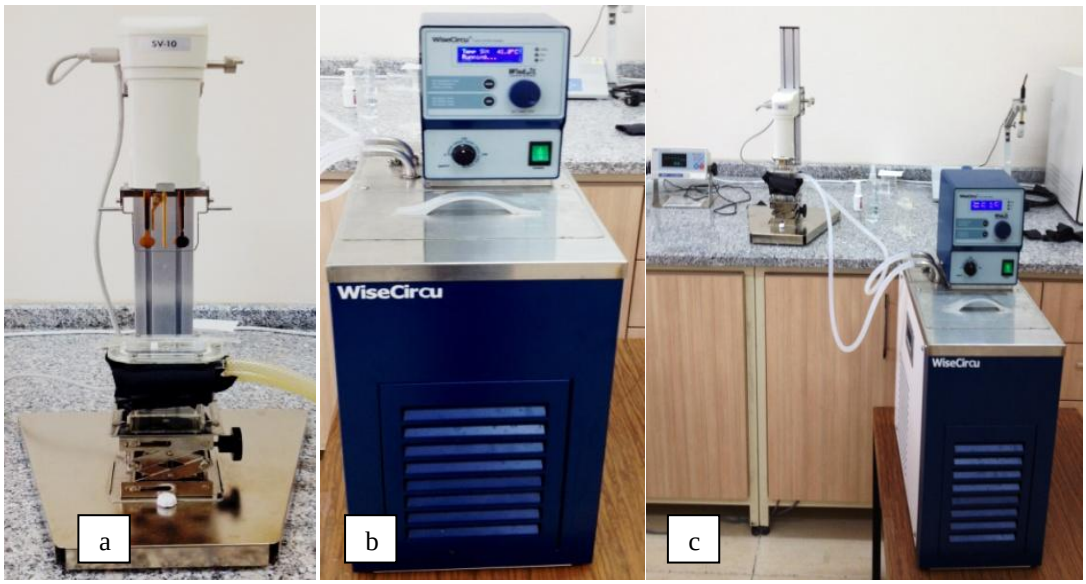

Figure 20. a) The Sine Wave Vibro Viscometer SV-10 (with black insulation on its sample cup), b) the WiseCircu circulating water bath WCR-P8 and c) the viscometer and the water bath.

3.3.2.2.2. Experimental Procedure

In this Section, the experimental procedure is described. Viscosity of nanofluids was measured with a Sine Wave Vibro Viscometer SV-10 manufactured by A&D Company Ltd. (Japan), with a measurement range of 0.3 mPa.s to 10,000 mPa.s. SV-10 vibrates with a sine wave frequency of 30 Hz and an amplitude of approximately 0.2 mm (0.4 mm peak to peak) [97]. In Figure 21, the schematic description of the viscosity detection unit is given [98].

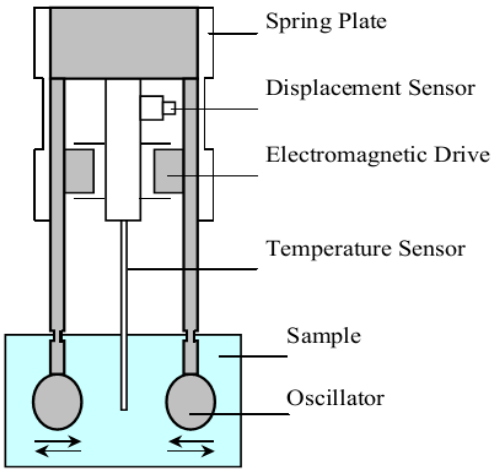

Figure 21. Schematic description of the viscosity detection unit [98]

As it is seen in Figure 21, the viscometer has two sensor plates (oscillators), which are driven with an electromagnetic force at the same frequency, by a sine-wave vibration in reverse phase, similar to a tuning-fork [97]. The tuning-fork vibration viscometer utilizes the same measurement principle as the vibration method. But, the vibromotive force generated due to vibration is a problem of the vibration method, which is eliminated by the adoption of a tuning-fork structure with two oscillator plates. The tuning fork and two oscillator plates function as a resonance system that is a highly sensitive viscosity sensor. The problem is eliminated by balancing the viscous resistance of the liquid and the driving force generated in the electromagnetic unit, since the amplitude of the oscillators is always feedback-controlled to remain constant [98]. In SV-10, the electromagnetic drive controls the vibration of the sensor plates to maintain constant amplitude. The drive electric current, i.e. an exciting force, will be detected as the magnitude of the viscidity produced between the sensor plates and the sample fluid. The coefficient of viscosity is obtained by the correlation between the drive electric current and the magnitude of the viscidity [97].

It is a widely known fact that, viscosity is very sensitive to temperature. Therefore, accurate measurement of the temperature of the samples is very important. With SV-10 viscometer, it is possible to measure the temperature of the sample accurately in a short period of time (since the sample and the sensor plates have small surface area, thermal capacity reaches thermal equilibrium only in a few seconds) [97].

Experiments are conducted in such a way that, the viscometer is calibrated before and after every nanofluid viscosity measurement with a reference fluid (H_2O), to ensure the validity of the results.

3.3.2.3. Analysis Phase

Step 11. Analyzing and interpreting the results of the experimental trials: For the analysis of the experimental data, ANOVA and graphics showing the mean effects of the factors and/or their interactions are used [99]. The experimental results are analyzed, and the effects of the factors and their interactions on the quality characteristic are determined by use of ANOVA. The optimum conditions of factors can also be determined as a Taguchi-specific step by drawing the mean effects graphics of the regarding factors, if there is a "best scenario" defined. However, for the present experimental investigation, the optimization of the factors and obtaining the best scenario is out of the scope.

Step 12. Conducting confirmation experiments: This step is not required for the present experimental investigation, since the objective of the investigation is not the optimization of the factors and obtaining the best scenario. If the objective of the investigation involves optimization and improvement of the process, the confirmation experiments should be done after obtaining the ANOVA results, in order to check whether the best scenario is obtained with the optimum conditions (levels) of the factors determined.

3.3.3. Performing the Statistical Analysis

Design of Experiments can be employed using different approaches, depending on the data collection. When an F test is used to test a hypothesis concerning the means of three or more populations, the technique is called ANOVA [100]. Taguchi Method can be employed to design the experiments with standard orthogonal arrays, and the experimental data can be analyzed with ANOVA. In this Section, the analysis procedure is handled, whereas the analysis results are presented in Chapter 4, Section 4.3.

At this point, it is useful to give an insight on the analysis procedure. Firstly, the experimental data should be well-arranged. A sample arrangement of experimental data for a two leveled three factor experiment is given in Table 15.

Table 15. Arrangement template of experimental data (for a two leveled (1, 2) three factor (*A, B,* and *C*) experiment with *m* repetitions)

Repetitions	Factors	A1		A2	
		B1	B2	B1	B2
1	C1				
	C2				
2	C1				
	C2				
⋮	C1				
	C2				
m	C1				
	C2				

The analysis is constructed on the model selected. Among the models available, which are fixed effects model, random effects model, and mixed effects model (the combination of the fixed effects model and the random effects model), the fixed effects model is appropriate for the present experimental investigation. The regarding additive model is given as Equation (47).

$$\mu = \bar{T} + \sum_{i=1}^{k} (\overline{CF}_i - \bar{T}) \tag{47}$$

In Equation (47), μ is the response (the quality characteristic), *CF* denotes the factors, whose effects are determined as significant on the quality characteristic through ANOVA, and *T* is the sum of all observations. The sign "–" upon the terms in Equation (47) denote the average of the corresponding terms. The *CF* can be one or more among the following: the factors (*A, B,* and *C*), their two factor interactions (*AB, AC,* and *ABC*), and their three factor interaction (*ABC*).

Detailed formulations of ANOVA are given below. The formulations (Equation (48-54)) are taken from [92]. One can refer to [92] for more detailed explanations on calculations.

The sum of squares of the main effects of the factors is calculated for each factor (*A, B,* and *C*) using Equations (48-50). The subscripts are provided as 1 and 2 for convenience, since each factor has two levels. In Equations (48-50), *N* is the total number of observations, and *n* is the number of observations for i^{th} level of the corresponding factor.

$$SS_A = \frac{(A_1 - A_2)^2}{N} = \frac{{A_1}^2}{n_{A_1}} + \frac{{A_2}^2}{n_{A_2}} - \frac{T^2}{N} \tag{48}$$

$$SS_B = \frac{(B_1 - B_2)^2}{N} = \frac{{B_1}^2}{n_{b_1}} + \frac{{B_2}^2}{n_{b_2}} - \frac{T^2}{N} \tag{49}$$

$$SS_C = \frac{(C_1 - C_2)^2}{N} = \frac{{C_1}^2}{n_{c_1}} + \frac{{C_2}^2}{n_{c_2}} - \frac{T^2}{N} \tag{50}$$

The sum of squares of the two factor interactions (*AB, AC* and *BC*) are calculated through Equations (51-53). Before providing the formulas for the calculations of SS_{AB}, SS_{AC}, and SS_{BC}, it is useful to touch on to the subtotal tables of *a*×*b, a*×*c* and *b*×*c*. Construction of these subtotal tables are not compulsory for ANOVA calculations, but their utilization makes the calculations more clear and easier. Sample templates for the subtotal tables of *a*×*b, a*×*c*, and *b*×*c* tables are given in Tables 16-18.

Table 16. Subtotal table of *a*×*b*

a×*b*	*B1*	*B2*
A1	Sum of the terms corresponding to *(A1B1)*	Sum of the terms corresponding to *(A1B2)*
A2	Sum of the terms corresponding to *(A2B1)*	Sum of the terms corresponding to *(A2B2)*

Table 17. Subtotal table of *a*×*c*

a×*c*	*C1*	*C2*
A1	Sum of the terms corresponding to *(A1C1)*	Sum of the terms corresponding to *(A1C2)*
A2	Sum of the terms corresponding to *(A2C1)*	Sum of the terms corresponding to *(A2C2)*

Table 18. Subtotal table of *b*×*c*

b×*c*	*C1*	*C2*
B1	Sum of the terms corresponding to *(B1C1)*	Sum of the terms corresponding to *(B1C2)*
B2	Sum of the terms corresponding to *(B2C1)*	Sum of the terms corresponding to *(B2C2)*

The S_{AB}, S_{AC}, and S_{BC} are calculated by using the subtotal tables (see Table 16-18) with Equations (51-53).

$$S_{AB} = \frac{(AB_1 - AB_2)^2}{N} = \frac{(AB_1)^2}{n_{AB_1}} - \frac{(AB_2)^2}{n_{AB_2}} - \frac{T^2}{N} \tag{51}$$

$$S_{AC} = \frac{(AC_1 - AC_2)^2}{N} = \frac{(AC_1)^2}{n_{AC_1}} - \frac{(AC_2)^2}{n_{AC_2}} - \frac{T^2}{N} \tag{52}$$

$$S_{BC} = \frac{(BC_1 - BC_2)^2}{N} = \frac{(BC_1)^2}{n_{BC_1}} - \frac{(BC_2)^2}{n_{BC_2}} - \frac{T^2}{N} \tag{53}$$

The sum of squares of the three factor interaction (ABC) is calculated through Equation (54). At this point, one can refer to the *a*×*b*×*c* subtotal table (see Table 19).

$$SS_{ABC} = \frac{(ABC_1 - ABC_2)^2}{N} = \frac{(ABC_1)^2}{n_{ABC_1}} - \frac{(ABC_2)^2}{n_{ABC_2}} - \frac{T^2}{N} \tag{54}$$

where S_{ABC} denotes the sum of squares of the cells in the *a*×*b*×*c* table. A sample template for the subtotal table of *a*×*b*×*c* is given in Table 19.

Table 19. Subtotal table of $a \times b \times c$

$a \times b \times c$	*A1*		*A2*	
	B1	*B2*	*B1*	*B2*
C1	Sum of the terms corresponding to *(A1B1C1)*	Sum of the terms corresponding to *(A1B2C1)*	Sum of the terms corresponding to *(A2B1C1)*	Sum of the terms corresponding to *(A2B2C1)*
C2	Sum of the terms corresponding to *(A1B1C2)*	Sum of the terms corresponding to *(A1B2C2)*	Sum of the terms corresponding to *(A2B1C2)*	Sum of the terms corresponding to *(A2B2C2)*

After the calculation of the sum of squares of the main effects of the factors (SS_A, SS_B, and SS_C), their two factor interactions (SS_{AB}, SS_{AC}, and SS_{BC}) and their three factor interaction (SS_{ABC}); the sum of squares of the error SS_E should be determined using Equation (55).

$$SS_E = SS_T - (SS_A + SS_B + SS_C + SS_{AB} + SS_{AC} + SS_{BC} + SS_{ABC}) \quad (55)$$

where the SS_T denotes the total sum of squares, which is calculated using Equation (56). In Equation (56), Y_i denotes the all the observations taken (see Table 15).

$$SS_T = \left[\sum_{i=1}^{N} {Y_i}^2\right] - \frac{T^2}{N} \quad (56)$$

As it was mentioned in Section 3.3.1, two different hypotheses, namely the null hypothesis (H_0) and the alternative hypothesis (H_a) are tested. The H_0 claims that there is no difference between the levels of a particular factor, which means the effect of the factor is insignificant on the quality characteristic at a significance level of α. The H_a claims that the levels of a particular factor are different, which means the effect of the factor is significant on the quality characteristic at a significance level of α.

At the hypothesis testing step, the α error is very important. As it was given in Figure 16 in Section 3.3.1, the α error is the probability that the null hypothesis (H_0) will be rejected, when in fact, it is true [92]. If the α is selected as 0.05, this means that the chance of rejecting H_0 when it is true is 0.05, whereas the chance of accepting H_0 when it is true is 0.95. The α error is therefore called as significance level, as well. As it is seen from this explanation, as the α value decreases, the probability of the correct decision and the level of analysis being sophisticated are getting higher.

The hypothesis testing involves six steps. In order to give example, these steps are explained below for factor A, only. For all the other factors and interactions considered, the below given steps should be followed, as well.

Step 1. Construction of the hypotheses:

At this step; two different hypotheses, i.e. the null hypothesis (H_0) and the alternative hypothesis (H_a) are employed, and the H_0 is tested. If the H_0 is rejected, then the H_a is accepted. The H_0 and H_a hypotheses are given below. The term μ_{A_i} in the hypotheses statements is the average of the observations for the each level (1, 2) of factor *A*.

H_0: $\mu_{A_1} = \mu_{A_2}$ (The effect of *A* is insignificant at a significance level of α)
H_a: $\mu_{A_1} \neq \mu_{A_2}$ (The effect of *A* is significant at a significance level of α)

Step 2. Determination of the test statistic: The F test is used to compare the means of the factor levels. The *F* statistic is defined as the ratio of the mean square of the factor to the mean square of the error, as in Equation (57).

$$F_A = \frac{MS_A}{MS_E} \tag{57}$$

Step 3. Selection of the significance level:

The significance level (α) is selected. It is important to recall that, the significance level (α error) is the probability of the acceptance of a hypothesis, which is not in fact true. Therefore, the smaller the α is, the more sophisticated the analysis gets. As a widely used value in pure sciences and engineering practices, α can be selected as 0.05.

Step 4. Development of the decision rule:

if $F_A \leq F_{table}$; the H_0 is accepted.

if $F_A > F_{table}$; the H_a is accepted.

F_{table} is the reference value taken from the F table. For a particular factor (e.g. *A*) F_{table} is the value corresponding to $F_{\alpha, v1, v2,}$ such as the *v1* is the degree of freedom of *A*, and *v2* is the degree of freedom of the error (see Table 20).

Step 5. Calculations: Calculation of the test statistic F (for A: F_A) is done.

Step 6. Result and decision:

If $F_A \leq F_{table}$; the H_0 is accepted.
Decision: The effect of *A* is insignificant at a significance level of α.

If $F_A > F_{table}$; the H_a is accepted.
Decision: The effect of *A* is significant at a significance level of α.

After performing the abovementioned steps, the ANOVA table can be constructed in the form given in Table 20.

Table 20. ANOVA: Standard table and formulas

Source of variation	*SS*	d_f	*MS*	*F*	F_{table}
A	SS_A	$d_{f_A}=a\text{-}1$	SS_A/d_{f_A}	MS_A/MS_E	$F_{\alpha,d_{f_A},d_{f_E}}$
B	SS_B	$d_{f_B}=b\text{-}1$	SS_B/d_{f_B}	MS_B/MS_E	$F_{\alpha,d_{f_B},d_{f_E}}$
C	SS_C	$d_{f_C}=c\text{-}1$	SS_C/d_{f_C}	MS_C/MS_E	$F_{\alpha,d_{f_C},d_{f_E}}$
AB	SS_{AB}	$d_{f_{AB}}=d_{f_A}.\,d_{f_B}$	$SS_{AB}/d_{f_{AB}}$	MS_{AB}/MS_E	$F_{\alpha,d_{f_{AB}},d_{f_E}}$
AC	SS_{AC}	$d_{f_{AC}}=d_{f_A}.\,d_{f_C}$	$SS_{AC}/d_{f_{AC}}$	MS_{AC}/MS_E	$F_{\alpha,d_{f_{AC}},d_{f_E}}$
BC	SS_{BC}	$d_{f_{BC}}=d_{f_B}.\,d_{f_C}$	$SS_{BC}/d_{f_{BC}}$	MS_{BC}/MS_E	$F_{\alpha,d_{f_{BC}},d_{f_E}}$
ABC	SS_{ABC}	$d_{f_{ABC}}=d_{f_A}.\,d_{f_B}.\,d_{f_C}$	$SS_{ABC}/d_{f_{ABC}}$	MS_{ABC}/MS_E	$F_{\alpha,d_{f_{ABC}},d_{f_E}}$
Error	SS_E	$d_{f_E}=d_{f_T}\text{-}\,d_{f_{ABC}}$	SS_E/d_{f_E}		
Total	SS_T	$d_{f_T}=\,d_{f_{ABC}}\text{-}\,1$			

In Table 20, the parameters *SS*, d_f, *MS*, *F* and F_{table} denote the sum of squares, degree of freedom, mean square, the calculated *F* value of the factor, and the *F* value obtained from F table, respectively. In addition to the aforementioned parameters, the "pure sum of squares (*SS'*)", which is the sum of squares of a factor that is purified from the error, can be calculated for factor *A* as in Equation (58), which will help at the estimation of the contribution (%) of the factors, as indicated in Equation (59). The calculation is the same for the other factors, as well.

$$SS'_A = SS_A - \left(MS_E \,.\, d_{f_A}\right) \tag{58}$$

$$Contribution\,\%\ of\ A = \frac{SS'_A}{SS_T} \tag{59}$$

In this Section, the calculations and decision making procedures in ANOVA are given in detail. This procedure is applied on the data of present experimental investigation, which is presented in Chapter 4, Section 4.3.

3.3.4. Conclusions

In this Chapter, the material and method are described, in order to construct the basis of the experimental study and the statistical analysis presented in Chapter 4.

Regarding the material topic, information is given on the nanofluid samples used in experiments, first. The characterization of the nanofluid samples is considered as very important, thus the zeta potential and the particle size distribution analyses are explained in detail. Since the effects of the zeta potential and particle size distribution are important on the colloidal behavior of nanofluids, they should be investigated when studying nanofluid viscosity.

After the information given on the experiment samples, the methodology of the experimental study is given, in detail. The methodology used for constructing the experimental study is DOE, which is a very useful tool based on statistics. DOE is widely used and appreciated for a considerable time for many fields, but its implementation for the field nanofluid viscosity is novel, to the best of the author's knowledge.

It is important to point out to the importance of employing DOE, since the determination of the effects of the factors (temperature, nanoparticle volumetric fraction and nanoparticle diameter, for the present investigation) on the quality characteristic (nanofluid viscosity and relative viscosity, for the present investigation) will have a more solid basis with DOE, by means of the statistical results. In addition, utilization of the statistics with experimental studies can be regarded as crucial, since statistics helps the researchers to have a stronger understanding on the results, which considerably helps provide valuable comments on the research.

CHAPTER 4

EXPERIMENTAL INVESTIGATION AND STATISTICAL EVALUATION OF Al_2O_3-H_2O NANOFLUID VISCOSITY

In this Chapter, the experimental investigation on Al_2O_3–H_2O nanofluid viscosity for varying temperature, nanoparticle volumetric fraction, and nanoparticle diameter is presented, first. The relationships between the aforementioned parameters and nanofluid viscosity and relative viscosity are shown. The experimental study involves stability evaluation of the nanofluids, as well. After that, the statistical evaluation of the experimental data is done. Two different correlations for the nanofluid viscosity and relative viscosity based on the present investigation are presented. Finally, some conclusions are drawn.

4.1. Introduction

In this Chapter, Section 4.2 is concerned with the experimental investigation on the Al_2O_3–H_2O nanofluid viscosity. The experimental setup and the experimental procedure of the measurement of Al_2O_3–H_2O nanofluid viscosity were presented in Chapter 3, in detail.

The experiments were planned with DOE before they were performed. Therefore, the current experimental investigation is based on a systematic approach. Section 4.3 is concerned with the statistical evaluation of the experimental data. The calculation procedure and the outputs of the statistical evaluation are presented in detail.

4.2. Experimental Study on the Al_2O_3–H_2O Nanofluid Viscosity

The viscosity of Al_2O_3–H_2O nanofluids are measured for varying temperatures (T= 20°C, 30°C, 40°C, and 50°C), nanoparticle volumetric fractions (φ= 0.01, 0.02, and 0.03), and nanoparticle diameters (d_p= 10 nm and 30 nm). In the experiments, the 40 ml and 10 ml samples are examined. When the viscosity of the sample is to be measured irrespective of temperature, the 40 ml samples are used, whereas if the temperature of the sample is to be regulated, the 10 ml samples are used.

The measurements are concerned with the evaluation on the nanofluid viscosity at room temperature (Section 4.2.1), nanofluid viscosity for varying temperatures (Section 4.2.2), nanofluid viscosity for varying nanoparticle volumetric fractions (Section 4.2.3), and nanofluid viscosity for varying nanoparticle diameters (Section 4.2.4). The stability of the examined nanofluids is evaluated at room temperature for different relaxation durations. In addition to the aforementioned, the representability of the samples, i.e. the effect of the differences in sample volumes on nanofluid viscosity is evaluated, as well.

4.2.1. Measurement of Al_2O_3-H_2O Nanofluid Viscosity at Room Temperature

Nanofluid viscosity measurement at room temperature is done as a starting point. The experiments done at room temperature are concerned with the effect of ultrasonication on nanofluid viscosity, and the evaluation of the small volume samples' representativeness on the sample in the main container.

The effect of ultrasonication on the viscosity of nanofluids is evaluated in terms of the ultrasonication time and power. The effect of ultrasonication on nanofluid viscosity is investigated by comparing the viscosities of the relaxed nanofluid samples that were ultrasonicated for different durations and powers.

The nanofluid samples examined at room temperature are of 40 ml volume. Since the nanofluids can be poly disperse and heterogeneous, the nanoparticle fraction within the samples in the small containers can be different than the sample in the main container. Therefore, evaluation of the representativeness of the small volume samples is important.

4.2.1.1. Decision Making on the Ultrasonication Time and Power

In the experiments, the nanofluids are used as they were supplied. The only process done on the nanofluid samples is the ultrasonication, by a high speed stirring of the suspension to ensure the mono dispersed and homogeneous condition of the particles within the suspension. The ultrasonication of the samples is applied as in Figure 22.

Figure 22. Ultrasonication of the nanofluids. The nanofluid is in the middle of the container, in which the ultrasonication tip is submerged. The containers at the corners are full of cold water, in order to limit the heating of the nanofluid, as a result of the ultrasonication.

It is important to obtain the optimum stability of the nanofluid samples. For this purpose, the ultrasonication is applied to the nanofluids, and it is regulated by the ultrasonication time and power. Therefore, the viscosity of nanofluids is investigated for different ultrasonication periods and powers applied on the samples. The results of the investigation on the viscosities of nanofluids at room temperature are provided below in Table 21.

Table 21. Viscosities of d_p= 10 nm and d_p= 30 nm nanofluids. Effect of different ultrasonication conditions on viscosity is shown.

Sample	After ultrasonication (mPa.s) *, **	After relaxation of few hours (mPa.s)	After one night relaxation (mPa.s)	Relative difference (%) between the first ultrasonication and one night relaxation ***
d_p= 10 nm (50 ml)****	2.84 *	3.01	3.18	11.97
	2.65 **	2.66	2.68	1.13
d_p= 30 nm (50 ml)****	3.65 *	4.24	4.13	13.15
	3.73 **	3.75	3.85	3.22

* The sign indicates the ultrasonication is done for 2 minutes at 30 W.
** The sign indicates the ultrasonication is done for 2 minutes at 70 W.
*** Relative difference % = [((new value) - (reference value)) / (reference value)] * 100
**** The ultrasonication samples were more than 40 ml to make up for losses during material transfer.

The relative differences given in Table 21 show that, the nanofluids ultrasonicated for 2 minutes at 70 W are more stable than the nanofluids ultrasonicated for 2 minutes at 30 W. Therefore, the ultrasonication to be applied on the nanofluids for the investigation is decided as 2 minutes at 70 W, in order to ensure their stability. As a result, the samples of the temperature dependent measurements are ultrasonicated for 2 minutes at 70 W, and used straightaway.

4.2.1.2. Viscosity of Nanofluids After Ultrasonication at Room Temperature and the Evaluation on Sample Representability

In Section 4.2.1.1, the decision making on the ultrasonication time and power was provided. The ultrasonication on the nanofluids was decided to be applied for 2 minutes at 70 W, since the most stable viscosity results (with less relative difference between after ultrasonication and after one night relaxation, see Table 21) were obtained with these ultrasonication conditions.

The viscosity of nanofluids is measured at room temperature, first. Since the possibilities of the nanofluids being poly disperse and heterogeneous is significant, it is important to examine whether there is a difference between the viscosities of the samples of different volumes. In order to ensure the objectivity of the following measurements, the representability of the small volume samples of the sample in main container, which is filled with nanofluid of 1 kg (1,1709 ml), should be evaluated. For this purpose, whether the samples in the small containers (Figure 23b) represent the sample in the main containers (Figure 23a) is examined. All samples other than φ= 0.01 are examined, since the differences are thought to be more significant for concentrated samples.

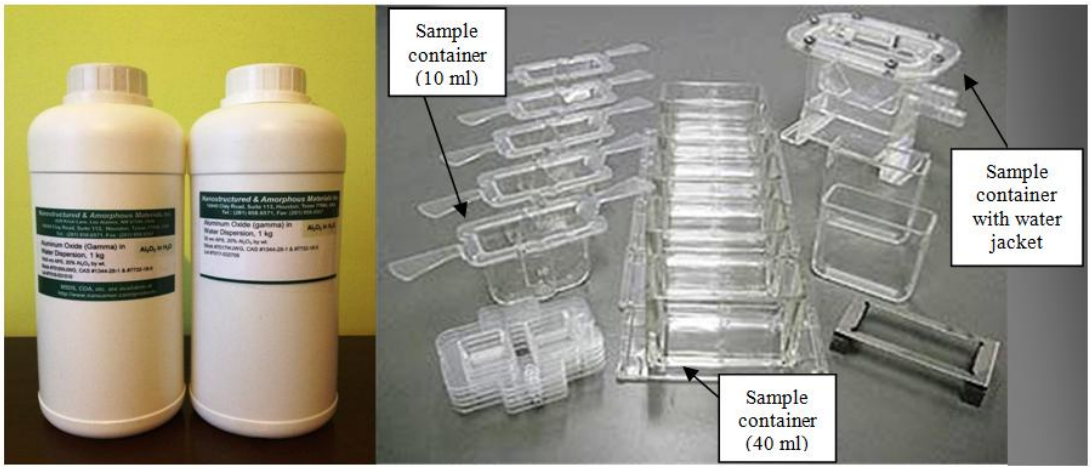

Figure 23. a) Nanofluids purchased from NanoAmor, b) Sample containers of Sine Wave Vibro Viscometer SV-10. Adapted from [102]

The magnitudes of the viscosities of φ= 0.0633, 0.03, and 0.02 nanofluids are illustrated in Figure 24 and Figure 25 for d_p= 10 nm and d_p= 30 nm, respectively.

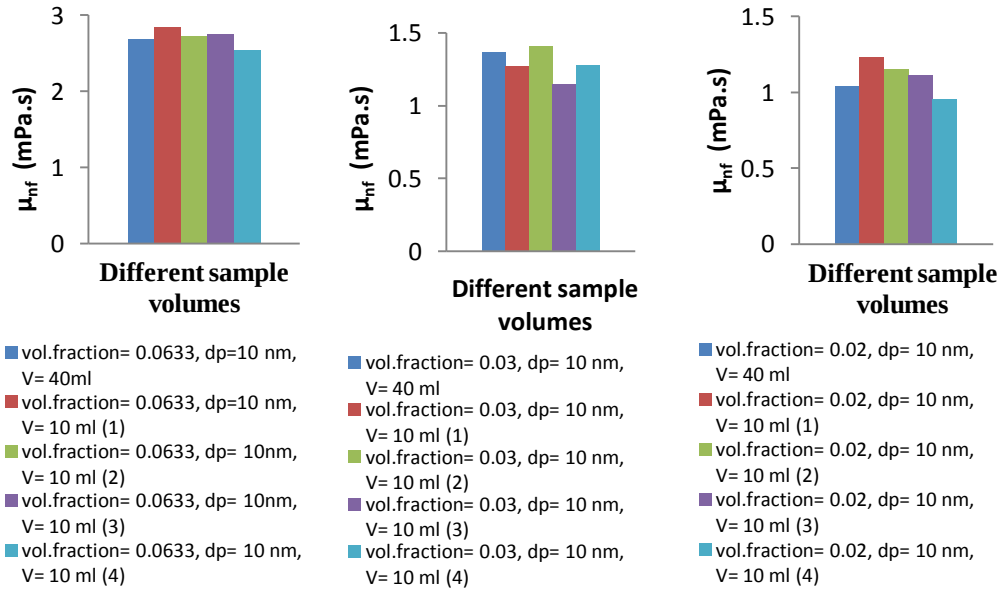

Figure 24. The viscosities of 40 ml and 10 ml, φ= 0.0633, 0.03, and 0.02*;* d_p= 10 nm Al_2O_3–H_2O nanofluids at room temperature

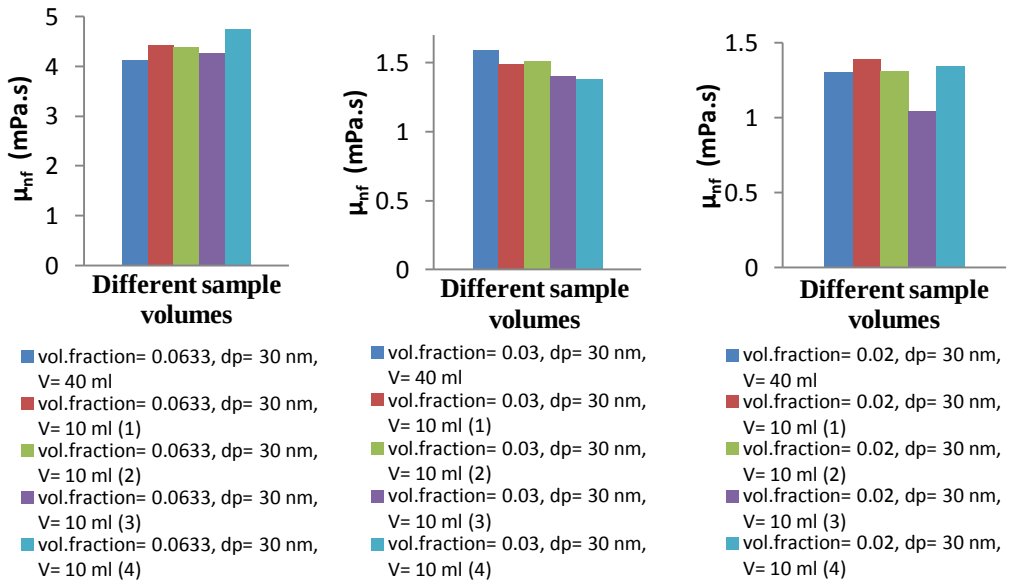

Figure 25. The viscosities of 40 ml and 10 ml, φ= 0.0633 (a), 0.03 (b) and 0.02 (c); d_p= 30 nm Al_2O_3–H_2O nanofluids at room temperature

In Table 22, the averages of the viscosities of the samples of 10 ml and the viscosities of the samples of 40 ml are given with the relative differences between them.

Table 22. The representability evaluation of the samples of 10 ml on the samples of 40 ml

Sample	Average* viscosity of the 10 ml sample	Viscosity of the 40 ml sample	Relative difference (%) **
φ= 0.0633, d_p= 30 nm	4.4525	4.1200	8.0704
φ= 0.0633, d_p= 10 nm	2.7150	2.6900	0.9294
φ= 0.03, d_p= 30 nm	1.4450	1.5900	-9.1195
φ= 0.03, d_p= 10 nm	1.2775	1.3700	-6.7518
φ= 0.02, d_p= 30 nm	1.2700	1.3000	-2.3077
φ= 0.02, d_p= 10 nm	1.1100	1.0400	6.7308

* Average = [($\mu_{sample(1)}$ + $\mu_{sample(2)}$ + $\mu_{sample(3)}$ + $\mu_{sample(4)}$) / 4]
** Relative difference % = [((new value) - (reference value)) / (reference value)] * 100

As it is illustrated in Figure 24 and Figure 25 and provided in Table 22, the viscosities of the samples of 10 ml are different from the samples of 40 ml, for the φ= 0.02, 0.03 and 0.066, d_p= 10 and 30 nm nanofluids considered. From this point forth, it is decided to measure the viscosities of each of the 10 ml of 40 ml nanofluids prepared for each condition (this approach will be called as four repetitions for each case, herein), and use their averages when presenting the data with graphics, to be able to obtain more objective results.

The averages of the four measurements taken for T= 20, 30, 40, and 50°C, φ= 0.01, 0.02, and 0.03, and d_p= 10 and 30 nm samples are presented in Table 23. Raw data of the entire experiment is provided in Appendix F. For completeness, Table 18 presents all data used for the graphs appearing in the next three sections, which are specifically about the effects of temperature, nanoparticle

volumetric fraction, and nanoparticle diameter, respectively. Therefore, their discussion is not given here.

Table 23. Experimental results for the viscosity (mPa.s) of Al_2O_3–H_2O nanofluids

		d_p (nm)	
T (°C)	φ	10	30
20	0.01	1.1650	1.1475
20	0.02	1.1500	1.5425
20	0.03	1.6200	1.7850
30	0.01	0.8800	0.9700
30	0.02	0.9800	1.2250
30	0.03	1.2900	1.3900
40	0.01	0.6800	0.8050
40	0.02	0.7500	0.9800
40	0.03	1.0000	1.1900
50	0.01	0.5725	0.6425
50	0.02	0.5975	0.7150
50	0.03	0.8900	1.0025

4.2.2. Viscosity of Al_2O_3–H_2O Nanofluids: Temperature Dependence

In this Section, the temperature dependent nanofluid viscosity is presented. In the experiments, water is used as the reference fluid for calibration of the viscometer. Since calibration of the equipment is very important to ensure the validity of the measurements, the measured viscosity values of water, and the reference viscosity values of water (which are the calibration values of the viscometer) is presented in Figure 26, to see whether the viscometer measures the viscosity of water as close as possible to the reference viscosity values of water.

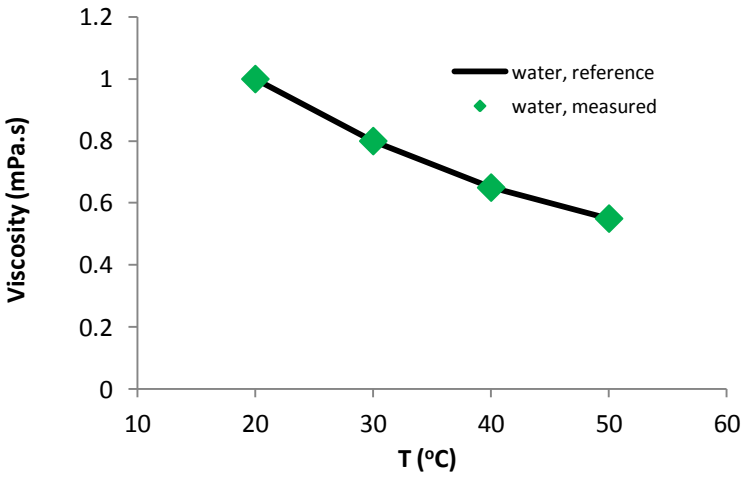

Figure 26. The viscosity of water: reference and measured values.

As it is seen in Figure 26, the reference viscosity values of water are very consistent with the measurement of the viscometer, therefore the validity of the following viscosity measurements is ensured. From this point of view, calibration of the viscometer is done before and after every nanofluid measurement.

After the calibration of the viscometer is done, and the validity of the viscosity measurements is ensured, the viscosity of nanofluids is investigated for varying temperatures. The temperature dependent nanofluid viscosity is illustrated in Figure 27.

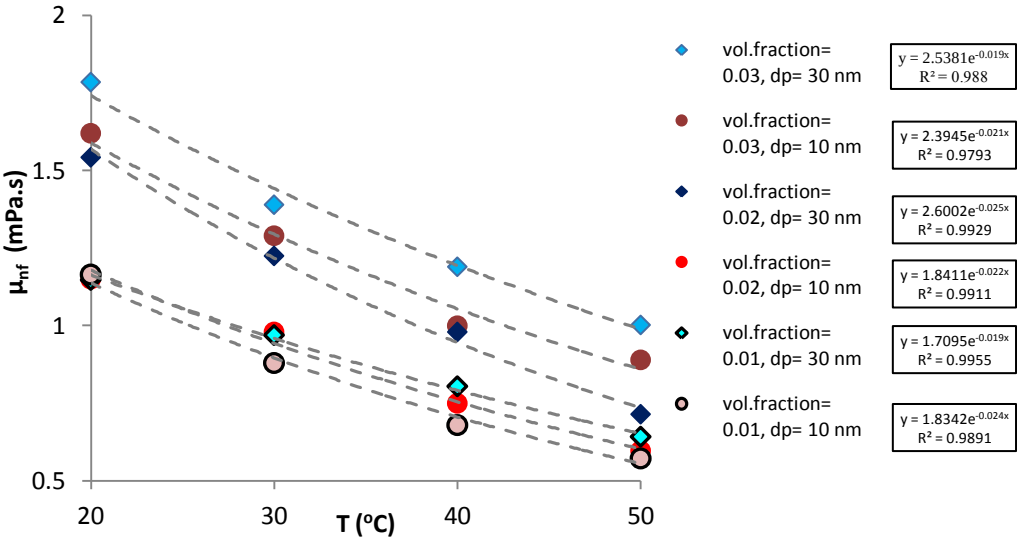

Figure 27. Nanofluid viscosity for varying temperature. Each marker represents the average of the four measurements. The grey dashed lines are the fitted exponential curves.

The experimental results of nanofluid viscosity presented in Figure 27 show that, the viscosity of nanofluids significantly decrease with increasing temperature. When the decrements in viscosities with increasing temperatures are fitted to representative curves, it is seen that exponential relationships between the nanofluid viscosity and temperature explain all the cases very well. Therefore, it can be concluded that, the viscosity of nanofluids decreases exponentially with increasing temperature.

The relative viscosity variation with temperature is illustrated in Figure 28.

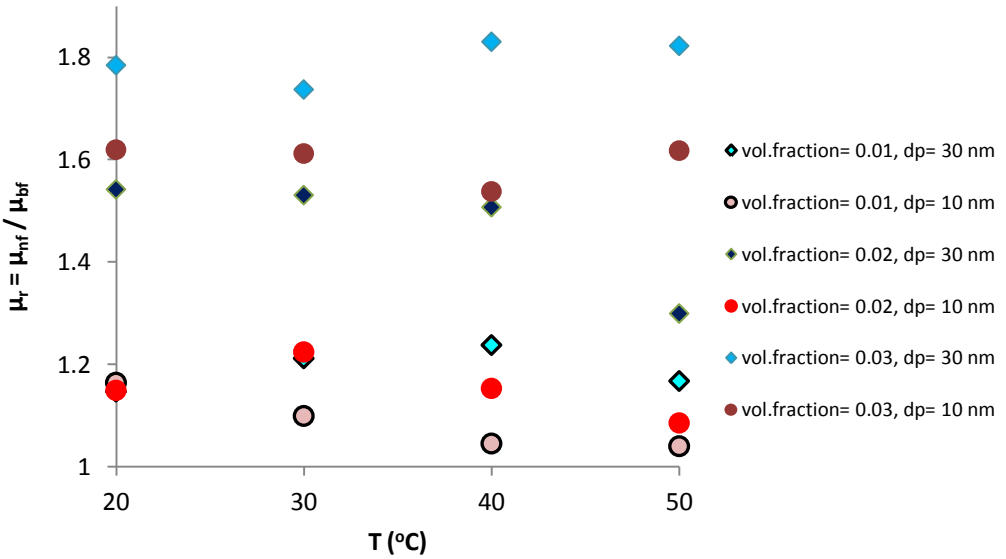

Figure 28. Relative viscosity for varying temperature. Each marker represents the average of the four measurements.

As it is seen in Figure 28, the variation of relative viscosity with temperature does not follow a classical trend, therefore for the current case, it is independent of temperature. In addition, as it was mentioned in Section 2.3.4, explaining the temperature dependence of relative viscosity may not be as simple as the temperature dependence of the nanofluid viscosity, since both the nanofluid and base fluid viscosities depend strongly on temperature.

4.2.3. Viscosity of Al_2O_3–H_2O Nanofluids: Nanoparticle Volumetric Fraction Dependence

In this Section, the nanoparticle volumetric fraction dependent nanofluid viscosity is presented. The nanofluid viscosity for varying nanoparticle volumetric fraction is illustrated in Figure 29.

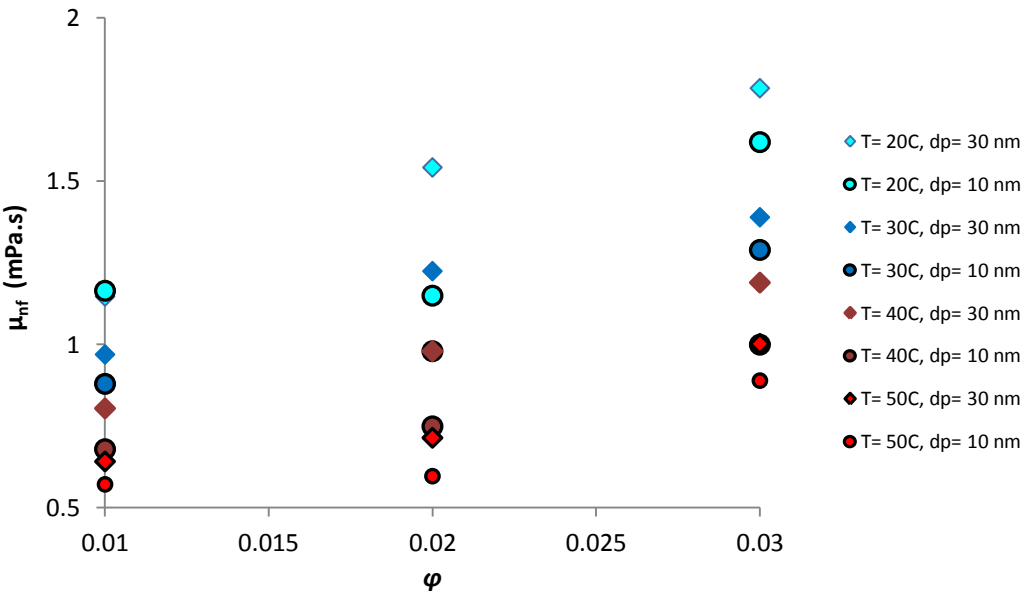

Figure 29. Nanofluid viscosity for varying nanoparticle volumetric fraction. Each marker represents the average of the four measurements.

The experimental results presented in Figure 29 show that, the viscosity of nanofluids increases with increasing nanoparticle volumetric fraction. It is an expected result, since the viscosity of suspensions (also the conventional ones) is expected to increase with increasing solid content. But, the viscosities of the present nanofluids are within moderate levels, can be considered as acceptable, and can be compensated, if needed. Since, the stability of the nanofluids of the present investigation are found to be very high, unusual increases in nanofluid viscosity due to the phenomena such as the increased nanoparticle aggregation and/or sedimentation are not expected, and not observed.

The experimental results illustrated in Figure 29 lead to a further discussion on the amount of the viscosity increment obtained. The relative viscosity values are presented in Figure 30 for varying nanoparticle volumetric fraction.

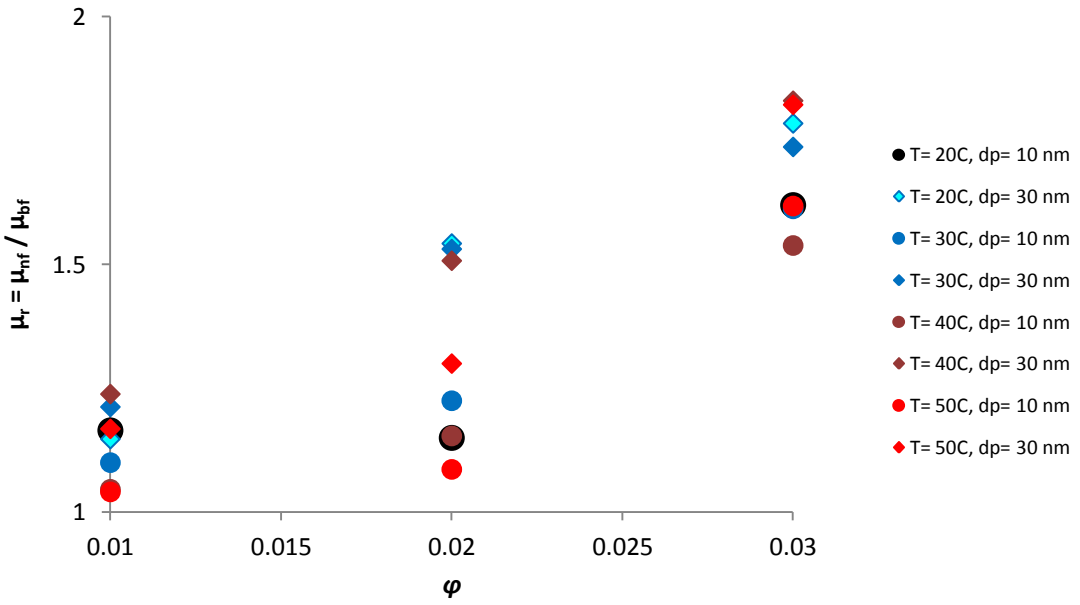

Figure 30. Relative viscosity for varying nanoparticle volumetric fraction. Each marker represents the average of the four measurements.

As it is seen in the Figure 30, the relative viscosity increases with increasing nanoparticle volumetric fraction and greater than 1 for each case considered, meaning the viscosity of examined nanofluids are higher than the viscosity of base fluid (water). The maximum viscosity increment obtained is about 1.83 times of the viscosity of water (for T= 40°C and d_p= 30 nm), which can be considered as not very critical in terms of pressure drop considerations, unless the application is very sensitive to the increment of viscosity.

4.2.4. Viscosity of Al_2O_3–H_2O Nanofluids: Nanoparticle Diameter Dependence

In this Section, the nanoparticle diameter dependent nanofluid viscosity is presented. The nanofluid viscosity for varying nanoparticle diameter is illustrated in Figure 31.

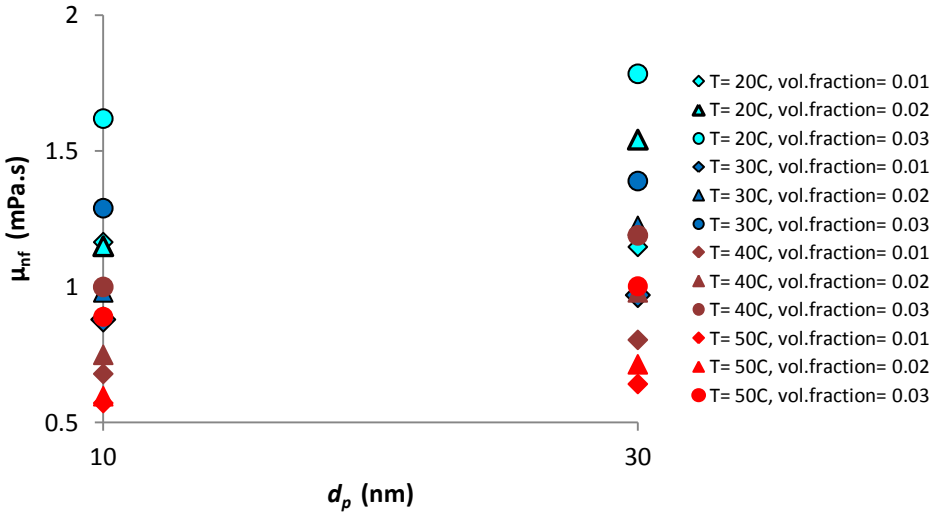

Figure 31. Nanofluid viscosity for varying nanoparticle diameter. Each marker represents the average of the four measurements.

The nanofluid viscosity literature on the nanoparticle diameter dependence is very inconsistent. However, the experimental results presented in Figure 31 shows that, the viscosity of nanofluids slightly increases with increasing nanoparticle diameter.

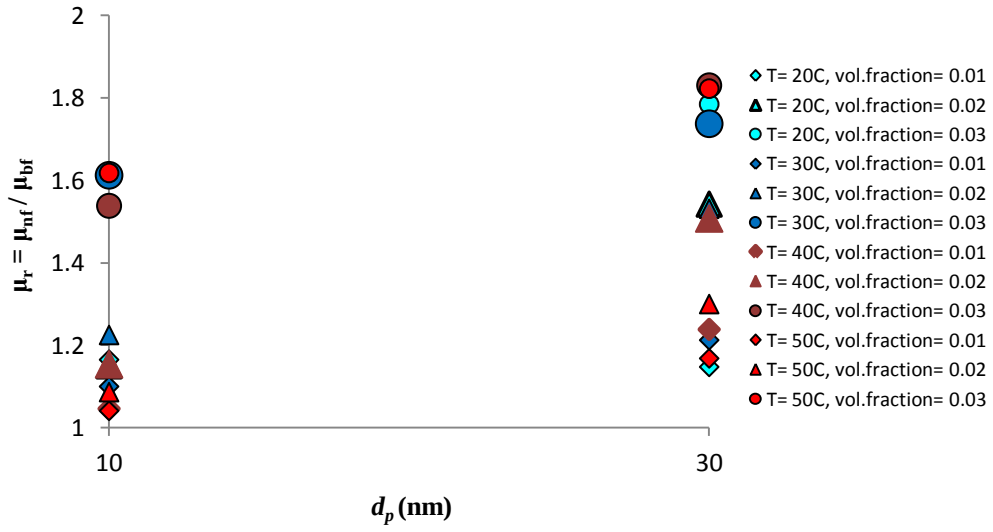

Figure 32. Relative viscosity for varying nanoparticle diameter. Each marker represents the average of the four measurements.

The relative viscosity data are presented in Figure 32 for varying nanoparticle diameter. As it is seen in the Figure, the relative viscosity generally increases with increasing nanoparticle diameter (only the relative viscosity of T= 20^{o}C and φ= 0.01 nanofluid does not show any increment with d_p), and greater than 1 for each case considered, meaning the viscosity of examined nanofluids are higher than the viscosity of base fluid (water).

The relative viscosity increment (in general) with increasing nanoparticle diameter may be attributed to the termination of the existing similarity of nanofluid with the base fluid (no solid content within). As the nanofluid contains larger-sized particles, the nanofluid differs more from the base fluid, and the increment obtained in viscosity gets higher.

4.2.5. Improvements Attempted on the Experimental Process

The efficiency evaluation of the equipments used in experiments is out of the scope of the present investigation. However, brainstorming on the improvements that can be done on the experimental process is considered as necessary. Since the experiments are highly dependent on the temperature, temperature related losses are very significant during the experiments.

The experiments are done at 20^{o}C, 30^{o}C, 40^{o}C and 50^{o}C, most of which are significantly higher than the room temperature in winter conditions, when the experiments were performed. Thus, stabilizing the temperature of the sample, and limiting the heat losses to the environment is a difficult task. In addition, instabilities of temperature can result in instabilities in the results. In order to stabilize the temperature as much as possible, the following are done.

- The water jacket (see Figure 23) placed in the measurement unit is insulated using black foam insulation, and a rubber/silicon flexible pipe is used to connect the water bath and water jacket around the sample container (see Figure 33).

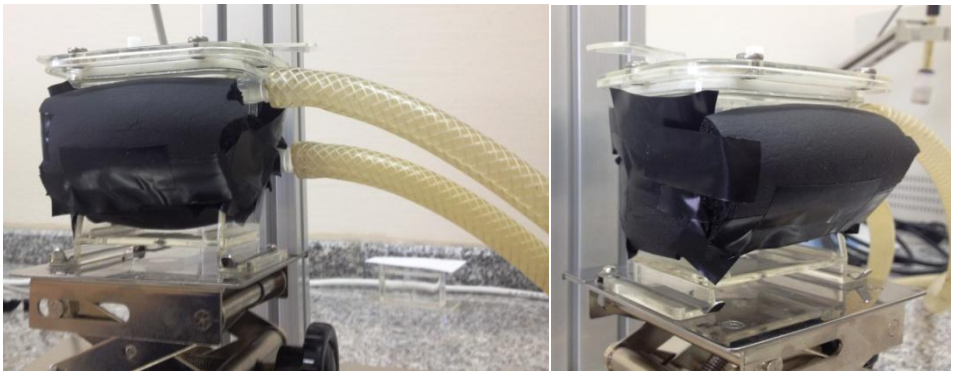

Figure 33. Insulated water jacket of the measurement unit

- The samples are stored at the examination temperature, as much as possible. For this purpose, the samples in glass bottles are submerged in large containers filled with hot water, whose temperature is near the examination temperature (see Figure 34).

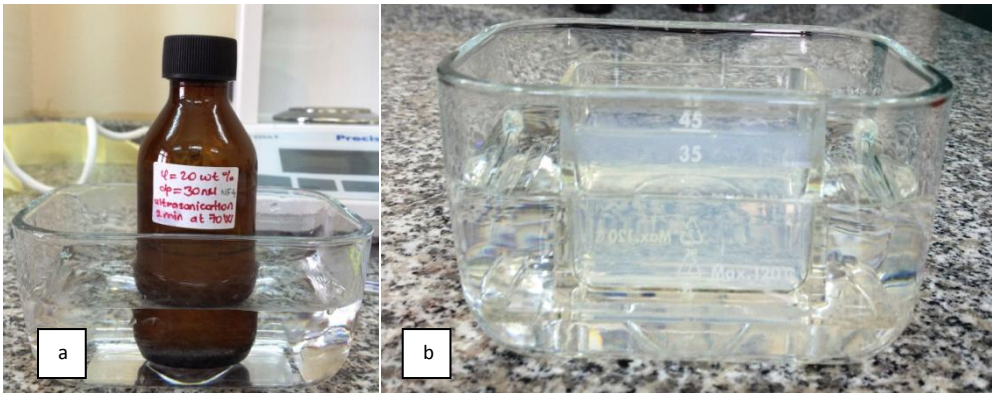

Figure 34. Nanofluid samples placed in hot water filled containers. a) nanofluid sample in a dark coloured glass bottle, b) nanofluid sample of 40 ml in sample container

- The evaporation of the sample is very significant, especially at around 40°C and 50°C (see Figure 35 for the sample stored in a sample cup, which was previously closed with a paper folio). Therefore, all nanofluids used in experiments are stored in dark colored closed bottles (as in Figure 12 and 34(a)).

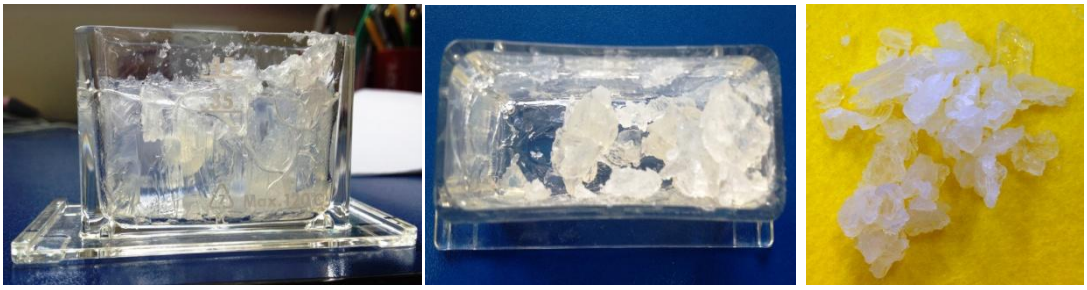

Figure 35. Evaporated nanofluids: stored in room condition for two weeks

The brainstorming done for the improvements attempted on the experimental study is considered as important, since developing an understanding of the experimental setup and experimental procedure helps conduct the experiments with minimum expense on both cost and time, in addition to its help on commenting on the results.

4.3. Statistical Evaluation on the Al_2O_3–H_2O Nanofluid Viscosity and Relative Viscosity

The detailed information and the calculation procedure of the statistical analysis done on the experimental data were given in Section 3.3. To mention briefly, the experiments were designed with Taguchi Method, and the L_8 standard orthogonal array was selected for the arrangement of experiments. The algorithm given in Section 3.3.2 was followed and the ANOVA results are showing the effects of the temperature, nanoparticle volumetric fraction, and nanoparticle diameter on nanofluid viscosity.

As it can be recalled from Section 3.3.2.1, ANOVA results show the effects of the factors (i.e. *A*: temperature, *B*: nanoparticle volumetric fraction and *C*: nanoparticle diameter) on the quality characteristic (i.e. nanofluid viscosity, and relative viscosity). The comparison of the magnitude (importance) of these parameters' effects on the quality characteristic is also possible.

From this point of view, it is decided to compare whether the minimum and maximum values of the factors (i.e. 20°C and 50°C for temperature (*A*), 0.01 and 0.03 for nanoparticle volumetric fraction (*B*), and 10 nm and 30 nm for nanoparticle diameter (*C*)) make any difference on the nanofluid viscosity and relative viscosity, first. The reason of this decision is to enhance the resolution and applicability of the experimental results. The results of the analysis on the nanofluid viscosity are presented in Section 4.3.1, whereas the results of the analysis on the relative viscosity are presented in Section 4.3.2.

In consequence of the statistical analyses presented in Section 4.3.1 and Section 4.3.2, new correlations for the nanofluid viscosity and relative viscosity are suggested in Section 4.3.3 and Section 4.3.4, respectively.

4.3.1. Statistical Evaluation of the Nanofluid Viscosity: Analysis Results

The ANOVA results showing the effects of temperature (*A*), nanoparticle volumetric fraction (*B*), nanoparticle diameter (*C*), and their two and three factor interactions on the nanofluid viscosity, at a significance level of α= 0.05, are given in Table 24. The data entering to the program for ANOVA is provided in Table 38 in Appendix E.

Table 24. ANOVA results for the nanofluid viscosity

Source of variation	*SS*	d_f	*MS*	*F*	F_{table}	*Significant effect ?*	α
A	3.40605	1	3.40605	533.237	4.26	YES	5 %
B	1.56645	1	1.56645	245.237	4.26	YES	
C	0.05445	1	0.05445	8.524	4.26	YES	
AB	0.08611	1	0.08611	13.481	4.26	YES	
AC	0.00061	1	0.00061	0.096	4.26	NO	
BC	0.02531	1	0.02531	3.963	4.26	NO	
ABC	0.00980	1	0.00980	1.534	4.26	NO	
Error	0.15330	24	0.00639				
Total	5.30209	31	3.40605				

As a reminder, in Table 24, *SS* is the sum of squares of the regarding terms (see Section 3.3.3 for the calculation procedure), d_f is the degree of freedom of the regarding factor (which is 1 less than its number of levels), *MS* is the mean square of the regarding terms and defined as the ratio of *SS* to d_f. For a particular factor (here, let the factor be *A*), *F* is the ratio of the *MS* of factor *A* to the *MS* of the error (i.e. $F_A=MS_A/MS_E$). F_{table}, which is defined as $F_{\alpha,d_{f_{factor}},d_{f_E}}$ in Table 20 of Section 3.3.3, is a standard value taken from the F table [101]. For the case in Table 19, the d_f of all the factors and interactions is 4.26, which is the value corresponds to α= 0.05, d_f =1 and d_{f_E}=24. For the cases when $F > F_{table}$ the effect of the factor is significant.

As it was mentioned in Section 3.3.2.3 that, the mean effects graphics of the factors are used to determine the optimum conditions of the regarding factors, if there is a "best scenario" defined. Since the determination of the optimum values of the factors are out of the scope of the present investigation, the main effects graphics are provided in Figure 36 to visualize the general trend.

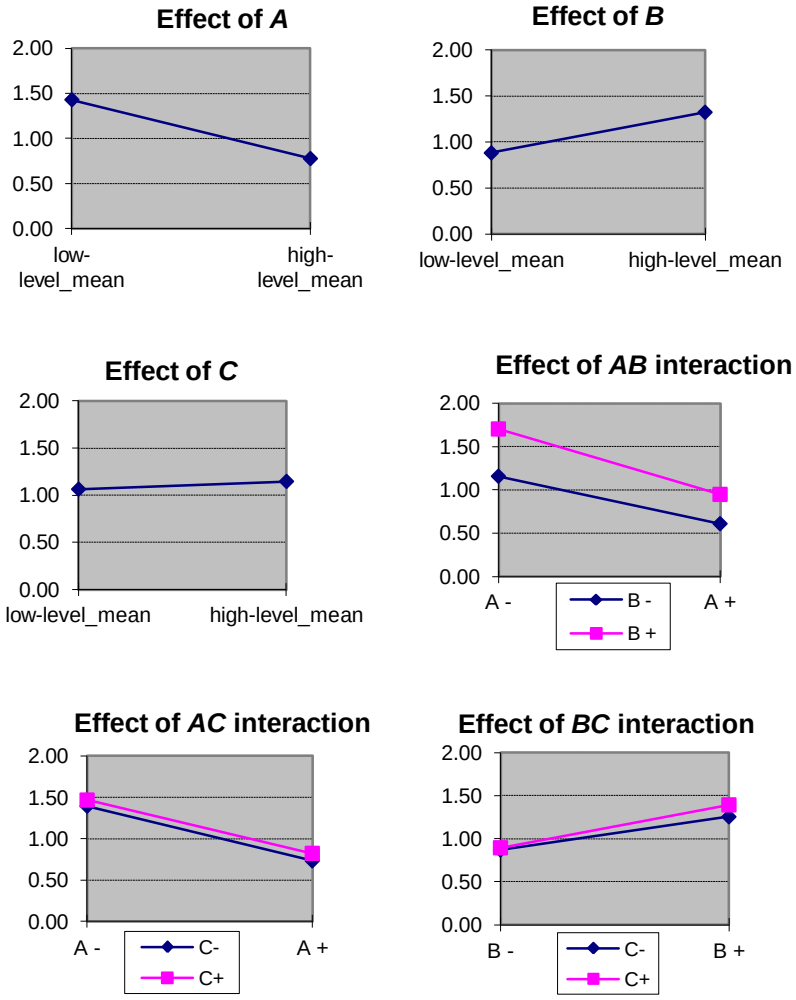

Figure 36. Main effects graphics corresponding the effects of *A*, *B*, *C*, *AB*, *AC* and *BC* on the nanofluid viscosity. The factors on the figures are: *A*: temperature, *B*: nanoparticle volumetric fraction, *C*: nanoparticle diameter, *AB*: two factor interaction of *A* and *B*, *AC*: two factor interaction of *A* and *C*, *BC*: two factor interaction of *B* and *C*

The decision on the significance of the effect of a factor is based on the comparison of the F value of the factor with F_{table}. As can be recalled from Section 3.3.3, if F > F_{table}, the effect of the factor is significant at that significance level (α).

From the results presented in Table 24, the following can be concluded:

- The main effects of *A* (temperature), *B* (nanoparticle volumetric fraction), and *C* (nanoparticle diameter) on the nanofluid viscosity are significant. The importance of the main effects of the factors

on the nanofluid viscosity can be described from high to low sequence as: $A > B > C$ (because the F values of the regarding factors are: $F_A > F_B > F_C$).

- The effect of *AB* interaction is significant on the nanofluid viscosity. Meaning, the effect of the A (temperature) on nanofluid viscosity for varying *B* (nanoparticle volumetric fraction) does not follow the same trend for all *B* (nanoparticle volumetric fractions) considered, or vice versa. As the temperature increases, the interaction of the molecules, thus, particles (due to their similar size range at the nanometer scale) increases; and as the nanoparticle volumetric fraction increases, the nanoparticle aggregation tendency also increases, which both can explain the physical mechanisms behind the significance of the *AB* interaction.

In addition to the aforementioned results from the ANOVA, the contributions (%) of the effects of *A, B, C, AB, AC, BC,* and *ABC* on the nanofluid viscosity can be obtained calculating *SS'* (the pure sum of squares: the sum of squares of a factor that is purified from the error) first, using Equation (58) and Equation (59) in Section 3.3.3. The *SS'* values and contributions (%) of *A, B, C, AB, AC, BC* and *ABC* to the nanofluid viscosity are provided in Table 25.

Table 25. *SS'* values and contributions (%) of *A, B, C, AB, AC, BC* and *ABC* to the nanofluid viscosity

Source of variation	*SS'*	Contribution %
A	3.39966	64.1
B	1.56006	29.4
AB	0.07973	1.5
C	0.04806	0.9
AC	-0.00577	-0.1
BC	0.01893	0.4
ABC	0.00341	0.1
Error		3.7
Total		

As it is seen in Table 25, the factor *A* (temperature) has the highest contribution to the nanofluid viscosity and, *B* (nanoparticle volumetric fraction), *AB* (two factor interaction of temperature and nanoparticle volumetric fraction) and *C* (nanoparticle diameter) follow it. Negative and/or small contribution values imply that the corresponding term(s) may be disregarded from the calculation of μ_{nf}.

4.3.2. Statistical Evaluation of the Relative Viscosity: Analysis Results

The ANOVA results showing the effects of temperature (*A*), nanoparticle volumetric fraction (*B*), nanoparticle diameter (*C*) and their two and three factor interactions on the relative viscosity, at a significance level of $\alpha = 0.05$, are given in Table 26. The data entering to the program for ANOVA is provided in Table 39 in Appendix E.

Table 26. ANOVA results for the relative viscosity

Source of variation	*SS*	d_f	*MS*	*F*	F_{table}	*Significant effect ?*	α
A	0.00228	1	0.00228	0.20600	4.26	NO	5 %
B	2.70123	1	2.70123	244.25346	4.26	YES	
C	0.11487	1	0.11487	10.38717	4.26	YES	
AB	0.00970	1	0.00970	0.87754	4.26	NO	
AC	0.01699	1	0.01699	1.53598	4.26	NO	
BC	0.03374	1	0.03374	3.05096	4.26	NO	
ABC	0.00554	1	0.00554	0.50062	4.26	NO	
Error	0.26542	24	0.01106				
Total	3.14977	31					

Brief information regarding the parameters and their calculations (referring to Section 3.3.3) was provided right after Table 24, therefore will not be repeated here.

As it was mentioned in Section 3.3.2.3 as well as in the Section 4.3.1 that, the mean effects graphics of the factors are used to determine the optimum conditions of the regarding factors, if there is a "best scenario" defined. Since the determination of the optimum values of the factors are out of the scope of the present investigation, the main effects graphics factors are provided in Figure 37 to visualize the general trend.

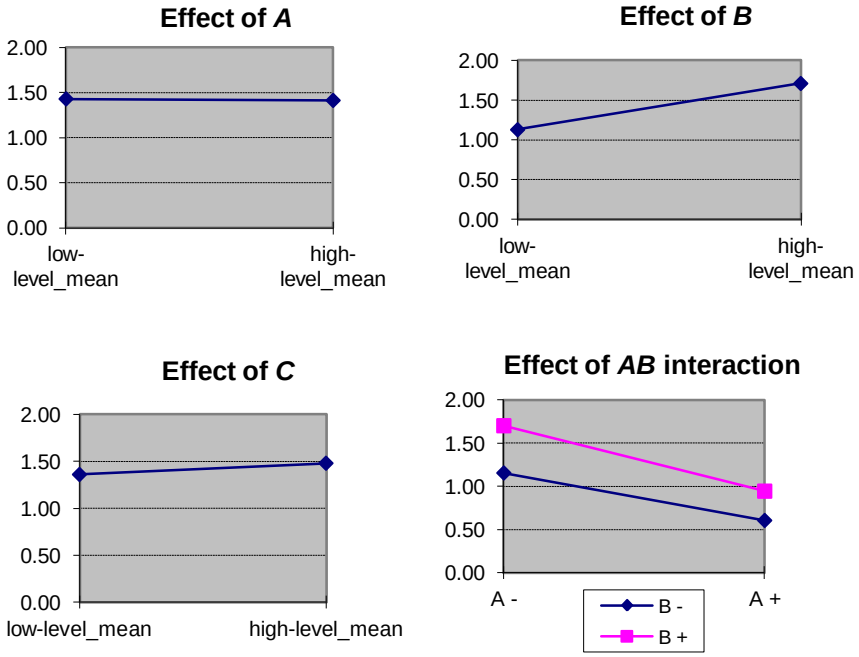

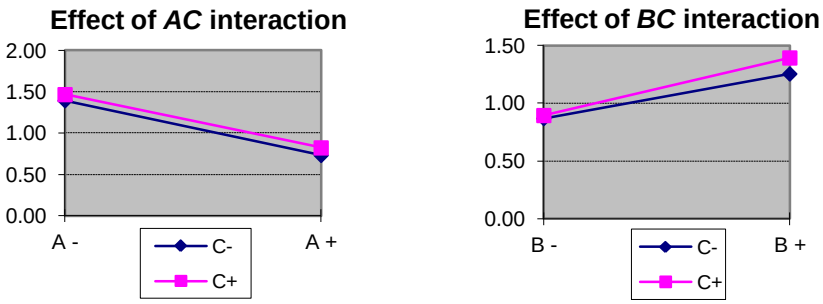

Figure 37. Main effects graphics corresponding the effects of *A, B, C, AB, AC* and *BC* on the relative viscosity. The factors on the figure are: *A*: temperature, *B*: nanoparticle volumetric fraction, *C*: nanoparticle diameter, *AB*: two factor interaction of *A* and *B*, *AC*: two factor interaction of *A* and *C*, *BC*: two factor interaction of *B* and *C*

The effect of a factor is considered as significant if F > F_{table} at that significance level (α).

From the results presented in Table 26, the following can be concluded:

- The main effects of *B* and *C* on the relative viscosity are significant. The importance of the main effects of the factors on the relative viscosity can be described from high to low sequence as: *B* > *C* (because the F values of the regarding factors are: $F_B > F_C$).

- The effect of two-factor and three-factor interactions are not significant on the relative viscosity.

In addition to the aforementioned results from the ANOVA, the contributions of the effects of *A, B, C, AB, AC, BC,* and *ABC* on the relative viscosity is obtained calculating *SS'* (the pure sum of squares: the sum of squares of a factor that is purified from the error) first, using Equation (58) and Equation (59) in Section 3.3.3. The *SS'* values and contributions (%) of *A, B, C, AB, AC, BC* and *ABC* to the relative viscosity are provided in Table 27.

Table 27. *SS'* values and contributions (%) of *A, B, C, AB, AC, BC* and *ABC* to the relative viscosity

Source of variation	*SS'*	Contribution %
A	-0.00878	-0.3
B	2.69017	85.4
AB	-0.00135	0
C	0.10381	3.3
AC	0.00593	0.2
BC	0.02268	0.7
ABC	-0.00552	-0.2
Error		10.9
Total		

As it is seen in Table 27, the factor *B* (nanoparticle volumetric fraction) has the highest contribution to the nanofluid relative viscosity and, *C* (nanoparticle diameter) and *BC* (two factor interaction of nanoparticle volumetric fraction and nanoparticle diameter) follow it. As it was mentioned in Section

4.3.1., negative and/or small contribution values imply that the corresponding term(s) may be disregarded from the calculation of μ_r.

4.3.3. New Correlation for Nanofluid Viscosity

The results of ANOVA (see Table 24) showed the effects of the factors on nanofluid viscosity. If one defines the viscosity of nanofluids based on the statistical analysis, the right approach is to define it by means of the parameters that have significant effect on nanofluid viscosity. As it can be recalled from Table 24, the effects of *A, B, C,* and *AB* are significant, whereas *AC, BC,* and *ABC* are insignificant on nanofluid viscosity at α=0.05. From this point of view, the correlation to be presented for the nanofluid viscosity based on the present experimental investigation will be dependent on *A, B, C* and *AB.*

Based on the present experimental investigation, the resulting nanofluid viscosity correlation is expressed below as Equation (60) in terms of the factors' names (i.e. *A, B, C,* and *AB*). These types of equations are called as "coded" equations, and while using the coded equations, one should substitute the levels (1 and 2) of the terms (e.g. factors: *A, B, C;* and their interactions*: AB, AC, BC, and ABC*) into the coded equation, rather than substituting the actual values of the factors (i.e. to calculate the nanofluid viscosity for T= 20^{o}C, φ= 0.01 and d_p= 10, one should substitute 1, 1, and 1, respectively for A, B and C in Equation (60)).

$$\left(\mu_{nf}\right)_{coded} = 0.8275 - 0.3413A + 0.7538B + 0.0825C - 0.2075AB \tag{60}$$

As a post-processing step, the "uncoded" equation is developed for the calculation of the nanofluid viscosity directly by substituting the actual values of the factors. For the development of the uncoded equation, the coefficients of the Equation (60) should be converted appropriately. The conversion is provided with Equation (61) for factor *A*, and the conversion for the other factors should be done in the same way (see [91] for details).

$$A_{coded} = \frac{A_{actual} - \left[(A_{high} + A_{low})/2\right]}{(A_{high} - A_{low})/2} \tag{61}$$

In Equation (61), A_{coded} and A_{actual} denote the coefficient of *A* in the coded and uncoded equation, respectively; whereas A_{high} and A_{low} are the values of the factor *A*, which correspond to its high and low levels (i.e. T= 20 and 50^{o}C). Calculating the actual values of the coefficients of the factors using Equation (61) for the each term in Equation (60); the Equation (60), which is coded, can be converted to its uncoded version. The uncoded nanofluid viscosity correlation is presented below as Equation (62).

$$\left(\mu_{nf}\right)_{uncoded} = 1.0973 - 0.0148T + 34.2292\varphi + 0.0041d_p - 0.3458T\varphi \tag{62}$$

As a reminder, in Equation (62), T, φ, and d_p are the temperature (^{o}C), nanoparticle volumetric fraction, and nanoparticle diameter (nm), respectively. Equation (62) can be used for different values of T, φ, and d_p provided they are within the intervals, i.e. for T: 20-50 ^{o}C, φ: 0.01-0.03, and d_p: 10-30 nm.

The estimations of the Equation (62) for the nanofluid viscosity for the each level of the factors *A, B,* and *C* are provided in Table 28 with the collected experimental data (in mPa.s) and the calculated relative differences between them.

Table 28. The estimations of nanofluid viscosity with Equation (62) with the measured values and relative differences (%)

A (°C)	1 (20)	1 (20)	1 (20)	1 (20)	2 (50)	2 (50)	2 (50)	2 (50)
B	1 (0.01)	1 (0.01)	2 (0.03)	2 (0.03)	1 (0.01)	1 (0.01)	2 (0.03)	2 (0.03)
C (nm)	1 (10)	2 (30)	1 (10)	2 (30)	1 (10)	2 (30)	1 (10)	2 (30)
μ_{nf} estimate (mPa.s)	1.115	1.198	1.661	1.744	0.566	0.649	0.905	0.988
μ_{nf} measured (mPa.s)	1.165	1.148	1.620	1.785	0.573	0.643	0.890	1.003
% difference*	-4.292	4.355	2.531	-2.297	-1.222	0.933	1.685	-1.496

* Relative difference % = [((new value) - (reference value)) / (reference value)] * 100

In Figure 38, the estimations obtained from Equation (62) and the experimental nanofluid viscosity data are compared, in order to see the representability of Equation (62) on the experimental data of present investigation.

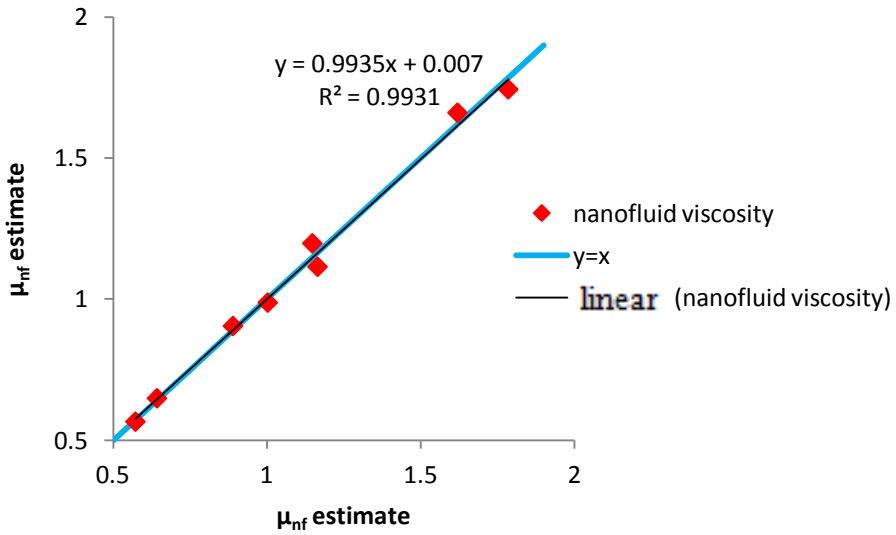

Figure 38. The comparison of the estimations of Equation (62) with the measured nanofluid viscosity

When interpreting the results illustrated in Figure 38, it should be noted that, if the number of values on the y = x line (or close to y = x line) is high, the measured values and the estimated values (using Equation (62)) are in a good agreement. As it is seen in Figure 38, the measured nanofluid viscosity and the estimated nanofluid viscosity values are in a very good agreement, which also can be explained in terms of the linear fit that represents the measured data (y = 0.9935x+0.007, R^2 = 0.9931) being very close to the y = x reference line. Therefore, the validity of Equation (62) for the experimental data of the present investigation is very high.

4.3.4. New Correlation for Relative Viscosity

The results of ANOVA (see Table 26) showed the effects of the factors on relative viscosity. As it was emphasized in Section 4.3.3, the resulting correlation should be dependent on the parameters, which have significant effect on relative viscosity. As can be recalled from Table 26, the effects of *B* and *C* are significant, whereas *A, AB, AC, BC,* and *ABC* are insignificant on relative viscosity at α=0.05. From this point of view, the correlation to be presented for the relative viscosity based on the present experimental investigation will be dependent on *B* and *C*.

Based on the present experimental investigation, the resulting relative viscosity correlation in its coded form is expressed below as Equation (63) in terms of the factors' names (i.e. *A*, *B*, and *C*). Even though the factor A appeared to be insignificant based on the results of ANOVA (see Table 26), in order to make comparison obtained relative viscosity with estimated relative viscosity and compliance with operating conditions being used in experimental setup in terms of T, φ , and d_p, the factor *A* is included in Equation (63). As a reminder, Equation (63) can be used by substituting the levels (1 and 2) of the factors (*A*, *B* and *C*), since it is in coded form.

$$(\mu_r)_{coded} = 0.3949 - 0.0169A + 0.5811B + 0.1198C \quad (63)$$

Equation (63) can be converted its' uncoded form using Equation (61). Explanations on the conversion of the coded equations to uncoded equations were provided in Section 4.3.3., therefore will not be repeated here.

The uncoded correlation for the relative viscosity nanofluids, in which the actual values of the factors can be substituted directly, is expressed below as Equation (64).

$$(\mu_r)_{uncoded} = 0.739716 - 0.000563T + 29.054\varphi + 0.006d_p \quad (64)$$

As a reminder, in Equation (64), φ, and d_p are the nanoparticle volumetric fraction, and nanoparticle diameter (in nm), respectively. Equation (64) can be used for the estimation of the relative viscosity for different values of φ, and d_p provided they are within the intervals, i.e. for φ: 0.01-0.03, and d_p: 10-30 nm.

The estimations of the Equation (64) for the relative viscosity for the each level of the factors *A*, *B*, and *C* are provided in Table 29, with the collected experimental data and the calculated relative differences between them.

Table 29. The estimations of relative viscosity with Equation (64) with the values obtained from the experiments and the relative differences (%)

A (°C)	1 (20)	1 (20)	1 (20)	1 (20)	2 (50)	2 (50)	2 (50)	2 (50)
B	1 (0.01)	1 (0.01)	2 (0.03)	2 (0.03)	1 (0.01)	1 (0.01)	2 (0.03)	2 (0.03)
C (nm)	1 (10)	2 (30)	1 (10)	2 (30)	1 (10)	2 (30)	1 (10)	2 (30)
μ_r estimate	1.079	1.199	1.660	1.780	1.062	1.182	1.643	1.763
μ_r obtained	1.165	1.148	1.620	1.785	1.041	1.168	1.618	1.823
% difference*	-7.382	4.443	2.469	-0.28	2.017	1.199	1.545	-3.291

* Relative difference % = [((new value) - (reference value)) / (reference value)] * 100

In Figure 39, the estimations of Equation (64) and the relative viscosity data obtained from the experiments are compared, in order to see the representability of the Equation (64) on the relative viscosity data of present investigation.

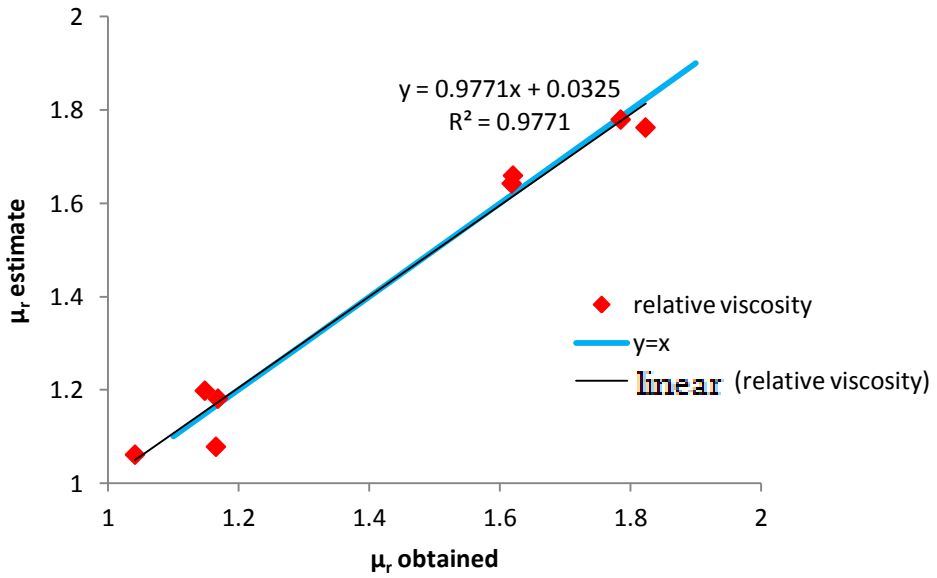

Figure 39. The comparison of the estimations of Equation (64) with the obtained relative viscosity

Interpretation of the Figure 39 was explained under Figure 38 in Section 4.3.3, therefore will not be repeated here. Figure 39 shows that, the obtained relative viscosity and the estimated relative viscosity values (using Equation (64)) are in a very good agreement. The linear fit that represents the obtained data (y = 0.9771x+0.0325, R^2 = 0.9771) is very close to the y= x reference line. Therefore, the validity of Equation (64) for the experimental data of the present investigation is very high.

4.4. Conclusions

In this Section, the conclusions arising from the experimental study and statistical evaluation are presented.

Regarding the Al_2O_3–H_2O nanofluid viscosity, the following were observed:

- The nanofluid viscosity decreases exponentially with increasing temperature.

- The nanofluid viscosity slightly increases with increasing nanoparticle volumetric fraction.

- The nanofluid viscosity increases with increasing nanoparticle diameter.

Regarding the relative viscosity of Al_2O_3–H_2O nanofluids, the following were observed:

- The relative viscosity variation with increasing temperature does not follow a classical trend, since the viscosity of base fluid is also highly dependent on temperature.

- The relative viscosity increased with increasing nanoparticle volumetric fraction.

- The nanofluid viscosity generally increases with increasing nanoparticle diameter.

Regarding the statistical analysis performed on the Al_2O_3–H_2O nanofluid viscosity and relative viscosity data, the following can be concluded:

- The effects of temperature, nanoparticle volumetric fraction, nanoparticle diameter, and the interaction of temperature and nanoparticle volumetric fraction are significant on nanofluid viscosity

at α=0.05 (for a confidence interval of 95%). The physical mechanisms explaining the significance of the interaction was explained in Section 4.3.1.

- When the resolution of the confidence interval for the nanofluid viscosity is lowered to 94%, i.e. by taking α=0.06, the effect of the interaction of nanoparticle volumetric fraction and nanoparticle diameter is significant on nanofluid viscosity, as well. Here, the physical mechanism beyond this interaction may be due to the increased nanoparticle aggregation with increasing nanoparticle volumetric fraction and/or increased nanoparticle diameter.

- The effects of nanoparticle volumetric fraction and nanoparticle diameter are significant on relative viscosity α=0.05.

- When the resolution of the confidence interval for the nanofluid viscosity is lowered to 90%, (i.e. by taking α=0.10), the effect of the interaction of nanoparticle volumetric fraction and nanoparticle diameter is significant on relative viscosity, as well. The interpretation of the significance of the interaction effect of nanoparticle volumetric fraction and nanoparticle diameter on relative viscosity was done for nanofluid viscosity at α=0.06 case above, therefore not repeated here.

Additionally, two new correlations were proposed for the Al_2O_3–H_2O nanofluid viscosity (see Equation (62)) and relative viscosity (see Equation (64)).

CHAPTER 5

DISCUSSION

In this Chapter, the findings of the present experimental investigation are discussed in terms of the comparisons with the findings of the relevant studies in literature. The comparison is considered as very important, since it strengthens pointing out the inconsistencies in literature. In addition to the comparisons, some important points of the present investigation regarding the material and method are emphasized. Finally, some conclusions are drawn.

5.1. Introduction

The inconsistencies in nanofluid viscosity literature are abundant. The reasons for the inconsistencies are still not fully attributed to certain factors and/or mechanisms; therefore developing an epistemic understanding on the results is of great importance. For this purpose, discussion of the results is critical, since it may lead researchers to point out the possible reasons for the regarding inconsistencies.

In this Chapter, the data of the present investigation are compared with the data of the relevant studies selected from literature. The comparisons are done on the data collected at ambient (room) temperature (mostly) in Section 5.2.1, at varying temperatures in Section 5.2.2 for φ= 0.01, 0.02 and 0.03 nanofluids, and with Einstein Model [24] as a Classical Model in Section 5.2.3. The nanofluid viscosity data of both the present investigation and selected studies from literature are illustrated with graphs, as well. Some of the factors that are possibly responsible for the inconsistencies between the findings of the studies are suggested.

In addition to the aforementioned, some important points of the present investigation are emphasized in Section 5.3.

5.2. Comparison of the Experimental Data of the Present Study with Literature

In the present investigation, the experimental data collected for the viscosity of Al_2O_3–H_2O nanofluids are compared with the relevant studies in literature. The studies to be used for the comparisons are selected from the literature survey given in Section 2.2.2 in Chapter 2 (see Table 5). Only the studies concerned with the viscosity of Al_2O_3–H_2O nanofluids are considered, in order to enhance the sensitivity of the comparisons, since the effect of the nanoparticle material on nanofluid viscosity is shown as significant in the benchmark study presented in Section 2.3 in Chapter 2, and the effect of base fluid can be considered as significant as well, since it is the biggest component of a nanofluid.

The Section 5.2.1 is concerned with the comparison for the ambient temperature (mostly), whereas the Section 5.2.2 is concerned with the comparison for varying temperatures. In the graphs presented, the labels, which have the phrase “experimental data” in their names with black markers, are the data collected in the present experimental investigation.

5.2.1. Comparison for the Ambient (Room) Temperature

The experimental data of the present investigation for the Al_2O_3–H_2O nanofluids of d_p= 10 nm and d_p= 30 nm are compared with the relevant studies in literature, for ambient temperature condition (mostly), in Figure 40. Only the data of Wang et al. [38] is not known to be collected at ambient temperature, since there is no information given regarding the temperature of the measurements.

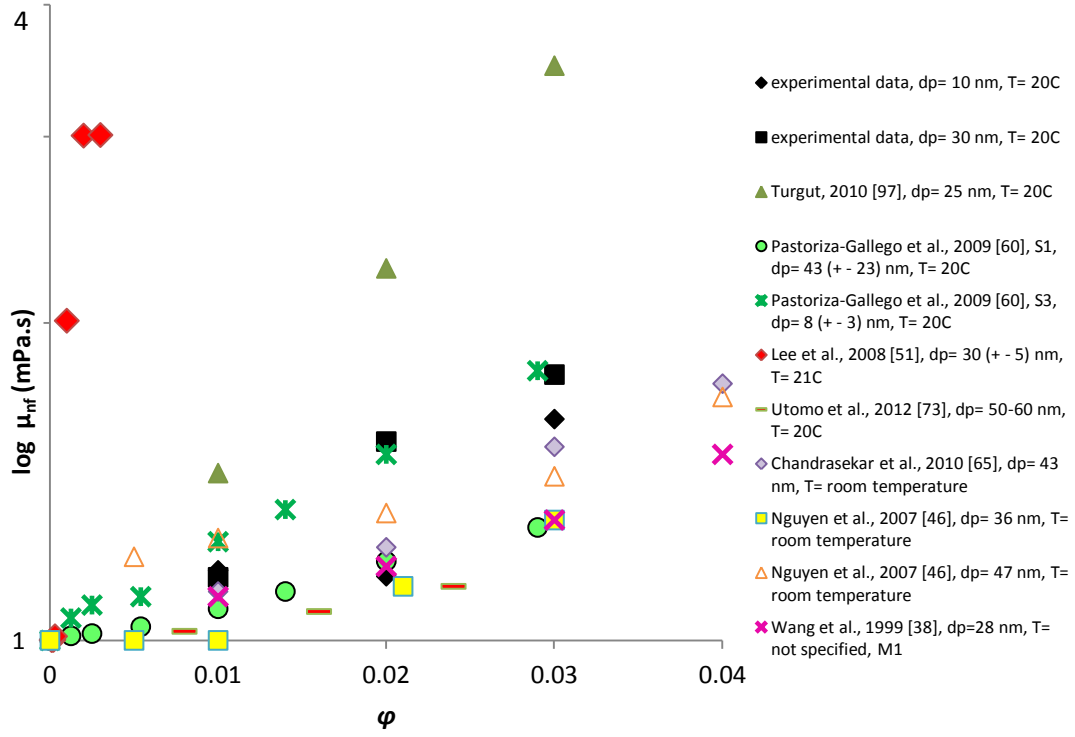

Figure 40. Comparison of Al_2O_3–H_2O nanofluid viscosity data at ambient temperature, mostly. The markers represent the averages of the four measurements taken at the same condition for the present investigation, and the data presented in literature.

The comparison between the Al_2O_3–H_2O nanofluid viscosity data between the present investigation and the selected data from literature (for a relevant interval of nanoparticle volumetric fraction to the present experimental investigation, i.e. φ= 0 to 0.04) is provided in Figure 40. Since it is more convenient for the illustration, the vertical axis is set as logarithmic.

As it is seen in Figure 40, the inconsistencies between the whole data are abundant. While the data presented in some of the studies are quite close to the data of the present investigation, there is no exact agreement between the data. The results arising from the comparison given in Figure 40 are specified below.

- The closest agreements observed are between the data of the present investigation (d_p= 10 nm) and the data of Chandrasekar et al. [65] (d_p= 43nm); the data of the present investigation (d_p= 30 nm) and the data of Pastoriza-Gallego et al. [60] (S3, d_p = 8±3 nm). Although the examined nanofluids in the corresponding studies differ in terms of the nanoparticle diameter, the viscosity values are quite close. The inconsistencies on the nanoparticle sizes certainly deserve attention.

- The data of Turgut [97] is higher; the data of Pastoriza-Gallego et al. [60] (S1, d_p = 43 ± 23 nm) and Wang et al. [38] are close (for φ= 0.01 and 0.02) to the experimental data of the present investigation (d_p= 10 nm); and the data of Nguyen et al. [46] are lower than the experimental data (d_p= 10 nm and d_p= 30 nm) of the present investigation.

- The disagreement between the results gets more pronounced as the nanoparticle volumetric fraction increases. As the nanoparticle volumetric fraction increases, the nanofluid gets more concentrated, thus the classical theories presented for relatively dilute suspensions (for Classical Models, see Table 5 in Chapter 2; for discussion and comparison with the experimental data, see Section 5.2.3) become insufficient on estimating the nanofluid viscosity. From the perspective of classical theories, Elçioğlu et al. [18] showed that, the underestimation of some of the Classical Models are more pronounced for increasing nanoparticle volumetric fraction, for which the aggregation tendency of the nanoparticles increases, therefore the classical theories assuming non-interacting particles (i.e. Einstein Model [24]) mostly give erroneous results.

The inconsistencies in literature are more abundant than the data presented only for Al_2O_3–H_2O nanofluids presented in Figure 40. The inconsistencies, which lead wide range of experimental results, are possibly due to uncontrolled parameters, such as nanofluid stability, (related to nanoparticle aggregation, use of surfactants, etc.). For example, the data of Lee et al. [51], which were collected at low nanoparticle volumetric fractions (φ= 0.0001–0.003), are significantly higher than the data collected in the present investigation, although they belong to d_p= 30 ± 5 nm Al_2O_3–H_2O nanofluids (But, Lee et al. [51] reported that, most of the nanoparticles' sizes were smaller than 30 nm, and there were a few aggregates.).

The possible reasons that can be regarded as responsible for these inconsistencies are not exactly specified in literature. In addition to the aforementioned, required information on the interpretation of the results are also mostly missing.

5.2.2. Comparison for Varying Temperature

The experimental data of the present investigation for the Al_2O_3–H_2O nanofluids of d_p= 10 nm and d_p= 30 nm are compared with the relevant studies in literature, for varying temperature condition, in Figure 41. Since it is more convenient for the illustration, the comparisons are given separately for φ= 0.01, 0.02 and 0.03 nanofluids in Figure 41 (for φ= 0.01 nanofluids, see the graph presented below; for φ= 0.02 and 0.03 nanofluids, see the following graphs presented in the next page).

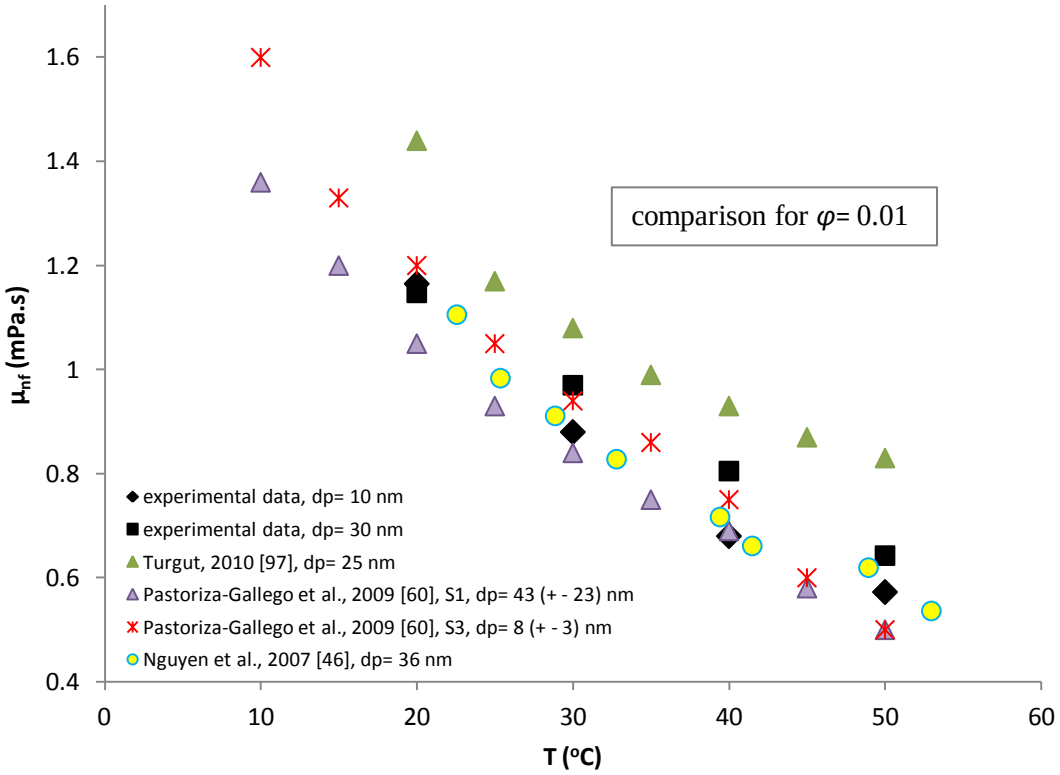
comparison for φ= 0.01
μnf (mPa.s)
T (°C)
experimental data, dp= 10 nm
experimental data, dp= 30 nm
Turgut, 2010 [97], dp= 25 nm
Pastoriza-Gallego et al., 2009 [60], S1, dp= 43 (+ - 23) nm
Pastoriza-Gallego et al., 2009 [60], S3, dp= 8 (+ - 3) nm
Nguyen et al., 2007 [46], dp= 36 nm

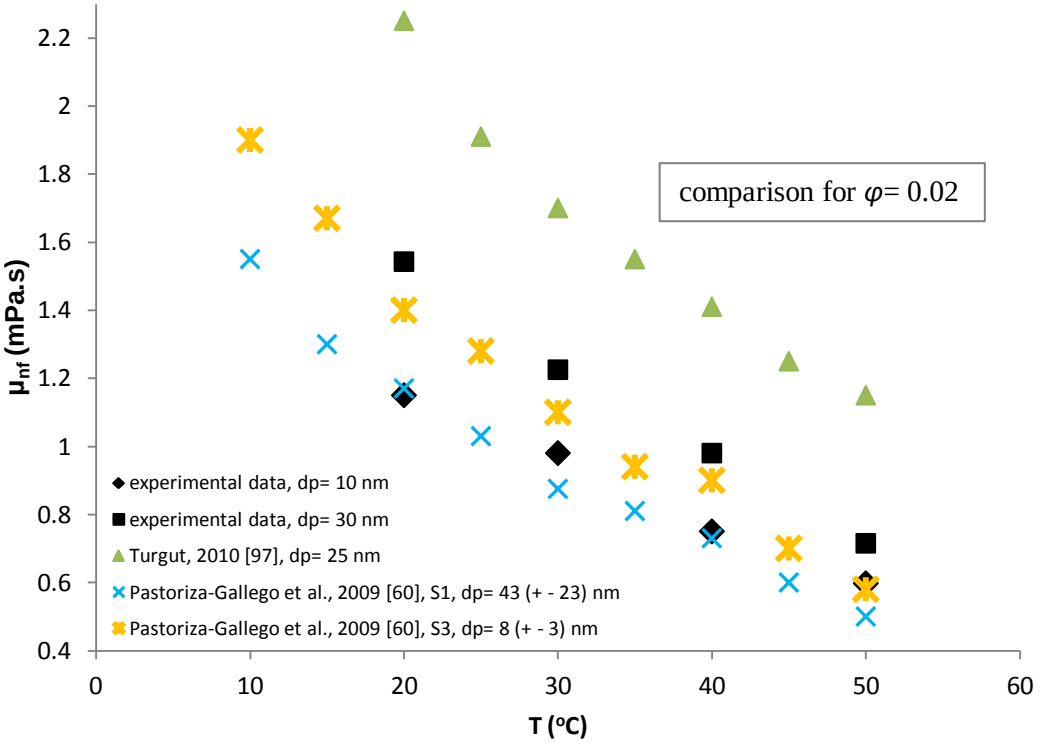
comparison for φ= 0.02
μnf (mPa.s)
T (°C)
experimental data, dp= 10 nm
experimental data, dp= 30 nm
Turgut, 2010 [97], dp= 25 nm
Pastoriza-Gallego et al., 2009 [60], S1, dp= 43 (+ - 23) nm
Pastoriza-Gallego et al., 2009 [60], S3, dp= 8 (+ - 3) nm

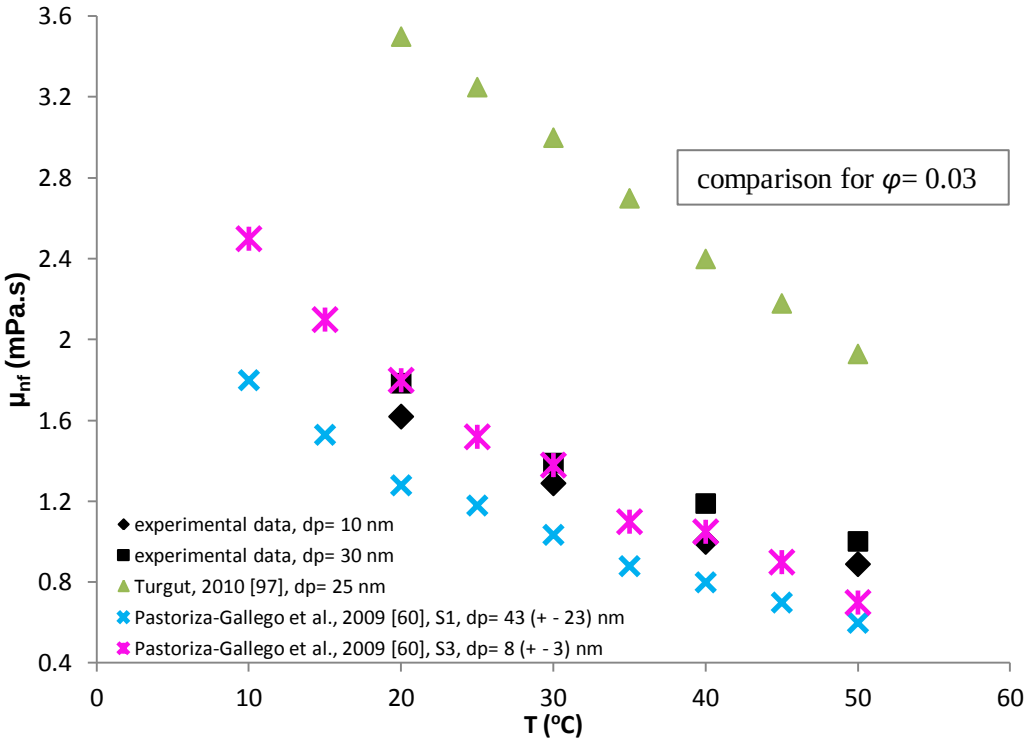

Figure 41. Comparison of Al_2O_3–H_2O nanofluid viscosity data for varying temperature. From top to bottom, the graphs belong to the nanofluids of φ= 0.01, 0.02, and 0.03. The markers represent the average of the four measurements taken at the same condition for the present investigation, and the data presented in literature.

In Figure 41, the experimental data (for φ= 0.01, 0.02, and 0.03) of the present investigation are compared with the data of the relevant studies in literature, for varying temperatures, for a relevant interval of temperature. As it is seen in Figure 41, some of the data presented for φ= 0.01, 0.02, and 0.03 nanofluids are pretty close to the data collected from literature. Nevertheless, there is no exact agreement between the data. The results arising from the comparison given in Figure 41 are specified below.

- For all the nanofluids of φ= 0.01, 0.02 and 0.03 considered, the data of Turgut [97] is significantly greater than the data of the present investigation.

- Regarding the φ= 0.01 Al_2O_3–H_2O nanofluid viscosity data, it is observed that, the data of Nguyen et al. [46] are quite close to the data of the present investigation for the d_p= 10 nm and 30 nm nanofluids, whereas the data of Pastoriza-Gallego et al. [60] for S1 (d_p= 43 ± 23 nm) and S3 (d_p= 8 ± 3 nm) are in a relatively good agreement with the data of the present investigation for the nanofluids of d_p= 10 nm and 30 nm, respectively.

- Regarding the φ= 0.02 Al_2O_3–H_2O nanofluid viscosity data for d_p= 10 nm, it is observed that the data of Pastoriza-Gallego et al., [60] for S1 (d_p= 43 ± 23 nm) are in an agreement with the experimental data for d_p= 10 nm nanofluids of the present investigation. The data of Pastoriza-Gallego et al. [60] for S2 (d_p= 8 ± 3 nm) are in an agreement with the experimental data for d_p= 30 nm nanofluids of the present investigation.

- Regarding the φ= 0.03 Al_2O_3–H_2O nanofluid viscosity data for d_p= 10 nm, it is observed that the data of Pastoriza-Gallego et al. [60] for S2 (d_p= 8± 3 nm) are quite close to the data of the present experimental investigation.

- It should be noted that, the most significant agreement is observed for φ= 0.01 nanofluids, for which the unforeseen behavior is less compared to φ= 0.02 and φ= 0.03 nanofluids. This issue can be interpreted to the tendency of the nanoparticles to interact as the nanoparticle volume fraction increases. Therefore, the disagreements for the more concentrated nanofluids are relatively acceptable compared to the dilute nanofluids.

5.2.3. Comparison Between the Experimental Data and Classical Models

The experimental data of the present investigation for the Al_2O_3–H_2O nanofluids of d_p= 10 nm and d_p= 30 nm are compared with Einstein Model [24] as one of the Classical Models, for varying temperature condition, in Figure 42. Only the predictions of Einstein Model are compared with the data of the present investigation, since the predictions of some Classical Models are shown to be very close to each other (see Table 4).

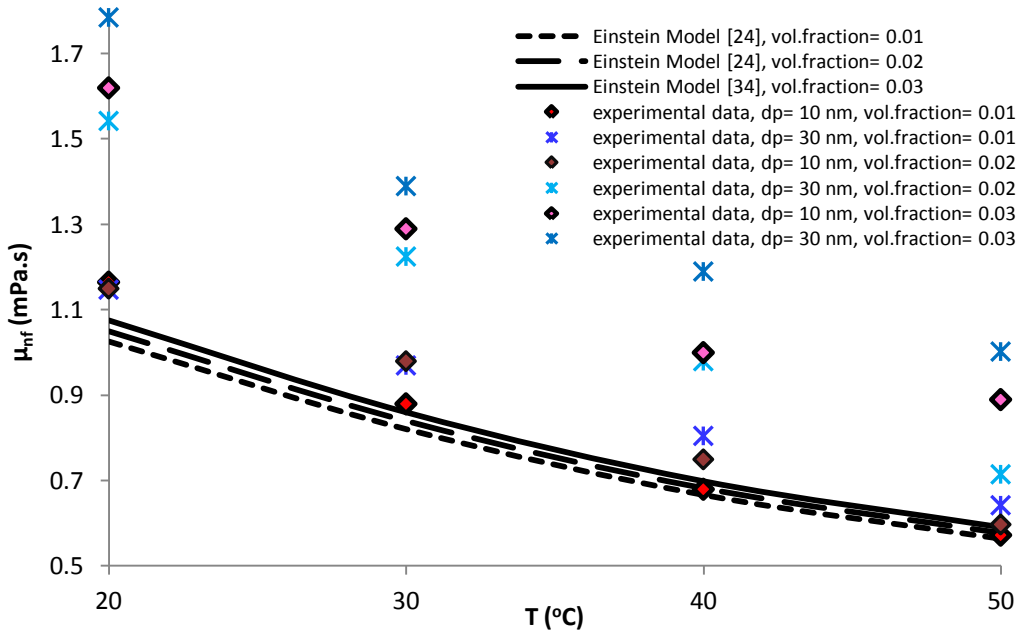

Figure 42. Comparison between the experimental data of the present investigation and the predictions of Einstein Model [24] for varying temperature

In general, the experimental data of the present investigation is higher than the predictions of Einstein Model [24], as it is seen in Figure 42. However, only the experimental data of d_p= 10 nm and φ= 0.01 Al_2O_3–H_2O nanofluids is significantly close to the predictions of Einstein Model [24], and this trend is attributed to the relatively dilute condition of the regarding nanofluid.

It is a widely known fact that, the Einstein Model defines the relative viscosity of suspensions in terms of a linear relationship with particle volumetric fraction, and the predictions of Einstein Model are more valid for dilute suspensions of hard spheres. Therefore, it can be said that, the Einstein Model is relatively successful on predicting the viscosity of the nanofluids of d_p= 10 nm and φ= 0.01 of the

present investigation, whereas it underpredicts the nanofluid viscosity for a wide margin of d_p and φ considered.

5.2.4. Suggestions on the Factors/Mechanisms that are Possibly Responsible for the Inconsistencies in Literature

In literature, the inconsistencies between the findings of the studies are attributed to some mechanisms and/or factors, but they are mostly roughly mentioned. The regarding mechanisms can be given as the nanofluid stability (nanoparticle aggregates within nanofluids, or stabilized nanofluids: both influence the viscosity), nanofluid production methods, equipments used for measurements, etc.

Other than the factors/mechanisms mentioned above, it can be concluded from the comparison provided in Section 5.2.1 that, the production method of nanofluids is a very significant factor, and has considerable effect on the experimental results. Effect of the nanofluid production method can be discussed based on the comparison presented in Section 5.2.1. Although the same type of equipments used for the experiments, the experimental data presented by Turgut [97] for Al_2O_3–H_2O nanofluids (d_p= 25 nm) are considerably higher than the experimental data of the present experimental investigation (for both d_p= 10 nm and 30 nm). More clearly, the nanofluids were produced by a two-step method in Turgut's study [97], whereas for the present investigation, the samples are supplied from a commercial source as nanofluids, and used as received. In addition, the nanofluids examined in the present investigation involve Acetic acid as surfactant, whereas the nanofluids of Turgut [97], which were examined for viscosity, did not involve any surfactant. Therefore, it can be concluded that, the difference in the nanofluid production method, results in a difference in the nanofluid viscosities, which were measured for the same conditions and with the same type of equipment.

In addition to the effect of nanofluid production method, some other parameters also have significant effects on the experimental results. During the experimental study conducted for the present investigation, it was seen that, the calibration of the equipment is of great importance, as well. Although calibration before and after every experiment elongates the experiment period, it minimizes the error coming from the equipment. While this can be eliminated by calculating the mean error and applying the error correction to the whole data to some extent, the magnitude of the error may be different for different experiment conditions (e.g. for different temperatures, etc). Therefore, intensive calibration is needed in order to ensure the validity of the results, and different calibration frequencies may result with different results.

5.3. Emphasis on the Important Points of the Present Investigation

In this Section, some important points of the present investigation are provided, which are mainly on the material selection, method selection and what is gained using the statistical methodology, which is novel for the field nanofluid viscosity.

5.3.1. Emphasis on Material Selection

The material to be investigated was selected as Al_2O_3–H_2O nanofluids, for the present investigation. The main reason for this selection was the high possibility of the Al_2O_3–H_2O nanofluids to be integrated in the industry, due to its relatively accessible cost. In addition, a considerable portion of nanofluid literature is concerned with the evaluation of the Al_2O_3–H_2O nanofluids.

However, there is a long way to produce the nanofluids very precisely for the applications, since the size and shape control of the nanoparticles within the base fluid are still difficult tasks, which directly affect the stability of the nanofluids.

5.3.2. Emphasis on Method Selection

The method employed to construct the experimental study was selected as DOE. This is a novel approach for the field nanofluid viscosity; therefore it is of great importance. When examining physical phenomena experimentally, using statistical approaches is very useful in understanding and interpreting the results.

The research on nanofluids is mainly based on the enhanced heat transfer performance of nanofluids, but the inconsistencies between the findings of the studies are abundant. Therefore, developing an epistemic understanding on the thermophysical properties of nanofluids is critical. This can be done with systematic studies combining the experimental and theoretical research. For this purpose, the present investigation is concerned with experimental investigation of the viscosity of Al_2O_3–H_2O nanofluids with statistical evaluation. However the experimental studies are bounded by the experimental facilities and material supplying opportunities, careful experimentation and statistical evaluation is a serious need.

5.3.3. Emphasis on Statistical Methodology: What is Gained?

By employing Taguchi Method, the desired conditions for the processes can be determined. If there is a best scenario, the required conditions (optimum conditions of the factors) to be established in order to achieve that scenario can be determined by drawing the main effects graphics of the regarding factors. After the determination of the optimum levels of the factors', whether the optimum conditions are giving the desired scenario can be evaluated with confirmation experiments. However, the optimization of the parameters is out of the scope of the present study.

The present investigation is concerned with the observation of a physical property (viscosity) of a material (i.e. nanofluid). The inconsistencies in experimental nanofluid viscosity literature are abundant, and the exact reasons that are responsible for these inconsistencies are not known, although some factors were presented in literature as suggestions. Therefore, pointing out these inconsistencies is a critical and a required task, which can be done using statistics, very effectively.

In this study, the effects of the factors (temperature, nanoparticle volumetric faction and nanoparticle diameter) and their two and three factor interactions on the quality characteristic (nanofluid viscosity, and the relative viscosity) are examined using DOE. It was a known fact that, the viscosity of nanofluids are strongly dependent on temperature and nanoparticle fraction, but the studies concerned with the nanoparticle diameter dependent nanofluid viscosity are less in number. As a result of the statistical analysis (ANOVA) performed, it was seen that, the effect of the nanoparticle diameter on nanofluid viscosity is less significant on the nanofluid viscosity compared to the temperature and nanoparticle volumetric fraction, but still significant. Therefore, this study points out to the requirement of the designation of nanoparticle diameter as a factor, which has considerable effect on nanofluid viscosity, and thus should be taken into account. Another important conclusion arising from the statistical analysis is that, the interaction effect of temperature and nanoparticle volumetric fraction is significant on nanofluid viscosity as well. This fact emphasizes that, the effect of the temperature on nanofluid viscosity for varying nanoparticle volumetric fractions does not follow the same trend for all nanoparticle volumetric fractions considered, or vice versa.

The effects of the aforementioned factors on the relative viscosity of nanofluids are also evaluated, since the relative viscosity defines the enhancement of viscosity obtained with nanofluids, compared to the base fluid. The viscosity enhancement obtained with nanofluids is a critical concern, which can seriously limit the potential applications of nanofluids. Regarding the effects of the factors (temperature, nanoparticle volumetric fraction, and nanoparticle diameter), and their two and three factor interactions on relative viscosity; it was found that, the effect of nanoparticle volumetric fraction and nanoparticle diameter are significant, whereas the effect of temperature is insignificant on the viscosity enhancement obtained with nanofluids. The effect of temperature on both the base fluids and nanofluids are very dominant and do not follow a classical trend, therefore the discussion is not straightforward. For example, even the viscosity of water varies exponentially with temperature [77].

Summarizing, the nanoparticle diameter dependence of nanofluid viscosity and relative viscosity should certainly be studied; and statistical evaluation of the experimental data gives very useful information, which can be used for the interpretation of the results.

CHAPTER 6

SUMMARY AND CONCLUSIONS

In this Chapter, a brief summary of the work performed is given, and the conclusions drawn from the present investigation are presented. Finally, some future work suggestions are given.

6.1. Summary

As it was presented in the previous Chapters, the current study was concerned with the experimental and theoretical investigations on the Al_2O_3–H_2O nanofluid viscosity, in a systematic way. Before the experimental investigation, the literature was reviewed carefully, in order to develop an understanding regarding the field nanofluid viscosity. A comprehensive literature survey and a benchmark study on the nanofluid viscosity and relative viscosity were performed in Chapter 2. With the light of the literature review given in Chapter 2; it was concluded that, the effects of the nanoparticle volumetric fraction, temperature and nanoparticle diameter are significant on nanofluid viscosity. Therefore these parameters were selected as factors for the present experimental investigation. In Chapter 3, the material and method (statistical methodology employed to construct the experiments) were presented, in detail. Chapter 4 was concerned with the experimental investigation and the statistical evaluation on the viscosity and relative viscosity of Al_2O_3–H_2O nanofluids. In Chapter 5, the results of the present experimental investigation were discussed, and emphasis on the important points of the material and method selection, as well as what is gained using the statistical methodology were presented.

This Chapter, as the final Chapter of this thesis, is concerned with the conclusions drawn from the experimental study and the statistical analysis.

6.2. Conclusions

The following conclusions can be made, regarding the experimental study:

- The Al_2O_3–H_2O nanofluid viscosity is found to decrease exponentially with increasing temperature; increase with increasing nanoparticle volumetric fraction; and increase with increasing nanoparticle diameter.
- The relative viscosity of Al_2O_3–H_2O nanofluids varied with increasing temperature without following a classical trend (independent of temperature), increased with increasing nanoparticle volumetric fraction, and generally increased with increasing nanoparticle diameter.

Regarding the statistical analysis, the following can be concluded:

- The effects of temperature, nanoparticle volumetric fraction, nanoparticle diameter and the interaction effect of temperature and nanoparticle volumetric fraction are significant on nanofluid viscosity at α= 0.05 (for a confidence interval of 95 %). For a slightly lower confidence interval (94 %) of the nanofluid viscosity, i.e. at α=0.06, the effect of the interaction of nanoparticle diameter and nanoparticle volumetric fraction is significant on nanofluid viscosity, as well.
- The effects of nanoparticle volumetric fraction and nanoparticle diameter are significant on relative viscosity at α=0.05. For a lower confidence interval (90 %) of the relative viscosity, i.e.

α=0.10, the effect of the interaction of nanoparticle volumetric fraction and nanoparticle diameter is significant on relative viscosity, as well.

- Based on the statistical analysis, Equations (60) as the nanofluid viscosity correlation and Equation (64) as the relative viscosity correlation were presented. These new kinds of correlations (i.e. the nanofluid viscosity correlation dependent on T, φ, d_p and $T\varphi$, and the relative viscosity correlation dependent on φ and d_p), have significantly different forms than the correlations and Classical Models provided in Table 5 and Table 6 in Chapter 2. These correlations are novel, since they emphasize the effects of some factors and/or interactions, based on the physical interpretation.

6.3. Future Work Suggestions

In this Section, some future work suggestions are provided.

- First of all, the experimental nanofluid viscosity research is strongly dependent on the material production. The researchers who have the facilities to produce the nanofluids have an advantage. The researchers, who do not have the opportunity to produce the nanofluids, as it is the case in the current work, mostly purchase them from commercial sources. While commercial sources provide precisely engineered materials; self production of the nanofluids would be more meaningful in terms of the development of a fundamental understanding on the material properties. Therefore, efforts can be made on precise production of nanofluids.

- As it is a known fact, the superior thermal conductivity of nanofluids to the commercial working fluids is very important, whereas the enhanced viscosity of nanofluids can be a limiting feature for the potential applications. Therefore, the performance evaluation of nanofluids can be done towards optimization of the thermal conductivity and viscosity, with their simultaneous investigation.

- Statistical approaches should definitely be used when examining a physical phenomenon. Since the random behaviors of nanoparticles are mainly responsible from the unforeseen behavior of nanofluids, developing an understanding on the behavior of nanofluids in terms of statistics is of great importance. DOE, which is employed in the present investigation, is not the only tool to be used. Other approaches (e.g. response surface methodology) should be sought, as well.

-Nanotechnology is a multidisciplinary research field and it combines numerous fields such as the pure sciences (e.g. physics, chemistry, etc.), engineering practices (e.g. mechanical, material, biomedical, etc.) and medicine. In addition, for the modeling, statistics is an important tool. Therefore, collaboration of the scientists from different fields is important, in order to understand and interpret the results in the best way.

REFERENCES

[1] Incropera, F.P., Dewitt, D.P., Bergman, T.L., Lavine, A.S., *Fundamentals of Heat and Mass Transfer*, Sixth Edition, John Wiley & Sons, Inc., USA, 2007.

[2] Kumar, T.S., Thakur, N.S., Kumar, A., Mittal, V., "Use of Artificial Roughness to Enhance Heat Transfer in Solar air Heaters – a Review", Journal of Energy in Southern Africa, Vol. 21, No. 1, pp. 35-51, 2010.

[3] Yu, W., Xie H., "A Review on Nanofluids: Preparation, Stability Mechanisms and Applications", Journal of Nanomaterials, doi:10.1155/2012/435873, 2011.

[4] Choi, S.U.S., Eastman, J.A., "Enhancing Thermal Conductivity of Fluids with Nanoparticles", ASME International Mechanical Engineering Congress & Exposition, November 12-17, San Francisco, CA, 1995.

[5] Yokoyama, T., Fukui, T., Masuda, H. et al., "Chapter 1: Basic Properties and Measuring Methods of Nanoparticles" in *Nanoparticle Technology Handbook (edited by: Hosokawa, M., Nogi, K., Naito, M., Yokoyama, T.)*, First Edition, Elsevier, Oxford, UK, 2007.

[6] Kakaç, S., Pramuanjaroenkij, A., "Review of Convective Heat Transfer Enhancement with Nanofluids", International Journal of Heat and Mass Transfer, 52, pp. 3187–3196, 2009.

[7] http://nano.anl.gov/news/highlights/2005_choi.html [date accessed: 24.04.2013]

[8] Das, S.K., Choi, S.U.S., Yu, W., Pradeep, T., *Nanofluids Science and Technology*, John Wiley & Sons, Inc., Hoboken, New Jersey and Canada, 2008.

[9] Brady, G.S., Clauser, H.R., Vaccari, J.A, *Materials Handbook*, Fifteenth Edition, McGraw Hill, US, ISBN: 0-07-136076-X, 2002.

[10] Ebrahimi, S., Gavili, A., Lajevardi, M. et al., "New Class of Coolants: Nanofluids" in *Cutting Edge Nanotechnology*, pp. 251-277, InTech, Vukovar, Croatia, ISBN: 978-953-7619-93-0, 2010.

[11] Wen, D., Lin, G., Vafaei, S., Zhang, K., "Review of Nanofluids for Heat Transfer Applications", Particuology, 7, pp. 141-150, 2009.

[12] Choi, S.U.S., "Nanofluid Technology: Current Status and Future Research", Second Korean-American Scientists and Engineers Association Research Trend Study Project Review and the Korea-U.S. Technical Conference on Strategic Technologies, Vienna, VA, 1998.

[13] Eastman, J.A., Choi, S.U.S., Li, S., Yu, W., Thompson, L.J., "Anomalously Increased Effective Thermal Conductivities of Ethylene Glycol-Based Nanofluids Containing Copper Nanoparticles", Appl. Phys. Lett., Vol. 78, No. 6, pp. 718-720, 2011.

[14] Li, Y., Zhou, J., Tung, S., Schneider, E., Xi, S., "A Review on Development of Nanofluid Preparation and Characterization", Powder Technology, 196, pp. 89–101, 2009.

[15] Mahbubul, I.M., Saidur, R., Amalina, M.A., "Latest Developments on the Viscosity of Nanofluids", International Journal of Heat and Mass Transfer, 55**,** pp. 874–885, 2012.

[16] Williams, W.C., Bang, I.C., Forrest, E., Hu, L.W., Buongiorno, J., "Preparation and Characterization of Various Nanofluids", NSTI-Nanotech 2006, Vol. 2, www.nsti.org, ISBN 0-9767985-7-3, 2006.

[17] Özerinç, S., Yazıcıoğlu, A.G., Kakaç, S., "Enhanced Thermal Conductivity of Nanofluids: A State-of-the-art Review", Microfluid Nanofluid, 8, pp. 145–170, 2010.

[18] Elçioğlu, E.B., Yazıcıoğlu, A.G., Kakaç, S., "Nanofluid Viscosity: A Comparative Summary of Experimental Work in Literature", 8th Nanoscience and Nanotechnology Congress, June 25-29, 2012, Book of the Abstract, Accepted Poster Presentations, pp. 508-509, Ankara, Turkey, 2012.

[19] Timofeeva, E.V., "Nanofluids for Heat Transfer – Potential and Engineering Strategies" in *Two Phase Flow, Phase Change and Numerical Modeling (edited by: Ahsan, A)*," pp. 435-450, InTech, Rijeka, Croatia, ISBN 978-953-307-584-6, 2011.

[20] Kakaç, S., Liu, H., *Heat Exchangers Selection, Rating and Thermal Design*, Second Edition, CRC Press LLC, Boca Raton, London, New York and Washington, D.C, 2002.

[21] Elçioğlu, E.B., Yazıcıoğlu, A.G., Kakaç, S., "A Comparative Evaluation on Nanofluid Viscosity (Nanoakışkan Viskozitesinin Karşılaştırmalı Değerlendirmesi)," Journal of Thermal Science and Technology, 2013 [article accepted].

[22] Muhesh Kumar, P.C., Kumar J., Suresh, S., "Review on Nanofluid Theoretical Viscosity Models", International Journal of Engineering Innovation & Research, Vol. 1, Issue 2, pp. 128-134, ISSN: 2277 – 5668, 2012.

[23] Hosseini, S.Sh., Shahrjerdi, A., Vazifeshenas , Y., "A Review of Relations for Physical Properties of Nanofluids", Australian Journal of Basic and Applied Sciences, 5(10): pp. 417-435, 2011.

[24] Einstein, A., "A New Determination of Molecular Dimensions (Ann Phys (4), 19, 1906, pp. 289-306. Corrections, ibid., 34, 1911, pp. 591-592,) in Investigations on the Theory of, the Brownian Movement." Edited with notes by: R. Fürth, Translated by: A.D. Cowper, Dover Publications, Inc, New York, pp. 37-62, 1956.

[25] Goodwin, J., *Colloids and Interfaces with Surfactants and Polymers: An Introduction*, John Wiley & Sons Ltd, West Sussex, England, 2004.

[26] Chen, H., Ding, Y., Tan, C., "Rheological Behaviour of Nanofluids", New Journal of Physics, 9, 367, pp. 1-24, 2007.

[27] Batchelor, G. K., "The Effect of Brownian Motion on the Bulk Stress in a Suspension of Spherical Particles", J. Fluidmech, 83, pp. 97-117, 1977.

[28] Andrade, E.N da C., XLI. "A Theory of the Viscosity of Liquids—Part I", Philosophical Magazine Series 7, Vol. 17, Issue 112, 1934.

[29] Brinkman, H.C., "The Viscosity of Concentrated Suspensions and Solutions", J. Chemistry Phy, 20, pp. 571-581, 1952.

[30] Krieger, I.M., Dougherty, T.J., "A Mechanism for Non-Newtonian Flow in Suspensions of Rigid Spheres", Transactions of the Society of Rheology III, pp. 137-152, 1959.

[31] Frankel, N.A., Acrivos, A., On the Viscosity of a Concentrate Suspension of Solid Spheres, Chem. Eng. Sci, 22, pp. 847–853, 1967.

[32] Nielsen, L.E., "Generalized Equation for the Elastic Moduli of Composite Materials", J. Appl. Phys. 41, pp. 4626-4627, 1970.

[33] Phuoc, T.X., Massoudi, M., "Experimental Observations of the Effects of Shear Rates and Particle Concentration on the Viscosity of Fe_2O_3–Deionized Water Nanofluids", International Journal of Thermal Sciences, 48, pp. 1294–1301, 2009.

[34] Lundgren, T. S., “Slow Flow through Stationary Random Beds and Suspensions of Spheres”, J. Fluid Mechanics, 51, pp. 847-853, 1972.

[35] Graham, A.L., “On the Viscosity of Suspensions of Solid Spheres”, Appl. Sci. Res, Vol. 37, Issue 3-4, pp. 275–286, 1981.

[36] Wang, X-Q., Mujumdar, A.S., “A Review on Nanofluids - Part I: Theoretical and Numerical Investigations”, Brazilian Journal of Chemical Engineering, Vol. 25, No. 04, pp. 613 - 630, 2008.

[37] Pak, B.C., Cho, Y.I., “Hydrodynamic and Heat Transfer Study of Dispersed Fluids with Submicron Metallic Oxide Particles”, Experimental Heat Transfer: A Journal of Thermal Energy Generation, Transport, Storage, and Conversion, 11:2, pp. 151-170, 1998.

[38] Wang, X., Xu, X., Choi, S.U.S., “Thermal Conductivity of Nanoparticle– Fluid Mixture”, Journal of Thermophysics and Heat Transfer, Vol. 13, No. 4, 1999.

[39] Tseng, W.J., Lin, K-C., “Rheology and Colloidal Structure of Aqueous TiO_2 Nanoparticle Suspensions”, Materials Science and Engineering A355, pp. 186-192, 2003.

[40] Prasher, R., Song, D., Wang, J., Phelan, P., “Measurements of Nanofluid Viscosity and its Implications for Thermal Applications”, Applied Physics Letters, 89, 133108, 2006.

[41] Namburu, P.K., Kulkarni, D.P., Misra, D., Das, D.K., “Viscosity of Copper Oxide Nanoparticles Dispersed in Ethylene Glycol and Water Mixture”, Experimental Thermal and Fluid Science, 32, pp. 397–402, 2007-a.

[42] Namburu, P.K., Kulkarni, D.P., Dandekar, A., D.K. Das, “Experimental Investigation of Viscosity and Specific Heat of Silicon Dioxide Nanofluids”, Micro & Nano Letters, Vol. 2, No. 3, pp. 67–71, 2007-b.

[43] Chen, H., Ding, Y., He, Y., Tan, C,. “Rheological Behaviour of Ethylene Glycol Based Titania Nanofluids”, Chemical Physics Letters 444, pp. 333–337, 2007.

[44] He, Y., Jin, Y., Chen, H., Ding, Y., Cang, D., Lu, H., “Heat Transfer and Flow Behaviour of Aqueous Suspensions of TiO_2 Nanoparticles (Nanofluids) Flowing Upward Through a Vertical Pipe”, International Journal of Heat and Mass Transfer 50, pp. 2272-2281, 2007.

[45] Chevalier, J., Tillement, O., Ayela, F., “Rheological Properties of Nanofluids Flowing Through Microchannels”, Applied Physics Letters 91, 233103, 2007.

[46] Nguyen, C.T., Desgranges, F., Roy, G., Galanis, N., Maré, T., Boucher, S., Angue Mintsa, H., “Temperature and Particle-Size Dependent Viscosity Data for Water-Based Nanofluids – Hysteresis Phenomenon”, International Journal of Heat and Fluid Flow, 28, pp. 1492–1506, 2007.

[47] Murshed, S.M.S., Leong, K.C., Yang, C., “Investigations of Thermal Conductivity and Viscosity of Nanofluids”, International Journal of Thermal Sciences, 47, pp. 560–568, 2008.

[48] Chen, H., Yang, W., He, Y., Ding, Y., Zhang, L., Tan, C., Lapkin, A.A., Bavykin, D.V., “Heat Transfer and Flow Behaviour of Aqueous Suspensions of Titanate Nanotubes (Nanofluids)”, Powder Technology, 183, pp. 63–72, 2008.

[49] Tavman, I., Turgut, A., Chirtoc, M., Schuchmann, H.P., Tavman, S., “Experimental Investigation of Viscosity and Thermal Conductivity of Suspensions Containing Nanosized Ceramic Particles”, Archives of Materials Science and Engineering, Vol. 34, Issue 2, pp. 99-104, 2008.

[50] Garg, J., Poudel, B., Chiesa, M., Gordon, J.B., Ma, J.J., Wang, J.B., Ren, Z.F., Kang, Y.T., Ohtani, H., Nanda, J., McKinley, G.H., Chen, G., “Enhanced Thermal Conductivity and Viscosity of Copper Nanoparticles in Ethylene Glycol Nanofluid”, Journal of Applied Physics, 103, 074301, 2008.

[51] Lee, J.-H., Hwang, K.S., Jang, S.P., Lee, B.H., Kim, J.H., Choi, S.U.S., Choi, C.J., "Effective Viscosities and Thermal Conductivities of Aqueous Nanofluids Containing Low Volume Concentrations of Al_2O_3 Nanoparticles", International Journal of Heat and Mass Transfer, 51, pp. 2651–2656, 2008.

[52] Xie, H., Chen, L., Wu, Q., "Measurements of the Viscosity of Suspensions (Nanofluids) Containing Nanosized Al_2O_3 Particles", High Temperatures-High Pressures, Vol. 37, pp. 127–135, 2008.

[53] Anoop, K.B., Kabelac, S., Sundararajan, T., Das, S.K., "Rheological and Flow Characteristics of Nanofluids: Influence of Electroviscous Effects and Particle Agglomeration", Journal of Applied Physics, 106, 034909, 2009.

[54] Chen, H., Ding, Y., Lapkin, A., Fan, X., "Rheological Behaviour of Ethylene Glycol-Titanate Nanotube Nanofluids", J Nanopart Res, 11, pp. 1513–1520, 2009.

[55] Turgut, A., Tavman, I., Chirtoc, M., Schuchmann, H.P., Sauter, C., Tavman, S., "Thermal Conductivity and Viscosity Measurements of Water-Based TiO_2 Nanofluids", Int J Thermophys, 30, pp. 1213–1226, 2009.

[56] Duangthongsuk, W., Wongwises, S., "Measurement of Temperature-Dependent Thermal Conductivity and Viscosity of TiO_2-Water Nanofluids", Experimental Thermal and Fluid Science, 33, pp. 706–714, 2009.

[57] Garg, P., Alvarado, J.L., Marsh, C., Carlson, T.A., Kessler, D.A., Annamalai, K., "An Experimental Study on the Effect of Ultrasonication on Viscosity and Heat Transfer Performance of Multi-Wall Carbon Nanotube-Based Aqueous Nanofluids", International Journal of Heat and Mass Transfer, 52, pp. 5090–5101, 2009.

[58] Timofeeva, E.V., Routbort, J.L., Singh, D., "Particle Shape Effects on Thermophysical Properties of Alumina Nanofluids", Journal of Applied Physics, 106, 014304, 2009.

[59] Zhao, J-F., Luo, Z-Y., Ni, M-J., Cen, K-F., "Dependence of Nanofluid Viscosity on Particle Size and pH Value", Chin. Phys. Lett., Vol. 26, No. 6, 066202, 2009.

[60] Pastoriza-Gallego, M.J., Casanova, C., Páramo, R., Barbés, B., Legido, J.L., Piñeiro, M.M., "A Study on Stability and Thermophysical Properties (Density and Viscosity) of Al_2O_3 in Water Nanofluid", Journal Of Applied Physics, 106, 064301, 2009.

[61] Naik, M.T., Ranga Janardhana, G., Kumar Reddy, K.V., Reddy, B.S., "Experimental Investigation into Rheological Property of Copper Oxide Nanoparticles Suspended in Propylene Glycol-Water Based Fluids", ARPN Journal of Engineering and Applied Sciences, Vol. 5, No. 6, pp. 29-34, 2010.

[62] Godson, L., Raja, B., Mohan Lal, D., Wongwises, S., "Experimental Investigation on the Thermal Conductivity and Viscosity of Silver-Deionized Water Nanofluid", Experimental Heat Transfer, 23:4, pp. 317-332, 2010.

[63] Tavman, I., Turgut, A., "An Investigation on Thermal Conductivity and Viscosity of Water Based Nanofluids", Microfluidics Based Microsystems NATO Science for Peace and Security Series A: Chemistry and Biology, pp 139-162, 2010.

[64] Kole, M., Dey, T.K., "Viscosity of Alumina Nanoparticles Dispersed in Car Engine Coolant", Experimental Thermal and Fluid Science, 34, pp. 677–683, 2010.

[65] Chandrasekar, M., Suresh, S., Chandra Bose, A., "Experimental Investigations and Theoretical Determination of Thermal Conductivity and Viscosity of Al_2O_3/Water Nanofluid", Experimental Thermal and Fluid Science, 34, pp. 210–216, 2010.

[66] Xie, H., Yu, W., Chen, W., "MgO Nanofluids: Higher Thermal Conductivity and Lower Viscosity Among Ethylene Glycol-Based Nanofluids Containing Oxide Nanoparticles", Journal of Experimental Nanoscience, Vol. 5, No. 5, pp. 463–472, 2010.

[67] Lee, S.W., Park, S.D., Kang, S., Bang, I.C., Kim, J.H., "Investigation of Viscosity and Thermal Conductivity of SiC Nanofluids for Heat Transfer Applications", International Journal of Heat and Mass Transfer, 54, pp. 433–438, 2011.

[68] Suresh, S., Venkitaraj, K.P., Selvakumar, P., Chandrasekar, M., "Synthesis of Al_2O_3–Cu/Water Hybrid Nanofluids Using Two Step Method and its Thermophysical Properties", Colloids and Surfaces A: Physicochem. Eng. Aspects, 388, pp. 41-48, 2011.

[69] Kole, M., Dey, T.K., "Effect of Aggregation on the Viscosity of Copper Oxide Gear Oil Nanofluids", International Journal of Thermal Sciences, 50, pp. 1741-1747, 2011.

[70] Pastoriza-Gallego, M.J., Casanova, C., Legido, J.L., Piñeiro, M.M., "CuO in Water Nanofluid: Influence of Particle Size and Polydispersity on Volumetric Behaviour and Viscosity", Fluid Phase Equilibria, 300, pp. 188–196, 2011.

[71] Kim, C.K., Lee, G-J., Rhee, C.K., "A Study on Heat Transfer Characteristics of Spherical and Fibrous Alumina Nanofluids", Thermochimica Acta 542, pp. 33-36, 2012.

[72] Aladag, B., Halelfadl, S., Doner, N., Maré, T, Duret, S., Estellé P., "Experimental Investigations of the Viscosity of Nanofluids at Low Temperatures", Applied Energy, 97, pp. 876-880, DOI: 10.1016/j.apenergy.2011.12.101, 2012.

[73] Utomo, A.T., Poth, H., Robbins, P.T., Pacek, A.W., "Experimental and Theoretical Studies of Thermal Conductivity, Viscosity and Heat Transfer Coefficient of Titania and Alumina Nanofluids", International Journal of Heat and Mass Transfer 55, pp. 7772–7781, 2012.

[74] Suganthi, K.S., Rajan, K.S., "Temperature Induced Changes in ZnO–Water Nanofluid: Zeta Potential, Size Distribution and Viscosity Profiles", International Journal of Heat and Mass Transfer, 55, pp. 7969–7980, 2012.

[75] Nabeel Rashin, N., Hemalatha, J., "Viscosity Studies on Novel Copper Oxide–Coconut Oil Nanofluid", Experimental Thermal and Fluid Science, Vol. 48, pp. 67-72, 2013.

[76] Syam Sundar, L., Singh, M.K., Sousa, A.C.M., "Investigation of Thermal Conductivity and Viscosity of Fe_3O_4 Nanofluid for Heat Transfer Applications", International Communications in Heat and Mass Transfer, Vol. 44, pp. 7-14, 2013.

[77] Kestin, J., Sokolov, M., Wakeham, W.A., "Viscosity of Liquid Water in the Range -8^{o}C to 150^{o}C", J. Phys. Re. Data, Vol. 7, No. 3, pp. 941-948, 1978.

[78] Kitano, T., Kataoka, T., Shirota, T., "An Empirical Equation of the Relative Viscosity of Polymer Melts Filled with Various Inorganic Fillers", Rheologica Acta, Volume 20, Issue 2, pp 207-209, 1981.

[79] Masoumi, N., Sohrabi, N., Behzadmehr, A., "A New Model for Calculating the Effective Viscosity of Nanofluids", Journal of Physics D: Applied Physics, 42, 055501, 2009.

[80] Maïga, S.E.B., Nguyen, C.T., Galanis, N, Roy, G., "Heat Transfer Behaviours of Nanofluids in a Uniformly Heated Tube", Superlattices and Microstructures 35, pp. 543–557, 2004.

[81] Munson, B.R., Young, D.F., Okiishi, T.H., Huebsch, W.W., *Fundamentals of Fluid Mechanics*, Sixth Edition, John Wiley & Sons, Inc., Asia, 2010.

[82] Sergis, A., Hardalupas, Y., "Anomalous Heat Transfer Modes of Nanofluids: a Review Based on Statistical Analysis", Nanoscale Research Letters, 6: 391, 2011.

[83] Turgut, A., Tavman, I., Cetin, L., Chirtoc, M., Fudym, O., "Preparation and Characterization of Nanofluids Containing Alumina Nanoparticles", ICHMT DIGITAL LIBRARY ONLINE, Volume 0, 2011 Issue - TMNN-2010. Proceedings of the International Symposium on Thermal and Materials Nanoscience and Nanotechnology - 29 May − 3 June, 2011, Antalya, Turkey, 2011.

[84] http://www.labx.com/v2/adsearch/detail3.cfm?adnumb=490604
[date accessed: April 11, 2013].

[85] http://www.silver-colloids.com/Tutorials/Intro/pcs12A.html
[date accessed: May 7, 2013].

[86] Fisher, R.A., *Statistical Methods for Research Workers*, Oliver and Buyd, Edinburgh, 1925. [http://psychclassics.yorku.ca/Fisher/Methods/]

[87] Fisher, R.A., *The Design of Experiments*, Oliver and Boyd, Edinburgh and London, 1935.

[88] Fisher, R.A., Statistical Methods and Scientific Induction, Journal of the Royal Statistical Society, Series B (Methodological), Vol. 17, No. 1, pp. 69-78, 1955.

[89] Mason, R.L., Gunst, R.F., Hess, J.L., *Statistical Design and Analysis of Experiments with Applications to Engineering and Science*, Second Edition, John Wiley & Sons Inc., Hoboken, New Jersey and Canada, 2003.

[90] Anderson, M., Design of Experiments, The Industrial Physicist, pp. 24-26, 1997.

[91] Kavak, D., Demir, M., Başsayel, B., Anagün, A.S., "Factorial Experimental Design for Optimizing the Removal of Lead Ions From Aqueous Solutions by Cation Exchange Resin", Desalination and Water Treatment, 51, pp. 1712-1719, 2013.

[92] Ross, P.J., *Taguchi Techniques for Quality Engineering. Loss Function, Orthogonal Experiments, Parameter and Tolerance Design*, Second Edition, McGraw Hill, New York, San Francisco, Washington, D.C., 1996.

[93] Cabilio, P., Masaro, J., *Basic Statistical Procedures and Tables*, Tenth Edition, Department of Mathematics and Statistics, Acadia University, 2001.

[94] Lu, J-C., Jeng, S-L, Wang, K., "A Review of Statistical Methods for Quality Improvement and Control in Nanotechnology", Journal of Quality Technology, Vol. 41, No. 2, pp. 148-164, 2009.

[95] Anagun, A.S., Ozcelik, F., "Optimization of Genetic Algorithm Parameters for Multi-channel Manufacturing Systems by Taguchi Method", AI 2005: LNAI 3809, Springer-Verlag Berlin Heidelberg, pp. 1021-1024, 2005.

[96] Phadke M.S., *Quality Engineering Using Robust Design*, AT&T Bell Laboratories, Prentice Hall PTR, Englewood Cliffs, New Jersey 07632, 1989.

[97] Turgut, A., "Investigation of Thermophysical Properties of Nanofluids", Ph.D. Thesis submitted to Graduate School of Natural and Applied Sciences of Dokuz Eylül University, 2010.

[98] Izumo, N., Koiwai, A., "Technological Background and Latest Market Requirements Concerning "Static Viscosity" Measurement with a Tuning-fork Vibration Viscometer", in Proceedings of Asia-Pacific Symposium on Measurement of Mass, Force and Torque (APMF 2009), 1-4 June 2009, Tokyo, Japan, pp. 51-57, 2009.

[99] Özalp, A., Anagün, A.S., "Yapay Sinir Ağı Performansına Etki Eden Faktörlerin Analizinde Taguchi Yöntemi: Hisse Senedi Fiyat Tahmini Uygulaması", İstatistik Araştırma Dergisi, 2(1), pp. 29-45, 2003.

[100] Bluman, A.G., *"Elementary Statistics a Brief Version"*, Second Edition, McGraw-Hill Companies, New York, 2003.

[101] Çömlekçi, N., *"Deney Tasarımı, İlke ve Teknikleri"*, Alfa Yayınları, İstanbul, 2003.

[102]http://www.aandd.jp/img/products/test_measuring/testinstruments/sv-a/ax-sv-54.jpg [date accessed: May 12, 2013].

APPENDIX A

COEFFICIENTS OF THE CORRELATIONS PROVIDED IN TABLE 6

Table 30. The values of the empirical constants (*A*, *B*, and *C*) of the correlation proposed by Chen et al. [26, 43]. (Provided as Equation (21).)

φ % (by weight)	*A*	*B*	*C*	MaxD[a] (%)	MinD[b] (%)
0.0	-3.2114	0.86973	-154.57	+0.62	-1.44
0.5	-3.1820	0.86285	-155.13	+0.31	-1.58
1.0	-3.3289	0.91603	-150.35	+1.38	-0.80
2.0	-3.5126	0.98375	-144.48	+0.75	-1.31
4.0	-3.2517	0.91226	-150.74	+0.38	-0.86
8.0	-3.7005	1.08082	-138.30	+0.26	-1.65

[a] Maximum discrepancies. [b] Minimum discrepancies.

Table 31. The values of the empirical constants (*a*, *b*, and *c*) of the correlation proposed by Duangthongsuk and Wongwises [56]. (Provided as Equation (34).)

Temperature (^{o}C)	*a*	*b*	*c*	R^2
15	1.0226	0.0477	-0.0112	0.9885
25	1.013	0.092	-0.015	0.9767
35	1.018	0.112	-0.0177	0.9937

Table 32. The values (at 25^{o}C) of the empirical constants (A_1 and A_2) of the correlation proposed by Timofeeva et al. [58]. (Provided as Equation (35).)

	Platelets	Blades	Cylinders	Bricks
A_1	37.1	14.6	13.5	1.9
A_2	612.6	123.3	904.4	471.4

Table 33. The values of the empirical constants (*A* and *B*) calculated by Kole and Dey [64]. Coefficients belong to the correlation proposed by Namburu et al. [41, 42]. (Provided as Equation (20).)

φ	*A*	*B*	R^2
0.001	1.83442	-0.01345	0.9993
0.004	1.88642	-0.01244	0.9994
0.007	1.98529	-0.01226	0.9995
0.010	1.98752	-0.01128	0.9954
0.0151	2.1355	-0.00999	0.9974

Table 34. The values of the empirical constants (*A*,*B*, and *C*) calculated by Kole and Dey [64]. Coefficients belong to the correlation proposed by Chen et al. [26, 43]. (Provided as Equation (21).)

φ (by volume)	*A*	*B*	*C*	Deviation (%)
0.005	-0.70784	0.70912	-171.04969	-1.398
0.010	-1.11379	1.23013	-104.97616	-0.0737
0.015	-4.94087	3.37827	-26.21399	-0.0565
0.020	-1.10774	1.43086	-87.08024	-0.0751
0.025	-1.61144	0.57409	-160.04291	0.6575

Table 35. The values of the empirical constants (*a* and *b*) of the correlation proposed by Nabeel Rashin and Hemalatha [75]. (Provided as Equation (41).)

Shear rate (s^{-1})	Temperature (K)	*a*	*b*
3.67	308	54	5111
	313	32	7312
	318	7	9868
	323	10	8226
	328	9	6527
7.34	308	46	2489
	313	33	3419
	318	17	4353
	323	14	4745
	328	15	4354
14.68	308	31	1887
	313	23	2875
	318	11	4090
	323	14	3428
	328	19	2370

Table 36. The values of the empirical constant (*c*) of the correlation proposed by Nabeel Rashin and Hemalatha [75]. (Provided as Equation (42).)

Shear rate (s^{-1})	Concentration (φ (%) by weight)	*c* (Pa s)
3.67	0	219
	0.5	380
	1.0	613
	1.5	837
	2	1359
	2.5	1790
7.34	0	326
	0.5	553
	1.0	625
	1.5	936
	2	1042
	2.5	1394
14.68	0	545
	0.5	773
	1.0	765
	1.5	912
	2	860
	2.5	1179

APPENDIX B

MATLAB CODE EMPLOYED TO CALCULATE THE REQUIRED AMOUNTS OF H_2O FOR DILUTED SAMPLE PREPARATION & OTHER CHARACTERISTICS WITH PROGRAM OUTPUTS

```
% This MATLAB Program calculates the required amounts of deionized
water to
% be added into the Al2O3-H2O nanofluids of 20wt% to dilute them to
3, 2 and 1 vol% (50mL each).

% NOMENCLATURE:
% np, w and nf: nanoparticles, water and nanofluid, respectively.
% phi: the fraction of nanoparticles in the nanofluid, i.e.
phi_weight:
% weight percentage, phi_vol: volumetric percentage of the
nanoparticles in the nanofluid.
% phi_vol_dilution1, phi_vol_dilution2 and phi_vol_dilution3:
volumetric fractions of the diluted nanofluids.
% phi_vol_confirm: confirmation value of the volumetric fraction of
% nanoparticles estimated from the volumes of nanoparticles and
water.

% GIVEN (KNOWN) VALUES :
density_np = 3.7; % provided by NanoAmor.
density_w = 1;
phi_weight = 0.20;
volume_nf = 50;

% CALCULATION ALGORITHM :
phi_vol = (phi_weight*density_w)/(density_np + phi_weight*density_w
- phi_weight*density_np); % formula given in the Turgut et al.
publication.

C1 = phi_vol;
V2 = 50;
C2 = 0.03;

% From phi_weight = 0.20, How can phi_vol = 0.30 be prepared?
% ConcentratedSampleVolume_1 * C1 = V2 * C2, C1 denotes the volume
fraction of the stock suspension, and C2 denotes the volume fraction
of the 50mL sample (3 vol%).
% Rearranging:
ConcentratedSampleVolume_1 = V2 * C2 / C1 ;

C3 = 0.02;

% From phi_weight = 0.20, How can phi_vol = 0.20 be prepared?
% ConcentratedSampleVolume_2 * C1 = V2 * C3 , C3 denotes the volume
fraction of the 50mL sample (2 vol%).
% Rearranging:
ConcentratedSampleVolume_2 = V2 * C3 / C1 ;

C4 = 0.01;
```

```
% From phi_weight = 0.20, How can phi_vol = 0.10 be prepared?
% ConcentratedSampleVolume_3 * C1 = V2 * C4 , C4  denotes the volume
fraction of the 50mL sample (1 vol%).
% Rearranging:
ConcentratedSampleVolume_3 = V2 * C4 / C1 ;



% The deionized water amounts to be added to
ConcentratedSampleVolume_1,
% ConcentratedSampleVolume_2 and ConcentratedSampleVolume_3 to form
3,2 and 1 vol% nanofluids (DIW_1, DIW_2 and DIW_3, respectively) can
be
% calcualted wiht the below equations:

DIW_1 = 50 - ConcentratedSampleVolume_1;
DIW_2 = 50 - ConcentratedSampleVolume_2;
DIW_3 = 50 - ConcentratedSampleVolume_3;
```

PROGRAM OUTPUTS

Table 37. Detailed results for the sample preparation characteristics

Name	Value	Min	Max
C1	0.0633	0.0633	0.0633
C2	0.0300	0.0300	0.0300
C3	0.0200	0.0200	0.0200
C4	0.0100	0.0100	0.0100
ConcentratedSampleVolume_1	23.700	23.700	23.700
ConcentratedSampleVolume_2	15.800	15.800	15.800
ConcentratedSampleVolume_3	7.900	7.900	7.900
DIW_1	26.300	26.300	26.300
DIW_2	34.200	34.200	34.200
DIW_3	42.100	42.100	42.100
V2	50	50	50
density_np	3.700	3.700	3.700
density_w	1	1	1
phi_vol	0.0633	0.0633	0.0633
phi_weight	0.2000	0.2000	0.2000
volume_nf	50	50	50

APPENDIX C

CHARACTERIZATION OF THE NANOFLUID STABILITY WITH ZETA POTENTIAL AND PARTICLE SIZE DISTRIBUTION MEASUREMENTS

1. Zeta Potential Results for φ= 0.01, d_p= 10 nm Alumina-Water Nanofluids of Present Investigation

Zeta Potential Report
v2.2

Malvern

Malvern Instruments Ltd - © Copyright 2008

Sample Details

Sample Name:	10280-04(10nm-%1) 1
SOP Name:	mansettings.dat
General Notes:	

File Name:	22Subat13.dts	**Dispersant Name:**	Water
Record Number:	77	**Dispersant RI:**	1,330
Date and Time:	03 Nisan 2013 Çarşamba 12:...	**Viscosity (cP):**	0,8872
		Dispersant Dielectric Constant:	78,6

System

Temperature (°C):	25,0	**Zeta Runs:**	12
Count Rate (kcps):	201,3	**Measurement Position (mm):**	2,00
Cell Description:	Clear disposable zeta cell	**Attenuator:**	9

Results

		Mean (mV)	Area (%)	Width (mV)
Zeta Potential (mV): 49,2	**Peak 1:**	49,6	85,9	8,06
Zeta Deviation (mV): 12,3	**Peak 2:**	24,2	7,9	3,90
Conductivity (mS/cm): 0,950	**Peak 3:**	76,9	5,3	5,46

Result quality See result quality report

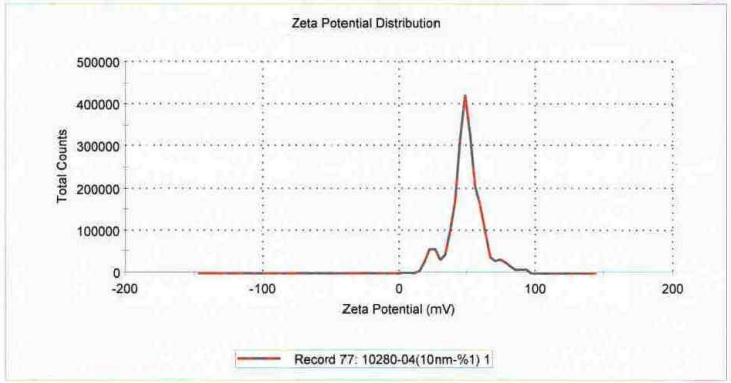

Malvern Instruments Ltd
www.malvern.com

DTS Ver. 5.10
Serial Number : MAL500109

File name: 22Subat13
Record Number: 77
03 Nis 2013 13:32:20

2. Zeta Potential Results for φ= 0.01, d_p= 30 nm Alumina-Water Nanofluids of Present Investigation

Zeta Potential Report

v2.2

Malvern

Sample Details

Sample Name: 10280-03(30nm-%1) 1
SOP Name: mansettings.dat
General Notes:

File Name:	22Subat13.dts	**Dispersant Name:**	Water
Record Number:	82	**Dispersant RI:**	1,330
Date and Time:	03 Nisan 2013 Çarşamba 12:...	**Viscosity (cP):**	0,8854
		Dispersant Dielectric Constant:	78,6

System

Temperature (°C):	24,9	**Zeta Runs:**	12
Count Rate (kcps):	510,8	**Measurement Position (mm):**	2,00
Cell Description:	Clear disposable zeta cell	**Attenuator:**	10

Results

		Mean (mV)	Area (%)	Width (mV)
Zeta Potential (mV): 48,0	**Peak 1:**	49,4	95,6	11,6
Zeta Deviation (mV): 14,8	**Peak 2:**	11,8	2,4	3,92
Conductivity (mS/cm): 0,977	**Peak 3:**	-12,3	0,9	3,34

Result quality See result quality report

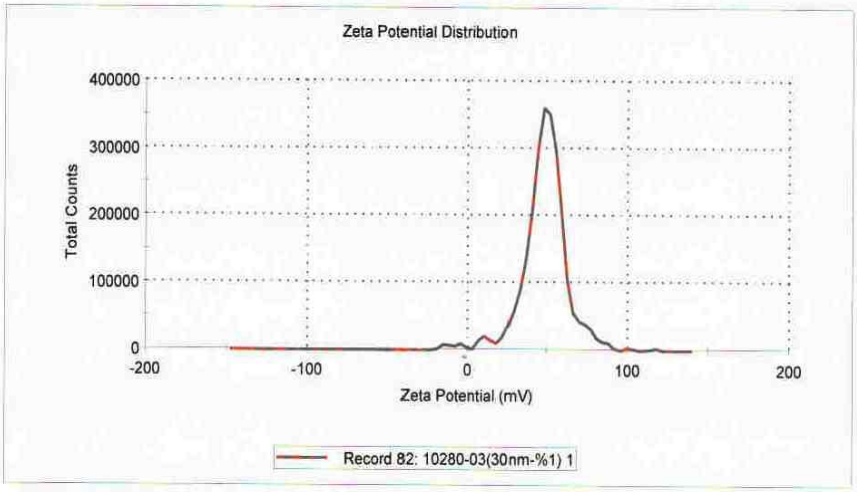

3. Particle Size Distribution Results for φ= 0.01, d_p= 10 nm Alumina-Water Nanofluids of Present Investigation

Size Distribution Report by Volume

v2.0

Malvern

Sample Details

Sample Name: 10281-01(10nm-%1) 1
SOP Name: mansettings.dat
General Notes:

File Name:	22Subat13.dts	**Dispersant Name:**	Water
Record Number:	69	**Dispersant RI:**	1,330
Material RI:	1,76	**Viscosity (cP):**	0,8896
Material Absorbtion:	0,10	**Measurement Date and Time:**	03 Nisan 2013 Çarşamba ...

System

Temperature (°C):	24,9	**Duration Used (s):**	60
Count Rate (kcps):	343,3	**Measurement Position (mm):**	4,65
Cell Description:	Disposable sizing cuvette	**Attenuator:**	8

Results

			Diam. (nm)	% Volume	Width (nm)
Z-Average (d.nm):	36,79	**Peak 1:**	19,79	100,0	11,40
PdI:	0,233	**Peak 2:**	0,000	0,0	0,000
Intercept:	0,943	**Peak 3:**	0,000	0,0	0,000
Result quality	Good				

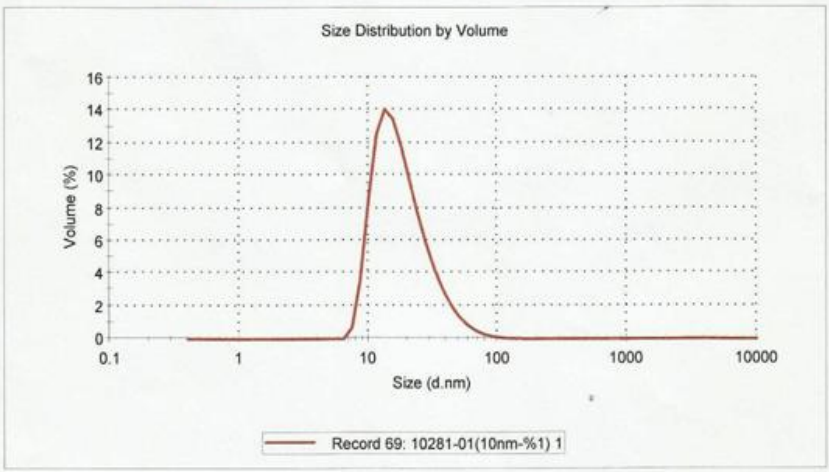

Size Statistics Report by Volume

v2.0

Sample Details

Sample Name: 10281-01(10nm-%1) 1

File Name: 22Subat13.dts

SOP Name: mansettings.dat

Measurement Date and Time: 03 Nisan 2013 Çarşamba 11:25:59

Z-Average (nm):	36,7932	**Derived Count Rate (kcps):**	7500,7667837...
Standard Deviation (nm):	0	**Standard Deviation (kc...**	0
%Std Deviation:	0	**%Std Deviation:**	0
Variance:	0	**Variance:**	0

Size d.nm	Mean Volume %	Std Dev Volume %
0,4000	0,0	
0,4632	0,0	
0,5365	0,0	
0,6213	0,0	
0,7195	0,0	
0,8332	0,0	
0,9649	0,0	
1,117	0,0	
1,294	0,0	
1,499	0,0	
1,736	0,0	
2,010	0,0	
2,328	0,0	
2,696	0,0	
3,122	0,0	
3,615	0,0	
4,187	0,0	
4,849	0,0	

Size d.nm	Mean Volume %	Std Dev Volume %
5,615	0,0	
6,503	0,0	
7,531	0,7	
8,721	3,6	
10,10	8,5	
11,70	12,5	
13,54	14,0	
15,69	13,4	
18,17	11,7	
21,04	9,6	
24,36	7,6	
28,21	5,8	
32,67	4,3	
37,84	3,0	
43,82	2,1	
50,75	1,4	
58,77	0,8	
68,06	0,5	

Size d.nm	Mean Volume %	Std Dev Volume %
78,82	0,3	
91,28	0,1	
105,7	0,1	
122,4	0,0	
141,8	0,0	
164,2	0,0	
190,1	0,0	
220,2	0,0	
255,0	0,0	
295,3	0,0	
342,0	0,0	
396,1	0,0	
458,7	0,0	
531,2	0,0	
615,1	0,0	
712,4	0,0	
825,0	0,0	
955,4	0,0	

Size d.nm	Mean Volume %	Std Dev Volume %
1106	0,0	
1281	0,0	
1484	0,0	
1718	0,0	
1990	0,0	
2305	0,0	
2669	0,0	
3091	0,0	
3580	0,0	
4145	0,0	
4801	0,0	
5560	0,0	
6439	0,0	
7456	0,0	
8635	0,0	
1,000e4	0,0	

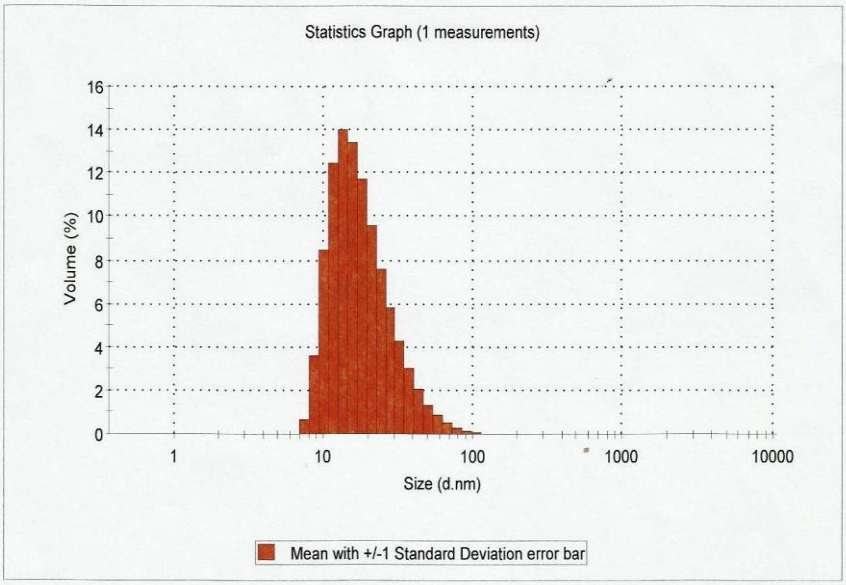

Size Distribution Report by Intensity

v2.0

Malvern

Sample Details

Sample Name: 10281-01(10nm-%1) 1

SOP Name: mansettings.dat

General Notes:

File Name:	22Subat13.dts	**Dispersant Name:**	Water
Record Number:	69	**Dispersant RI:**	1,330
Material RI:	1,76	**Viscosity (cP):**	0,8896
Material Absorbtion:	0,10	**Measurement Date and Time:**	03 Nisan 2013 Çarşamba 1...

System

Temperature (°C):	24,9	**Duration Used (s):**	60
Count Rate (kcps):	343,3	**Measurement Position (mm):**	4,65
Cell Description:	Disposable sizing cuvette	**Attenuator:**	8

Results

			Diam. (nm)	% Intensity	Width (nm)
Z-Average (d.nm):	36,79	**Peak 1:**	49,84	100,0	28,31
PdI:	0,233	**Peak 2:**	0,000	0,0	0,000
Intercept:	0,943	**Peak 3:**	0,000	0,0	0,000

Result quality Good

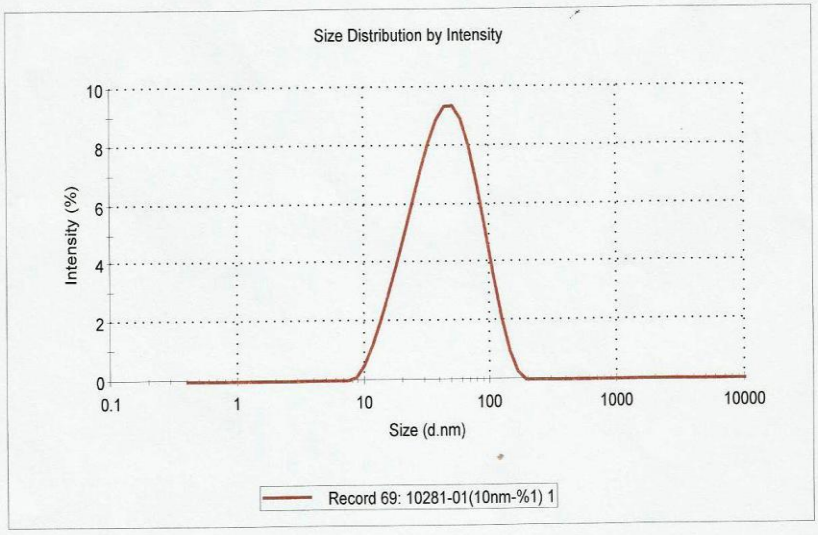

4. Particle Size Distribution Results for φ= 0.01, d_p= 30 nm Alumina-Water Nanofluids of Present Investigation

Size Distribution Report by Volume

v2.0

Malvern

Sample Details

Sample Name: 10281-02(30nm-%1) 1

SOP Name: mansettings.dat

General Notes:

File Name:	22Subat13.dts	**Dispersant Name:**	Water
Record Number:	87	**Dispersant RI:**	1,330
Material RI:	1,76	**Viscosity (cP):**	0,8862
Material Absorbtion:	0,10	**Measurement Date and Time:**	03 Nisan 2013 Çarşamba ...

System

Temperature (°C):	25,1	**Duration Used (s):**	60
Count Rate (kcps):	410,1	**Measurement Position (mm):**	4,65
Cell Description:	Disposable sizing cuvette	**Attenuator:**	9

Results

			Diam. (nm)	% Volume	Width (nm)
Z-Average (d.nm):	29,04	**Peak 1:**	11,48	99,9	7,577
PdI:	0,401	**Peak 2:**	4773	0,1	961,6
Intercept:	0,940	**Peak 3:**	0,000	0,0	0,000
Result quality	Good				

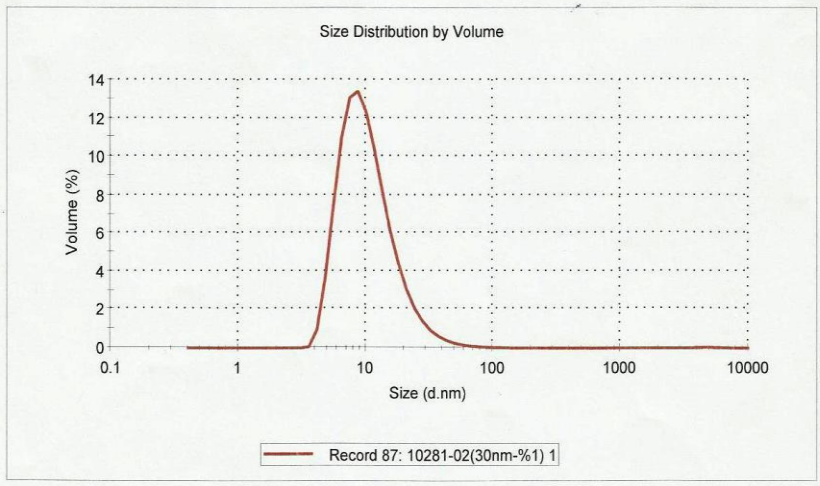

Size Statistics Report by Volume

v2.0

Malvern

Sample Details

Sample Name: 10281-02(30nm-%1) 1

File Name: 22Subat13.dts

SOP Name: mansettings.dat

Measurement Date and Time: 03 Nisan 2013 Çarşamba 12:49:48

Z-Average (nm):	29,04033	**Derived Count Rate (kcps):**	4264,6419165...
Standard Deviation (nm):	0	**Standard Deviation (kc...**	0
%Std Deviation:	0	**%Std Deviation:**	0
Variance:	0	**Variance:**	0

Size d.nm	Mean Volume %	Std Dev Volume %	Size d.nm	Mean Volume %	Std Dev Volume %	Size d.nm	Mean Volume %	Std Dev Volume %	Size d.nm	Mean Volume %	Std Dev Volume %
0,4000	0,0		5,615	7,5		78,82	0,1		1106	0,0	
0,4632	0,0		6,503	11,0		91,28	0,0		1281	0,0	
0,5365	0,0		7,531	13,0		105,7	0,0		1484	0,0	
0,6213	0,0		8,721	13,4		122,4	0,0		1718	0,0	
0,7195	0,0		10,10	12,3		141,8	0,0		1990	0,0	
0,8332	0,0		11,70	10,4		164,2	0,0		2305	0,0	
0,9649	0,0		13,54	8,2		190,1	0,0		2669	0,0	
1,117	0,0		15,69	6,1		220,2	0,0		3091	0,0	
1,294	0,0		18,17	4,4		255,0	0,0		3580	0,0	
1,499	0,0		21,04	3,0		295,3	0,0		4145	0,0	
1,736	0,0		24,36	2,1		342,0	0,0		4801	0,0	
2,010	0,0		28,21	1,4		396,1	0,0		5560	0,0	
2,328	0,0		32,67	0,9		458,7	0,0		6439	0,0	
2,696	0,0		37,84	0,6		531,2	0,0		7456	0,0	
3,122	0,0		43,82	0,4		615,1	0,0		8635	0,0	
3,615	0,1		50,75	0,2		712,4	0,0		1,000e4	0,0	
4,187	0,9		58,77	0,2		825,0	0,0				
4,849	3,6		68,06	0,1		955,4	0,0				

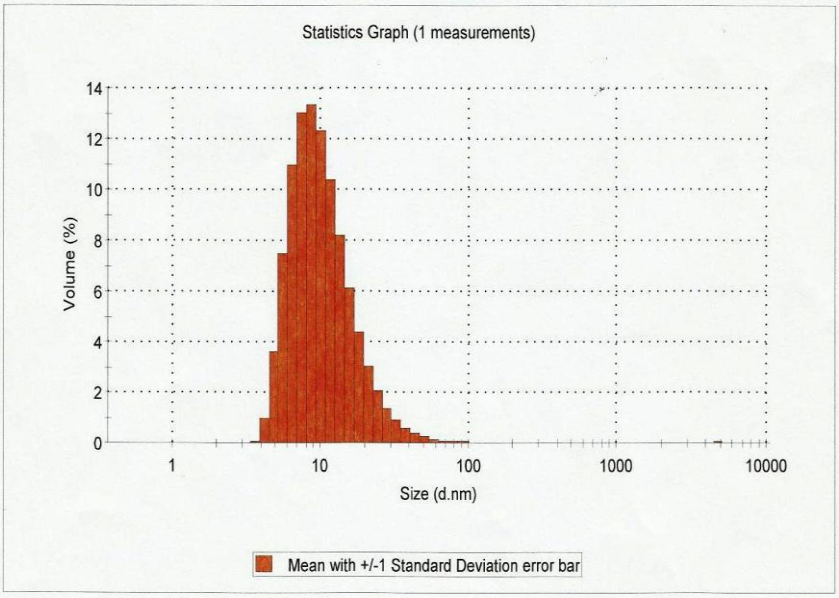

Size Distribution Report by Intensity

v2.0

Malvern

Sample Details

Sample Name: 10281-02(30nm-%1) 1

SOP Name: mansettings.dat

General Notes:

File Name:	22Subat13.dts	**Dispersant Name:**	Water
Record Number:	87	**Dispersant RI:**	1,330
Material RI:	1,76	**Viscosity (cP):**	0,8862
Material Absorbtion:	0,10	**Measurement Date and Time:**	03 Nisan 2013 Çarşamba 1...

System

Temperature (°C):	25,1	**Duration Used (s):**	60
Count Rate (kcps):	410,1	**Measurement Position (mm):**	4,65
Cell Description:	Disposable sizing cuvette	**Attenuator:**	9

Results

			Diam. (nm)	% Intensity	Width (nm)
Z-Average (d.nm):	29,04	**Peak 1:**	49,91	98,7	40,49
PdI:	0,401	**Peak 2:**	4430	1,3	909,4
Intercept:	0,940	**Peak 3:**	0,000	0,0	0,000

Result quality Good

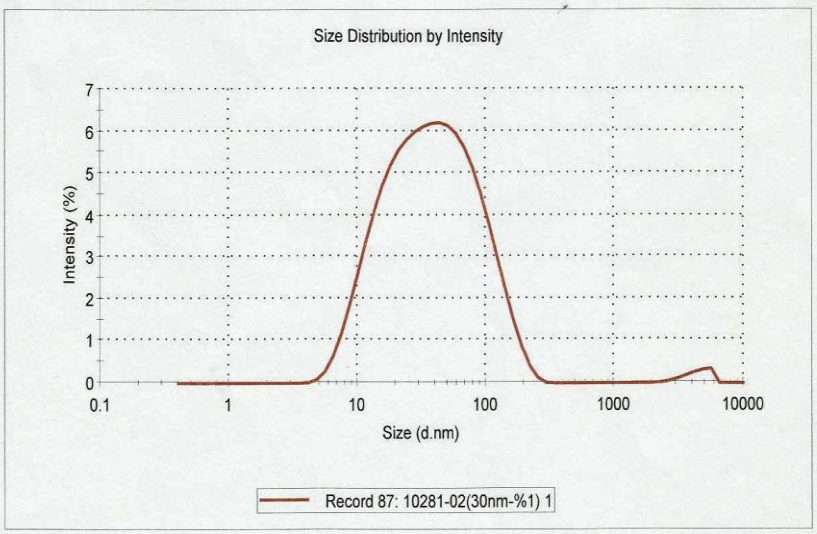

APPENDIX D

CHARACTERIZATION OF THE NANOFLUID PARTICLE SIZE DISTRIBUTION: DYNAMIC LIGHT SCATTERING (DLS) RESULTS

1. DLS Results for φ= 0.01, d_p= 10 nm Alumina-Water Nanofluids of Present Investigation

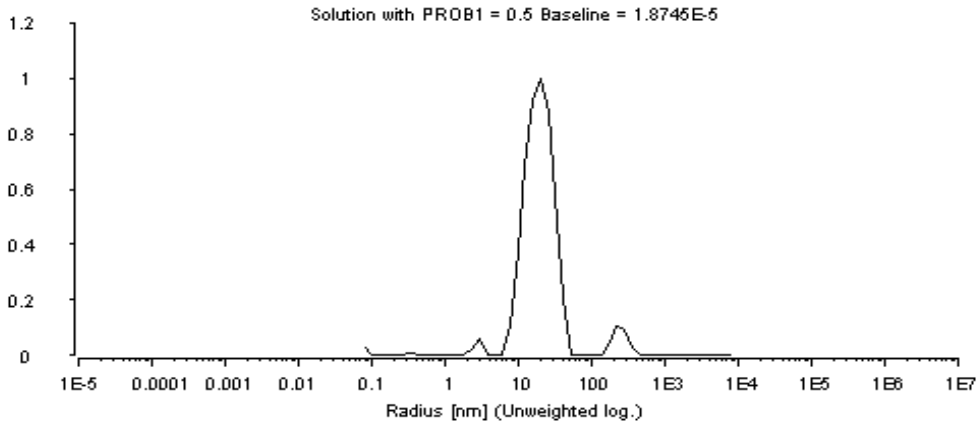

Peak 1, from 8.116E-002 [nm] to 8.116E-002 [nm]

Weight of Peak [%] : 0.52349

Mean Peak Position : 8.116E-002 [nm]

Relative Peak Width : ± 6.585E-010

Peak 2, from 3.423E-001 [nm] to 4.350E-001 [nm]

Weight of Peak [%] : 0.11653

Mean Peak Position : 3.653E-001 [nm]

Relative Peak Width : ± 1.067E-001

Peak 3, from 2.332E+000 [nm] to 2.964E+000 [nm]

Weight of Peak [%] : 1.46715

Mean Peak Position : 2.809E+000 [nm]

Relative Peak Width : ± 9.986E-002

Peak 4, from 7.736E+000 [nm] to 4.147E+001 [nm]

Weight of Peak [%] : 92.71538

Mean Peak Position : 1.902E+001 [nm]

Relative Peak Width : ± 4.049E-001

Peak 5, from 1.749E+002 [nm] to 3.591E+002 [nm]

Weight of Peak [%] : 5.17746

Mean Peak Position : 2.442E+002 [nm]

Relative Peak Width : ± 2.098E-001

2. DLS Results for φ= 0.01, d_p= 30 nm Alumina-Water Nanofluids of Present Investigation

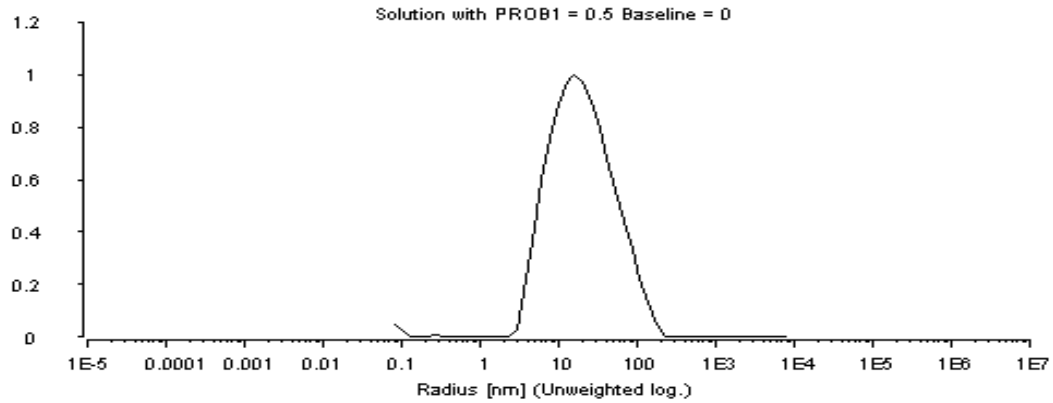

Peak 1, from 8.128E-002 [nm] to 1.033E-001 [nm]

Weight of Peak [%] : 0.60616

Mean Peak Position : 8.727E-002 [nm]

Relative Peak Width : ± 1.095E-001

Peak 2, from 2.697E-001 [nm] to 2.697E-001 [nm]

Weight of Peak [%] : 0.04491

Mean Peak Position : 2.697E-001 [nm]

Relative Peak Width : ± 0.000E+000

Peak 3, from 2.968E+000 [nm] to 1.751E+002 [nm]

Weight of Peak [%] : 99.34893

Mean Peak Position : 1.930E+001 [nm]

Relative Peak Width : ± 8.744E-001

APPENDIX E

DATA ENTERING PROCEDURE FOR ANOVA

1. Data Entering for ANOVA on Alumina-Water Nanofluid Viscosity

Table 40 represents the way employed to enter the data at performing ANOVA, for Al_2O_3-H_2O nanofluid viscosity.

Table 38. The data entering for ANOVA: the locations of the factors and observations employed for the present investigation on nanofluid viscosity

								Observations			
Experiment	***A***	***B***	***AB***	***C***	***AC***	***BC***	***ABC***	**1**	**2**	**3**	**4**
1	1	1	1	1	1	1	1	1.24	1.24	1.09	1.09
2	1	1	1	2	2	2	2	1.06	1.05	1.24	1.24
3	1	2	2	1	1	2	2	1.65	1.65	1.58	1.60
4	1	2	2	2	2	1	1	1.89	1.89	1.68	1.68
5	2	1	2	1	2	1	2	0.66	0.66	0.48	0.49
6	2	1	2	2	1	2	1	0.69	0.68	0.60	0.60
7	2	2	1	1	2	2	1	0.93	0.93	0.85	0.85
8	2	2	1	2	1	1	2	0.97	0.97	1.03	1.04

2. Data Entering for ANOVA on Alumina-Water Relative Viscosity

Table 41 represents the way employed to enter the data at performing ANOVA, for Al_2O_3-H_2O relative viscosity.

Table 39. The data entering for ANOVA: the locations of the factors and observations employed for the present investigation on relative viscosity

								Observations			
Experiment	***A***	***B***	***AB***	***C***	***AC***	***BC***	***ABC***	**1**	**2**	**3**	**4**
1	1	1	1	1	1	1	1	1.24	1.24	1.09	1.09
2	1	1	1	2	2	2	2	1.06	1.05	1.24	1.24
3	1	2	2	1	1	2	2	1.65	1.65	1.58	1.60
4	1	2	2	2	2	1	1	1.89	1.89	1.68	1.68
5	2	1	2	1	2	1	2	1.20	1.20	0.87	0.89
6	2	1	2	2	1	2	1	1.25	1.24	1.09	1.09
7	2	2	1	1	2	2	1	1.69	1.69	1.55	1.55
8	2	2	1	2	1	1	2	1.76	1.76	1.87	1.89

APPENDIX F

Al_2O_3-H_2O NANOFLUID VISCOSITY RAW DATA

(The data presented in the cells are in mPa.s)

Table 40. Experimental Al_2O_3-H_2O nanofluid viscosity raw data

		d_p (nm)							
T (^{o}C)	φ	10				30			
20	0.01	1.24	1.24	1.09	1.09	1.06	1.05	1.24	1.24
20	0.02	1.16	1.17	1.13	1.14	1.58	1.57	1.52	1.5
20	0.03	1.65	1.65	1.58	1.6	1.89	1.89	1.68	1.68
30	0.01	0.8		0.96		0.93		1.01	
30	0.02	0.95		1.01		1.23		1.22	
30	0.03	1.38		1.2		1.51		1.27	
40	0.01	0.6		0.76		0.81		0.8	
40	0.02	0.75		0.75		0.97		0.99	
40	0.03	1.06		0.94		1.18		1.2	
50	0.01	0.66	0.66	0.48	0.49	0.69	0.68	0.6	0.6
50	0.02	0.59	0.61	0.59	0.6	0.6	0.62	0.82	0.82
50	0.03	0.85	0.85	0.93	0.93	0.97	0.97	1.03	1.04